

Utah State University

DigitalCommons@USU

---

All Graduate Theses and Dissertations

Graduate Studies

---

8-2018

## Enhancing Spider-Silk Protein Materials through Continuous Electrospinning and Photo-Initiated Cross-Linking

Dan Gil

*Utah State University*

Follow this and additional works at: <https://digitalcommons.usu.edu/etd>



Part of the [Biology Commons](#)

---

### Recommended Citation

Gil, Dan, "Enhancing Spider-Silk Protein Materials through Continuous Electrospinning and Photo-Initiated Cross-Linking" (2018). *All Graduate Theses and Dissertations*. 7254.

<https://digitalcommons.usu.edu/etd/7254>

This Dissertation is brought to you for free and open access by the Graduate Studies at DigitalCommons@USU. It has been accepted for inclusion in All Graduate Theses and Dissertations by an authorized administrator of DigitalCommons@USU. For more information, please contact [digitalcommons@usu.edu](mailto:digitalcommons@usu.edu).



ENHANCING SPIDER SILK PROTEIN MATERIALS THROUGH CONTINUOUS  
ELECTROSPINNING AND PHOTO-INITIATED CROSS-LINKING

by

Dan Gil

A dissertation submitted in partial fulfillment  
of the requirements for the degree

of

DOCTOR OF PHILOSOPHY

in

Biology

Approved:

---

Randolph V. Lewis, Ph.D.  
Major Professor

---

Justin A. Jones, Ph.D.  
Committee Member

---

Ronald Sims, Ph.D.  
Committee Member

---

Lee F. Rickords, Ph.D.  
Committee Member

---

Dennis Welker, Ph.D.  
Committee Member

---

Richard S. Inouye, Ph.D.  
School of Graduate Studies

UTAH STATE UNIVERSITY  
Logan, Utah

2018

Copyright © Dan Gil 2018

All Rights Reserved

## ABSTRACT

Enhancing Spider Silk Protein Materials through Continuous Electrospinning and  
Photo-initiated Cross-linking

by

Dan Gil, Doctor of Philosophy

Utah State University, 2018

Major Professor: Dr. Randy Lewis  
Department: Biology

One of the most innovative techniques for creating robust fibers is that of electrospinning. Using this technique our dopes (solubilized spider silk proteins) are placed into a syringe with a positive electrode attached and the negative electrode attached to the target (rotating drum/funnel or stationary target). With the electrodes in place, an electric field is created. This forces the dope droplet at the end of the syringe to be ejected at an incredibly quick rate. The rate creates an elongation factor that induces nanofiber formation generating mats comprised of thousands of nanofibers. Traditionally electrospinning produces a mat that must then be processed into yarns/fibers. Our group has modified the electrospinner to be able to produce a continuous yarn composed of several hundred nanofibers (approximately 300-500 nanofibers). This continuous yarn is then reeled outside of the electrospinner and collected onto a spindle for further processing. Decreasing the diameter of spider-silk fibers will eliminate stress focal points, thus increasing mechanical properties surpassing that of natural silk.

To further enhance the spider-silk materials our group is employing a technique traditionally used to analyze protein-to-protein interactions. The method is known as photo-induced cross-linking of unmodified proteins (PICUP). This technique creates a direct carbon-to-carbon bond between tyrosines within the proteins. This di-tyrosine cross-link is how our spider-silk proteins will be enhanced. By incorporating two additives to our dopes, then irradiating them with a high power light source, tyrosines are covalently cross-linked enhancing the spider-silk protein materials. To increase the efficiency of this reaction our lab created the Cross-link Initiating Photodiode (CLIP), a 200w LED light source designed for maximum cross-link. Using the CLIP, our spider-silk protein materials have already seen a seven to ten fold increase in mechanical properties. These cross-linked materials can further be modified through post-treatments using alcohols, creating a plethora of diverse, tunable materials.

(122 pages)

## PUBLIC ABSTRACT

Enhancing Spider Silk Protein Materials through Continuous Electrospinning and  
Photo-initiated Cross-linking

Dan Gil

Spider-silk is known as one of the stronger natural materials, unfortunately it is impossible to farm spiders due to their territorial and cannibalistic nature. To address this issue, researchers have studied spider-silk to discover how it is produced in nature. From their results, spider-silk is composed of large sized proteins produced in two different cell types. Using this knowledge, researchers created transgenic organisms capable of producing spider-silk proteins in large quantities. Using these proteins, several groups have created fibers, films, hydrogels, and adhesives with robust and versatile properties.

Wet-spinning is a technique commonly used to create fibers from spider-silk proteins. These fibers unfortunately do not compare to the mechanical properties of natural silk. To address this researchers have used a method known as electrospinning to create spider-silk fibers with substantially smaller diameters. In doing so, these electrospun fibers have increased surface area and enhanced mechanical properties. Using this method, our group has modified the electrospinner to be able to produce continuous fine diameter yarns composed of hundreds of nanofibers with mechanical properties surpassing that of natural silk.

Fibers aside, spider-silk proteins can be used to create a variety of different biocompatible materials. To further enhance these materials, our group has utilized a technique traditionally used for observation. This technique employs a high intensity light

source to initiate cross-links within the proteins. With this method, our spider-silk protein materials have increased their mechanical properties by a factor of seven. These materials can further be modified through post-treatments, resulting in tunable materials with diverse and robust mechanical properties.

## ACKNOWLEDGMENTS

I would like to thank Dr. Randolph V. Lewis and Dr. Justin A. Jones for their guidance and support during my graduate career as well as making the funds available to me from the National Science Foundation, Department of Energy, and University Technology Acceleration Grant. I would especially like to thank my committee members, Drs. Ronald Sims, Dennis Welker, and Lee F. Rickords, for their support and assistance throughout the entire process. To my colleagues, thank you for your support and patience working together in the laboratory. To my undergrads, I would like to extend a special thank you for your unflinching devotion and hard work. To the Eccles Science Writing Center and Ann Elise, thank you so much for helping edit my dissertation.

I give special thanks to my wife for coming with me on this adventure in Utah, without her none of this would have been possible. Her encouragement, moral support, and most of all patience during this experience has been a guiding light. To my parents, thank you for pushing me to become the person I am today. Without your support and influence, I would never have had the opportunity to receive a Ph.D. To my friends, even with being on different ends of the country, their presence was always felt and missed. I could not have done it without all of you.

Dan Gil



## CONTENTS

	Page
ABSTRACT .....	iii
PUBLIC ABSTRACT .....	v
ACKNOWLEDGMENTS .....	vii
LIST OF TABLES .....	ix
LIST OF FIGURES .....	x
CHAPTER	
1. INTRODUCTION .....	1
2. CONTINUOUS ELECTROSPINNING OF SPIDER SILK PROTEINS CREATES NANOFIBER YARNS WITH UNPRECEDENTED PROPERTIES .....	24
3. ENHANCING SPIDER SILK PROTEIN MATERIALS THROUGH PHOTO-INITIATED CROSS-LINKING .....	62
4. CONCLUSION.....	86
APPENDICES .....	89
VITAE .....	108

## LIST OF TABLES

Table	Page
1.1 Comparisons of Mechanical Properties .....	5
2.1 Polymers and rSSp Used for Electrospinning .....	34
2.2 Aqueous Dope Composition and Electrospinning Results .....	44
2.3 Effects of Additives on Aqueous Dope Electrospinning .....	47
2.4 Composition of Composite Dopes and Electrospinning Results .....	49
2.5 Results of 80/20 HFIP Dopes at Different Concentrations .....	51
2.6 Optimal Post-treatments Results on Continuous Electrospun Yarns .....	52
2.7 Mechanical Properties of Natural Silk and Continuous Electrospun Yarns .....	53
2.8 Results from rSSp Fiber Verification.....	54
3.1 Post-treated Cross-linked Hydrogels, Foams, and Sponges .....	70
3.2 Average Mechanical Results for Compression of Uncross-linked Hydrogels and Post-treated Cross-linked Hydrogels .....	71
3.3a Average Mechanical Results for Post-treated Cross-linked Hydrogels Tested in Uniaxial Tension.....	73
3.3b Average Mechanical Results of Cross-linked Foams Tested in Compression .....	74
3.3c Average Mechanical Results for Cross-linked Sponges Tested in Cyclical Compressions.....	75

## LIST OF FIGURES

Figure	Page
1.1 <i>Nephila clavipes</i> , golden orb weaver .....	1
1.2 Orb-weaver glands responsible for the six different silks and one glue .....	2
1.3 Duct-work for spider glands.....	4
1.4 Taylor cone .....	10
1.5 Mat electrospinning.....	11
1.6 Mat with randomly oriented fibers.....	12
1.7 Deakin University design for continuous electrospinning.....	13
1.8 Highly twisted continuous electrospun yarn.....	13
2.1 Continuous electrospinning setup .....	32
2.2 SEM image of continuous composite yarn .....	38
2.3 Unpost-treated HFIP yarn .....	40
2.4 Post-treated electrospun HFIP rSSp yarn .....	41
2.5 rSSp verification 1-5 .....	55
2.6 rSSp verification 2-5 .....	56
2.7 rSSp verification 3-5 .....	57
2.8 rSSp verification 4-5 .....	58
2.9 rSSp verification 5-5 .....	59
3.1 CLIP activated. (A) Cooling unit (B) Staging area for samples .....	68
3.2 Average mechanical properties of cross-linked hydrogels, foams, and sponges .....	72
3.3 (A) Compressed post-treated cross-linked cylindrical hydrogel with no stress fractures (B) Post-treated cross-linked hydrogel as dog bone for uniaxial tensions testing .....	73
3.4 Average mechanical properties of cross-linked sponges tested in cyclical compression .....	74

3.5a Deconvoluted FT-IR Amide I of post-treated cross-linked hydrogels; 1600-1700cm <sup>-1</sup> (A) IPA (B) IPA frozen (C) MeOH (D) EtOH.....	76
3.5b Deconvoluted FT-IR Amide II of post-treated cross-linked hydrogels; 1500-1600cm <sup>-1</sup> (A) IPA (B) IPA Frozen (C) MeOH (D) EtOH .....	76
3.6a Deconvoluted FT-IR Amide I of post-treated cross-linked hydrogels; 1600-1700cm <sup>-1</sup> (A)Wet frozen foam (B) Dry frozen foam (C)Wet frozen sponge (D) Dry frozen sponge .....	77
3.6b Deconvoluted FT-IR Amide II of cross-linked foams and sponges; 1500-1600cm <sup>-1</sup> (A)Wet frozen foam (B) Dry frozen foam (C)Wet frozen sponge (D) Dry frozen sponge .....	78
3.7 Rinse results of Cross-linked hydrogels. (A) Unwashed (B) Washed (C) CLIP used to excited excess Ruthenium.....	79
3.8 BHK cell growth study using unwashed cross-linked post-treated hydrogels. (A) Control well (B) IPA post-treated (C) methanol post-treated .....	80
3.9 BHK cell growth study using washed cross-linked post-treated hydrogels. (A) Control well (B) IPA post-treated (C) methanol post-treated .....	80
A1 Metal funnel .....	91
A2 Stabilizing chamber with electrode attachment .....	92
A3 Reeling system for continuous electrospinning .....	93
B1 Back-opening for syringe pump .....	95
B2 Front end of housing with syringe tip exposed .....	95
D1 Cross-link Initiating Photodiode (CLIP) .....	100

# CHAPTER I

## INTRODUCTION

Spider-silks are some of the most unique and robust natural materials in existence. Created by arachnids and select insects, silk possesses unmatched physical and chemical properties. While some spiders are capable of producing only a few types of silk, the genus orb-weavers can produce up to six different silk fibers and one glue (Figure 1.1).<sup>1</sup> The properties of each silk type range from stretching to approximately 300% of their original length to absorbing 4 GPa of force.<sup>2</sup> These mechanical properties, as well as biocompatibility, are the reasons humans have aspired to use silk throughout time.



Figure 1.1: *Nephila clavipes*, golden orb weaver.<sup>1</sup>

### History of Silk

The novel uses of spider and moth silks were first noted in approximately 500 A.D., ancient Greeks used it in a medical setting as a gauze for wounds because there was no immunological response, representing biocompatibility. China recognized *Bombyx mori* silk's potential, attempting to keep it as a secret but to no avail.<sup>3</sup> Cultures spread across the globe have used spider-silk to create fishing lines, fishing nets, and garments.<sup>4,5</sup>

The earliest documented inquiries into the possible applications of spider-silk were during the 18<sup>th</sup> century. The French government asked two naturalists, Rene-Antoine Ferchault de Reaumur and Bon de Saint-Hilaire, to study the material.<sup>4,6,7</sup> Their research ended in failure due to difficulties associated with farming spiders; spiders' territorial,

cannibalistic nature made it relatively impossible to farm spiders efficiently.<sup>6-9</sup> Nevertheless, interest in using spider-silk in novel manners continued to grow as researchers set out to uncover how spiders make silk in nature.

## Spider-silk in Nature

The potential for spider-silk is widely acknowledged. However, the why and how were not understood until recently. *Nephila clavipes*, known as the Golden Orb Weaver, is one of the most studied species of spiders. This highly evolved spider is capable of producing orb webs that are comprised of six different silks (depicted in Figure 1.2)<sup>10</sup> which can

withstand weather, time, and extreme impact.<sup>11</sup> Each silk has

been tuned through evolution for a specialized function within the spiders' life, and each is named after its gland of origin. The most researched silk protein is that of major ampullate, which is known as dragline silk for its remarkable toughness. Making up the radial spokes in the web, as well as the safety line for spiders, dragline silk has been reported to absorb 4 GPa of force and stretch 30% prior to failure. An interesting discovery

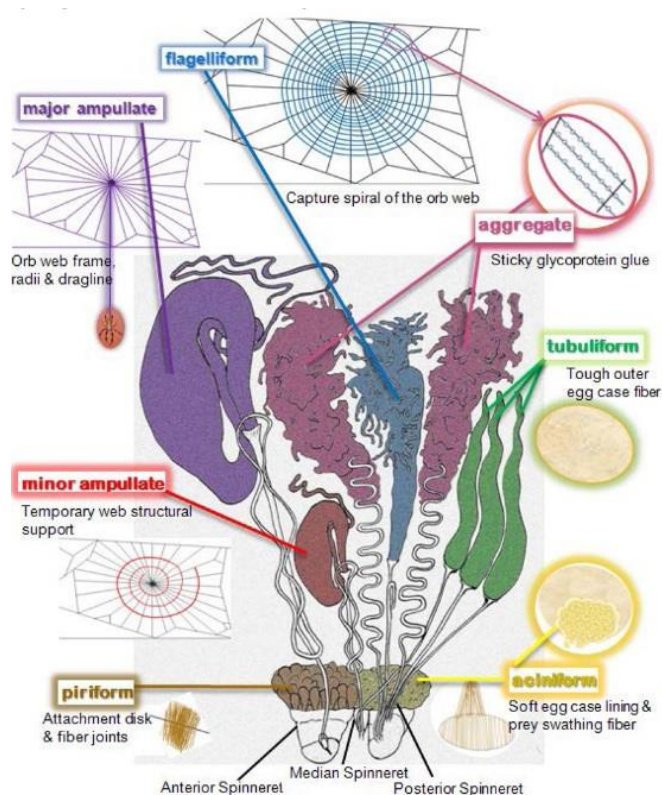


Figure 1.2: Orb-weaver glands responsible for the six different silks and one glue.<sup>10</sup>

is that dragline silk is composed of 2 proteins: major ampullate silk protein 1 (MaSp1)<sup>12</sup> and major ampullate silk protein 2 (MaSp2)<sup>13</sup>. To anchor the radial spokes and join silk strands together, spiders use piriform silk, which has been reported to have greater mechanical strength than dragline due to the fact that the dragline will fail prior to the anchor points. The capture spiral within the web is made up of flagelliform silk, designed to extend to up to 300% its original length. Aciniform silk, a strong yet soft silk, is used to wrap up prey. This silk makes up the first layer of egg cases, providing cushion, and is then wrapped in tubuliform silk, a tough, rigid silk used as a protective case. Instead of laying down an entirely new web, spiders make repairs to any destroyed region. They do so using a silk known as minor ampullate, which serves as a temporary solution until major remodeling can be performed on the web. The last silk type is in a class of its own because it's not a fiber at all. Aggregate silk is produced as a viscous liquid that can be seen as droplets along the web's structure. It is believed to keep the other silks hydrated by forming an aqueous coating and to possess adhesive properties.<sup>11</sup>

Silk glands are comprised of 2 different types of cells: specialized columnar epithelial cells responsible for synthesizing the protein and cells for excreting the protein into the lumen of the gland. Once the proteins are created and stored in the gland, spiders are able to create silk fibers through a pulling motion in which the proteins exit the spider through a spinneret located at the end of the abdomen. As the proteins move through the small ductwork within the glands, sheer stress is imparted (due to small diameter ducting and the S shaped curve, seen in Figure 1.3<sup>16</sup>) on the proteins, causing a conformational shift believed to be crucial in the switch from a liquid to solid state.<sup>14-16</sup> It was found that this conformational shift is due to a property seen few and far between with proteins, self-

assembly into higher structures. Whenever spider-silk proteins endure sheer stress, they undergo self-assembly into fibers, aligning into the proper orientation to create robust and versatile materials. Below in Figure 1.3<sup>16</sup> is the proposed process for the conversion of the proteins from a liquid to solid state.

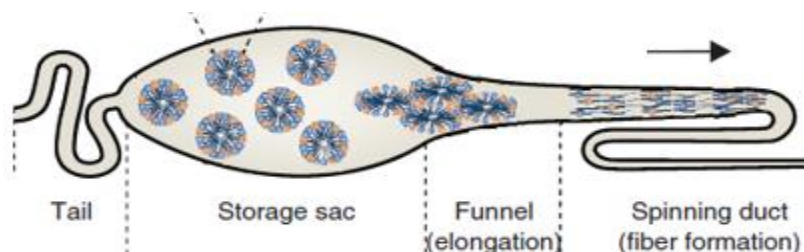


Figure 1.3: Duct-work for spider glands<sup>16</sup>

When the spinnerets were studied more closely, researchers discovered that each one is comprised of tiny spigots, a muscular structure that enables spiders to cut the silk fiber, “clamp” down onto the fiber pausing silk production, and chose a different silk type.<sup>17-19</sup> By isolating the glands, researchers were able to run PCR on each, creating a library of the genetic sequences for each specific silk type.<sup>20</sup>

With a better understanding of how spiders produce the liquid protein solution and convert it into a solid state, researchers set out to uncover the structure and thus the function of spider-silk proteins. Recent advances allowed us to analyze the genes responsible for producing spider-silk proteins, generating a vast amount of crucial information, such as their amino acid sequence. By understanding the protein structure, and thus their function, researchers hoped to recreate the process within the laboratory setting to create a novel manner for efficiently producing spider-silk proteins, eliminating the need to farm spiders.



## Composition and Structure of spider-silk proteins

Researchers during the late 1980s and into early 2000s used several advanced methods to uncover the mysteries within spider-silk proteins.<sup>21</sup> Some of the most valuable techniques that allowed them to define the composition and structure of the spider-silk proteins were nuclear magnetic resonance (NMR)<sup>22–29,29–33</sup>, Fourier transform infrared spectroscopy (FT-IR)<sup>34–36</sup>, X-ray diffraction (XRD)<sup>26,37–40</sup>, and Raman spectroscopy.<sup>41,42</sup>

Using these techniques, researchers were able to determine the exact amino acid sequence for each type of silk protein, giving an insight as to how spiders create such robust and versatile materials. The most studied silk type is dragline silk due to its impressive mechanical properties, seen below in Table 1.1.<sup>43</sup> Possessing such admirable properties, one would surmise that

**Table 1.1- Comparisons of Mechanical Properties<sup>a</sup>**

Material	Strength (MPa)	Strain (%)
Dragline silk	4000	35
Minor Ampullate silk	1000	5
Flagelliform	1000	>200
Tubiform silk	1000	20
<i>Bombyx mori</i> silk	600	20
Kevlar 49	3600	5
Rubber	50	850
Tendon	150	5
Bone	160	3

<sup>a</sup>Data from Gosline<sup>1</sup>, Lewis<sup>2</sup>, Altman<sup>3</sup>

dragline spider-silk proteins would have a very complex array of amino acids and structural motifs, making it rather challenging to synthesize them within the laboratory. Another fact about spider-silk that also lead researchers to believe it rather difficult to synthesize in the laboratory is the size of the proteins. MaSp1 and MaSp2 are approximately 250 kDa<sup>12,13</sup> each, making them some of the largest proteins in nature.

Fortunately for researchers, spider-silk proteins tend to be relatively simple with regards to the number of amino acids they're comprised of. Glycine, one of the smallest amino acids (with regards to the side chains) was found to be the major component of the

major ampullate protein making up approximately 46% of the sequence (with regards to total amino acid content). Only eight other amino acids were found to contribute any significant amount to the sequence.<sup>2,21,24,26,32,35,41,42,44-49</sup> Further analysis revealed that the proteins are made up of three sections: a C-terminus, repeating secondary structures (motifs), and an N terminus. The exact role of the C-terminus is unclear. Researchers believe it is responsible for enabling the proteins to be stored at high concentrations within the lumen of the glands, preventing them from solidifying in the gland (approximately 60% w/v within the gland), as well as a chemical switch for the protein to initiate its conformational shift from a liquid to solid state as it exits the spinneret.<sup>50,51</sup> The role of the N-terminus is hypothesized to be a secretion signal, exporting the proteins into the lumen of the gland.<sup>50,51</sup> It was also discovered that the N-terminus and C-terminus are highly conserved among spider-silk proteins across most species, leading researchers to believe they are important with regards to fiber formation.<sup>51</sup>

Without fully understanding the termini, the motifs are of highest interest due to the secondary structures observed within the proteins. There are three secondary structures predominately found within spider-silk proteins: beta-spirals, beta-sheets, and glycine-II-helices (Figure 1.4).<sup>2,43</sup> These secondary structures are motifs or repeating units throughout the sequence, hypothesized to be the source of the impressive properties of spider-silk. The beta-sheets are composed of predominately poly-alanine<sub>n</sub> or glycine-alanine<sub>n</sub> sequences and are responsible for the mechanical strength of dragline silk. Using XRD, this motif was also found to be highly crystalline in structure, creating a rigid backbone for the protein.<sup>37</sup> The beta-spirals are composed of either GPGGX (where X is usually Y or Q) or GPGQQ

repeating units. Extensive NMR testing demonstrated that the proline found within the sequences yields a 180° bend to the structure, creating a spring-like helix hypothesized to be responsible for the impressive strain found with some spider-silks. The third and final motif found in dragline silk is that of the glycine-II helices, which is composed of GGX sequences and is hypothesized to contribute to the overall strength of spider-silk.<sup>2,52,53</sup> All three of these motifs continuously repeat within the spider-silk sequence, creating a rigid backbone that is connected with spring-like helices, which creates a robust yet extensible material. The biocompatibility of silk is derived from the rather simplistic pallet of amino acids and structural motifs. The design of spider-silk proteins creates a material that the human body's cells can't create an antibody for. With all of this in mind, researchers set out to synthesize spider-silk proteins within the laboratory setting through a number of vectors.

### **Synthesizing Recombinant Spider-silk Proteins**

To eliminate the issues associated with farming spiders, researchers relied on genetic engineering to create a novel manner for producing spider silk proteins. The goal was to have viable amounts of spider silk proteins expressed through transgenic organisms, to be later purified and extracted for use within the laboratory setting. Due to the proteins' large size (250 kDa), researchers encountered issues incorporating genes. To overcome this issue, researchers created truncated versions of the proteins (15, 30, 60, 120 kDa), facilitating the gene transfer into a number of hosts. Using this method, the successful incorporation and expression of these proteins was observed in bacteria (*Escherichia coli*)<sup>54-60</sup>, yeast<sup>61</sup>, mammalian cells<sup>62</sup>, and Sf9 insect cell lines.<sup>60</sup> With advances in genetic

engineering techniques such as CRISPR-Cas9 and Talons, researchers were able to incorporate and express the genes through higher organisms such as *Bombyx mori*<sup>63</sup>, plants (potatoes and tobacco)<sup>64</sup>, and even goats.<sup>65,66</sup> With the goal achieved, researchers were capable of producing recombinant spider-silk proteins (rSSp) in large enough quantities to create a myriad of rSSp-based materials such as fibers, films, gels, foams, sponges, and even adhesives. In turn, these materials can be used in industrial, commercial, technological, and medical settings. There has even been evidence of the rSSp materials promoting healthy cell growth, creating a venue for robust, renewable, and biocompatible materials.<sup>67,68</sup>

To begin the process, the proteins must first be expressed in the transgenic organisms and then extracted and purified.<sup>65</sup> With the proteins purified and lyophilized into a powder, researchers initially used chaotropic agents such as 1,1,1,3,3,3-hexafluoro-2-propanol (HFIP) or 9M lithium bromide to solubilize the proteins into a viscous solution known as a dope. The downside to this approach is that by using chaotropic agents it cannot be upscaled to create large volume dopes. Attempting to find another means of solvation, researchers at Utah State University discovered that by using water as the solvent and using heat, as well as pressure, the proteins could be forced into solution, creating an aqueous-based rSSp dope.<sup>66</sup> By using water as the solvent, the researchers made it possible to upscale the process of creating large volume dopes for conversion of the above mentioned rSSp materials.

### **Producing rSSp Fibers through Wet-Spinning**

With a better understanding of how the proteins work, the next step was to discover

their possible applications. Instinctually what comes to mind is producing fibers and yarns made from rSSp that potentially have a strength-to-weight ratio outmatching any natural or synthetic fibers currently available. The first attempts at creating fibers from rSSp were performed using a technique known as wet-spinning, which got its name from the fact that the rSSp dope is extruded into a coagulation bath containing an alcohol (isopropyl alcohol, methanol, ethanol, etc). The coagulation bath is hypothesized to mimic the internal process of dehydrating the silk protein, aiding in maturing the proteins into their secondary, tertiary, and final quaternary structure. The dope is loaded into a syringe attached to peak tubing with a small internal diameter (0.245 mm). The small diameter peak tubing is used to mimic the size of the spinneret to induce shear force, hypothesized to initiate the conformational shift from a liquid to solid state. This peak tubing is then submerged into the coagulation bath and the dope is extruded. This causes a conformational shift from liquid to solid, resulting in a solid fiber. Fibers produced in this manner with no further processing have shown less-than-desirable properties, leading researchers to believe there are steps missing to achieve properties similar to natural spider-silk. It is also important to note that the fibers produced at this point are still much larger than those of natural spider-silk, at least double the diameter (approximately 20  $\mu\text{m}$ ), and do not compare to its mechanical strength.<sup>55</sup> To address this, researchers set out to further modify the fibers to decrease the fiber diameters and increase the mechanical properties. The synthetic wet-spun fibers were improved through a series of post-stretching while exposing the fibers to different post-stretch baths. When these fibers were analyzed, it was discovered that the post-stretching had increased the degree of crystallinity, inducing further beta-sheet formation and orienting the crystalline regions parallel to the fiber axis.<sup>55,69,70</sup>

Advances aside, there are still drawbacks to the wet-spinning method. Researchers were limited to producing one continuous fiber at a time, making it rather tedious and laborious to produce viable amounts of fiber. To address this, several groups attempted to create multi-head ports with the goal of creating up to 25 continuous fibers at a time. Problems continued to arise, such as large void spaces that needed to be filled with dope to have all 25 ports producing fibers, insufficient flow to have all 25 ports producing fibers, ports clogging and disrupting the process, etc. A new approach was needed to produce viable amounts of rSSp fibers to meet the demand for robust, renewable, biocompatible materials. To accomplish this, researchers used a novel technique that was discovered in the 16<sup>th</sup> century to create fibers.<sup>71</sup>

### **History of Electrospinning**

Discovered incidentally by William Gilbert, electrospinning has been used by researchers dating back to the 16<sup>th</sup> century. The first documented instance of creating fibers from electrospinning was later in 1887 by the Sir Charles Vernon Boys.<sup>72</sup> Later in 1914, John Zeleny established the parameters for successful electrospinning, such as humidity, temperature, and the distance between positive and negative electrodes.<sup>73</sup> The



Figure 1.4: Taylor cone  
biggest electrospinning discovery is credited to Sir Geoffrey Ingram Taylor and happened between 1964 to 1969. Taylor mathematically modelled the shape of the cone formed by the fluid droplet during electrospinning, which is crucial to produce nanofibers. This is known as the Taylor Cone (Figure 1.4), which is formed due to the entanglement property

in which the electric field causes the polymer chains to assemble into fibers, propagating continuous fiber formation from the solution.<sup>74</sup> With a better understanding of how and why the Taylor cone forms, researchers have been able to advance electrospinning techniques to produce fibers using a number of techniques and polymers.<sup>75</sup>

### Advancements in Electrospinning

Through electrospinning, materials composed of countless numbers of nanofibers are produced, creating products with remarkable properties. These, in turn, have increased surface area due to nanofiber composition. For this reason, electrospun materials are typically used in the medical setting for filtration purposes or in the automobile industry.<sup>76-78</sup> An illustration of traditional electrospinning can be seen below

in Figure 1.5.<sup>79</sup> Nanofibers have become well known in the scientific community due to their mechanical and chemical properties. It has been demonstrated that by decreasing the diameters of fibers and yarns, the stress and strain thresholds tend to increase. Fibers and yarns tend to fail

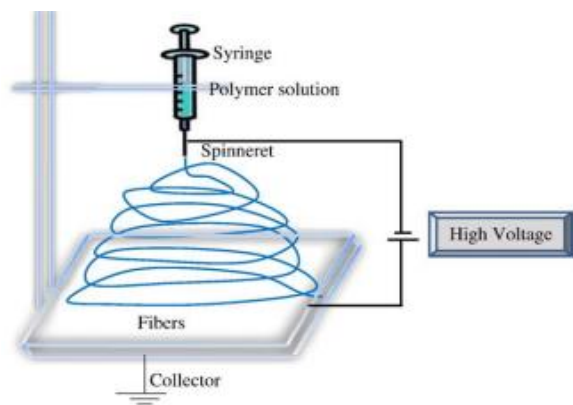


Figure 1.5: Mat electrospinning.<sup>91</sup>

due to stress focal points such as diameter inconsistencies, or anywhere stress can concentrate and cause the fiber to fail. By decreasing the diameters to nanofiber ranges, you are creating a perfect, uniform fiber capable of distributing the force throughout. This eliminates stress focal points resulting in fibers with unprecedented mechanical properties.<sup>80-82</sup>

Traditional electrospinning employs polymers to produce mats with varying properties composed of nanofibers with diameters ranging from 200-700 nm.<sup>83,84</sup> The result is a tough mat that appears solid but is porous, creating a material perfect for filtration. Initially, these mats were collected onto a stationary target, resulting in the nanofibers being oriented in every direction, seen in Figure 1.6.<sup>79,84</sup> To increase the mechanical properties, researchers started to incorporate a rotating drum to collect the electrospun fibers. This created mats with oriented fibers, thus increasing the mechanical properties of the materials

directionally.<sup>85</sup> There have been several variations of electrospinning aside from the rotating drum. These techniques attempted to increase the production capacity of electrospun fibers and create novel methods.

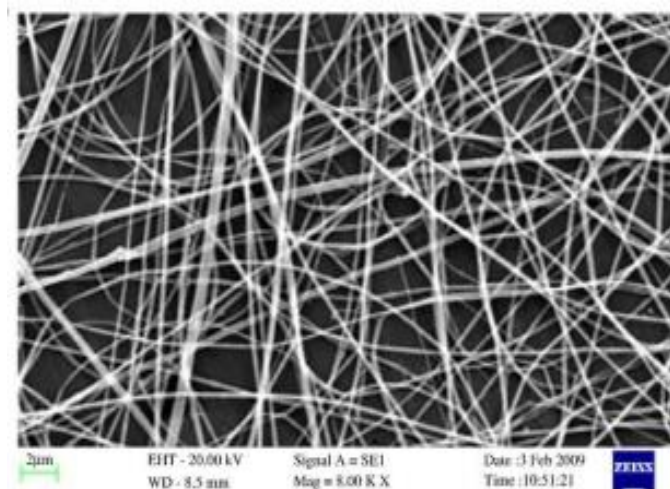


Figure 1.6: Mat with randomly oriented fibers.<sup>91</sup>

These methods include disc-electrospinning<sup>86</sup>, magneto-electrospinning<sup>87</sup>, and vortex electrospinning<sup>88</sup>. Even with the advancements of electrospinning, researchers were unable to create a process that resulted in a continuous electrospun material. These methods would either produce mats that had to be further processed into yarns or fibers of limited length. The only available solution to increase the electrospun products' length was to increase the size of the target, which came with its own limitations.

### **Reinventing Electrospinning**



In 2010, a group at Deakin University lead by Dr. Tong Lin created a novel method for producing continuous electrospun yarns.<sup>89</sup> This was performed by modifying the targets used for collecting the fibers. Their setup consisted of having two pumps holding syringes with metal tips containing polymers, one with the cathode attached and the other with the anode attached to the tips. The syringe tips are approximately 6 inches apart and angled towards one another. A grounded funnel connected to a motor is placed in front of the syringe tips, also 6 inches away, seen in Figure 1.7.<sup>89</sup>

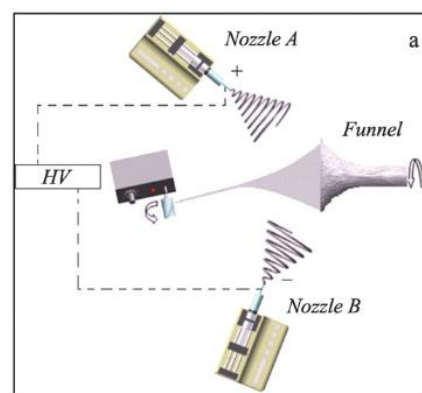


Figure 1.7: Deakin University design for continuous electrospinning.<sup>89</sup>

With the electric field in place, fibers collect at the mouth of the rotating funnel, creating a web across the mouth of the funnel. After a sufficient layer of fibers is formed across the funnel, a glass rod is brought in close proximity to the funnel. The capacity for glass to hold a charge causes the fibrous web to attach to the glass rod, creating a twisted fibrous cone due to the rotation of the funnel. The glass rod is then pulled away steadily from the funnel, resulting in a highly twisted yarn that is continuously produced from the fibers gathering at

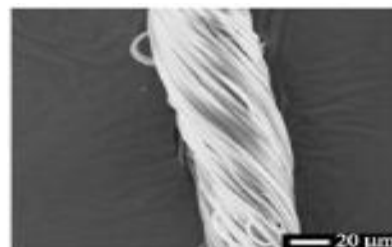


Figure 1.8: Highly twisted continuous electrospun yarn.<sup>97</sup>

the funnel mouth. The yarn in turn is made up of hundreds of nanofibers, resulting a yarn with increased mechanical properties with no length limitations, seen in Figure 1.8.<sup>97</sup> Utilizing this method, the problem of length limitation has been solved created a means of producing viable amounts of electrospun fibers and yarns.

## **Research Goals for Continuous Electrospinning of rSSp**

Recombinant spider-silk protein fibers produced from wet-spinning techniques possess remarkable mechanical properties. However, they have failed to match the tensile strength of its natural counterpart. Currently, *Bombyx mori* silk and rSSp have been electrospun to create mats that are processed into yarns. These possess mechanical properties approaching that of natural silk, but are limited in length due to traditional methods.<sup>80,90-95</sup> Employing the technique developed by Tong Lin, our goal is to modify our iMe electrospinner to produce continuous multi-nanofiber yarns derived from pure rSSp, as well as composites. The properties of these yarns will surpass those of natural silk, which is accomplished by decreasing the diameters of rSSp fibers from micrometers to nanometers creating a material with no stress focal points. By combining these fibers into a highly twisted yarn, the properties will surpass that of natural silk, resulting in continuous yarns with novel mechanical and chemical properties. The post-stretching of these yarns will allow us to tune the mechanical properties by modifying the structures within the proteins observed during wet-spinning. The result will be a product that is lightweight, robust and versatile, with exceptional mechanical properties when compared to natural silk. These materials will be studied for their mechanical properties, ability to be functionalized, and in appropriate cases, their protein structure. The techniques and results for these experiments are presented in Chapter 2- Continuous Electrospinning of Spider-silk Proteins Creates Nanofiber Yarns with Unprecedented Properties.

## **Using rSSp to Create Non-Fiber Biomaterials**

Fibers are just one of the remarkable products that can be created from rSSp. As

stated earlier, researchers have created a variety of other materials such as hydrogels, sponges, foams, films, and adhesives from rSSp.<sup>67,96-100</sup> The human body is capable of healing itself to a degree. However, when there is a large area that needs to be rebuilt, we cannot always compensate for the loss of cells. To address this, researchers have employed hydrogels for tissue engineering, placing them in the body and creating a scaffold for cells to thrive and build tissue.<sup>101-104</sup> Hydrogels, by definition, are a water-swollen network of cross-linked polymer chains.<sup>105</sup> Currently hydrogels are created from collagen, keratin, poly(vinyl alcohol) (PVA), poly(acrylic acid) (PAA), poly(lactide-co-glycolide) (PLG), just to name a few.<sup>102,105,106</sup> The creation of water-based, hydrophilic hydrogels has enabled researchers to create a biocompatible media, promoting healthy cell growth. However, the process involved with synthesizing these polymers is laborious and creates toxic byproducts.<sup>107-109</sup> To address these issues, some groups have created hydrogels using rSSp, yielding renewable biocompatible materials with novel properties. This was achieved when a small percentage of acid was combined with rSSp dopes. Within an hour, the solution would solidify into a hydrogel taking the form of the mold. Even with this advance, these hydrogels lack the mechanical properties necessary for certain applications such as a cartilage or bone replacement. Our group has applied a technique traditionally used for observation in a novel manner to address these issues.

### **Research Goals for Photo-initiated Cross-linking of rSSp Materials**

Photo-induced cross-linking of unmodified proteins, or PICUP, is traditionally used to observe protein-to-protein interactions. This reaction requires the proteins, tris(2,2'-bipyridyl) dichlororuthenium(II) hexahydrate (ruthenium), ammonium persulfate, and a

high-intensity light source.<sup>110</sup> These protein interactions are initiated when the sample is irradiated for an extended period of time and a direct carbon-to-carbon bond forms between tyrosines, producing intra-molecular cross-linking. Employing this technique, our rSSp dopes will be modified to instantaneously cross-link, solidifying in the process. Preliminary experiments with a 1000w flashlight have been able to enhance the mechanical properties of our cross-linked hydrogels by a factor of 4, expanding the use of our materials to a possible cartilage or bone replacement.

Our group has created the Cross-link Initiating Photo-diode, or CLIP — a high-intensity light source designed for maximum cross-linking to efficiently drive the intra-molecular cross-linking within our rSSp materials. The CLIP and our methods will force the reaction to become instantaneous, generating novel biomaterials. This will enable us to create shapes by “3D printing” rSSp materials instead of being confined to a mold. The cross-linking rSSp dopes will yield hydrogels, foams, sponges, and adhesives that can be activated with the CLIP to crosslink the rSSp material into a robust and stable form. These materials will be studied for their mechanical properties, ability to be functionalized, and in appropriate cases, their protein structure. The techniques and results for these experiments are presented in Chapter 3- Enhancing Spider-silk Protein Materials through Photo-Initiated Cross-linking.

## References

- (1) Lefèvre, T.; Leclerc, J.; Rioux-Dubé, J.-F.; Buffeteau, T.; Paquin, M.-C.; Rousseau, M.-E.; Cloutier, I.; Auger, M.; Gagné, S. M.; Boudreault, S.; et al. Conformation of Spider Silk Proteins In Situ in the Intact Major Ampullate Gland and in Solution. *Biomacromolecules* **2007**, *8* (8), 2342–2344.
- (2) Hayashi, C. Y.; Shipley, N. H.; Lewis, R. V. Hypotheses That Correlate the Sequence, Structure, and Mechanical Properties of Spider Silk Proteins. *Int. J. Biol. Macromol.* **1999**, *24* (2–3), 271–275.
- (3) Richter, G. M. A. Silk in Greece. *Am. J. Archaeol.* **1929**, *33* (1), 27–33.
- (4) Lewis, R. Unraveling the Weave of Spider Silk. *BioScience* **1996**, *46* (9), 636–638.
- (5) Leal-Egaña Aldo; Scheibel Thomas. Silk-based Materials for Biomedical Applications. *Biotechnol. Appl. Biochem.* **2010**, *55* (3), 155–167.
- (6) Daszkiewicz, P. René Antoine Ferchault de Réaumur (1683–1757), a Naturalist and Pioneer of Acarology and His Contacts with Poland. *Biol. Lett.* **2016**, *53* (1), 9–17.
- (7) Egerton, F. N. A History of the Ecological Sciences, Part 21: Réaumur and His History of Insects. *Bull. Ecol. Soc. Am.* **2006**, *87* (3), 212–224.
- (8) Berenbaum, M. R. Spin Control. *Sci. N. Y.* **1995**, *35* (5), 13.
- (9) Kaplan, D.; Adams, W. W.; Farmer, B.; Viney, C. Silk: Biology, Structure, Properties, and Genetics. In *Silk Polymers*; ACS Symposium Series; American Chemical Society, 1993; Vol. 544, pp 2–16.
- (10) Adrianos, S. L.; Teulé, F.; Hinman, M. B.; Jones, J. A.; Weber, W. S.; Yarger, J. L.; Lewis, R. V. Nephila Clavipes Flagelliform Silk-Like GGX Motifs Contribute to Extensibility and Spacer Motifs Contribute to Strength in Synthetic Spider Silk Fibers. *Biomacromolecules* **2013**, *14* (6), 1751–1760.
- (11) Vollrath, F. Spider Webs and Silks. *Sci. Am.* **1992**, *266* (3), 70–76.
- (12) Xu, M.; Lewis, R. V. Structure of a Protein Superfiber: Spider Dragline Silk. *Proc. Natl. Acad. Sci.* **1990**, *87* (18), 7120–7124.
- (13) Hinman, M. B.; Lewis, R. V. Isolation of a Clone Encoding a Second Dragline Silk Fibroin. Nephila Clavipes Dragline Silk Is a Two-Protein Fiber. *J. Biol. Chem.* **1992**, *267* (27), 19320–19324.
- (14) Eisoldt, L.; Thamm, C.; Scheibel, T. *Review: The Role of Terminal Domains during Storage and Assembly of Spider Silk Proteins*; 2012; Vol. 97.
- (15) Humenik, M.; Scheibel, T.; Smith, A. Spider Silk: Understanding the Structure–Function Relationship of a Natural Fiber. In *Progress in Molecular Biology and Translational Science*; Howorka, S., Ed.; Molecular Assembly in Natural and Engineered Systems; Academic Press, 2011; Vol. 103, pp 131–185.
- (16) Kronqvist, N.; Sarr, M.; Lindqvist, A.; Nordling, K.; Otikovs, M.; Venturi, L.; Pioselli, B.; Purhonen, P.; Landreh, M.; Biverstål, H.; et al. Efficient Protein Production Inspired by How Spiders Make Silk. *Nat. Commun.* **2017**, *8*, 15504.
- (17) Tokareva, O.; Jacobsen, M.; Buehler, M.; Wong, J.; Kaplan, D. L. Structure-Function-Property-Design Interplay in Biopolymers: Spider Silk. *Acta Biomater.* **2014**, *10* (4), 1612–1626.
- (18) Vollrath, F.; Knight, D. P. Structure and Function of the Silk Production Pathway in the Spider Nephila Edulis. *Int. J. Biol. Macromol.* **1999**, *24* (2), 243–249.

- (19) Vollrath, F.; Knight, D. P. Liquid Crystalline Spinning of Spider Silk. *Nature* **2001**, *410* (6828), 541–548.
- (20) Coe, J. V.; Nystrom, S. V.; Chen, Z.; Li, R.; Verreault, D.; Hitchcock, C. L.; Martin, E. W.; Allen, H. C. Extracting Infrared Spectra of Protein Secondary Structures Using a Library of Protein Spectra and the Ramachandran Plot. *J. Phys. Chem. B* **2015**, *119* (41), 13079–13092.
- (21) Lewis, R. V.; Xu, M.; Hinman, M. B. Spider Silk Protein. US5728810 A, March 17, 1998.
- (22) Work, R. W.; Morosoff, N. A Physico-Chemical Study of the Supercontraction of Spider Major Ampullate Silk Fibers. *Text. Res. J.* **1982**, *52* (5), 349–356.
- (23) Tillinghast, E. K.; Christenson, T. Observations on the Chemical Composition of the Web of *Nephila Clavipes* (Araneae, Araneidae). *J. Arachnol.* **1984**, *12* (1), 69–74.
- (24) Work, R. W.; Young, C. T. The Amino Acid Compositions of Major and Minor Ampullate Silks of Certain Orb-Web-Building Spiders (Araneae, Araneidae). *J. Arachnol.* **1987**, *15* (1), 65–80.
- (25) Kümmerlen, J.; van Beek, J. D.; Vollrath, F.; Meier, B. H. Local Structure in Spider Dragline Silk Investigated by Two-Dimensional Spin-Diffusion Nuclear Magnetic Resonance†. *Macromolecules* **1996**, *29* (8), 2920–2928.
- (26) Parkhe, A. D.; Seeley, S. K.; Gardner, K.; Thompson, L.; Lewis, R. V. Structural Studies of Spider Silk Proteins in the Fiber. *J. Mol. Recognit.* **1997**, *10* (1), 1–6.
- (27) Simmons, A.; Ray, E.; Jelinski, L. W. Solid-State <sup>13</sup>C NMR of *Nephila Clavipes* Dragline Silk Establishes Structure and Identity of Crystalline Regions. *Macromolecules* **1994**, *27* (18), 5235–5237.
- (28) Simmons, A. H.; Michal, C. A.; Jelinski, L. W. Molecular Orientation and Two-Component Nature of the Crystalline Fraction of Spider Dragline Silk. *Science* **1996**, *271* (5245), 84–87.
- (29) Jenkins, J. E.; Creager, M. S.; Lewis, R. V.; Holland, G. P.; Yarger, J. L. Quantitative Correlation between the Protein Primary Sequences and Secondary Structures in Spider Dragline Silks. *Biomacromolecules* **2010**, *11* (1), 192–200.
- (30) Jenkins, J. E.; Creager, M. S.; Butler, E. B.; Lewis, R. V.; Yarger, J. L.; Holland, G. P. Solid-State NMR Evidence for Elastin-like  $\beta$ -Turn Structure in Spider Dragline Silk. *Chem. Commun.* **2010**, *46* (36), 6714–6716.
- (31) Hronska, M.; van Beek, J. D.; Williamson, P. T. F.; Vollrath, F.; Meier, B. H. NMR Characterization of Native Liquid Spider Dragline Silk from *Nephila Edulis*. *Biomacromolecules* **2004**, *5* (3), 834–839.
- (32) Hijirida, D. H.; Do, K. G.; Michal, C.; Wong, S.; Zax, D.; Jelinski, L. W. <sup>13</sup>C NMR of *Nephila Clavipes* Major Ampullate Silk Gland. *Biophys. J.* **1996**, *71* (6), 3442–3447.
- (33) Holland, G. P.; Jenkins, J. E.; Creager, M. S.; Lewis, R. V.; Yarger, J. L. Quantifying the Fraction of Glycine and Alanine in  $\beta$ -Sheet and Helical Conformations in Spider Dragline Silk Using Solid-State NMR. *Chem. Commun. Camb. Engl.* **2008**, No. 43, 5568–5570.
- (34) Ling, S.; Qi, Z.; Knight, D. P.; Shao, Z.; Chen, X. Synchrotron FTIR Microspectroscopy of Single Natural Silk Fibers. *Biomacromolecules* **2011**, *12* (9), 3344–3349.
- (35) Papadopoulos, P.; Sölter, J.; Kremer, F. Structure-Property Relationships in Major Ampullate Spider Silk as Deduced from Polarized FTIR Spectroscopy. *Eur. Phys. J. E* **2007**, *24* (2), 193–199.
- (36) Van Nimmen, E.; De Clerck, K.; Verschuren, J.; Gellynck, K.; Gheysens, T.; Mertens, J.; Van Langenhove, L. FT-IR Spectroscopy of Spider and Silkworm Silks: Part I. Different

- Sampling Techniques. *Vib. Spectrosc.* **2008**, *46* (1), 63–68.
- (37) Sampath, S.; Isdebski, T.; Jenkins, J. E.; Ayon, J. V.; Henning, R. W.; Orgel, J. P. R. O.; Antipoa, O.; Yarger, J. L. X-Ray Diffraction Study of Nanocrystalline and Amorphous Structure within Major and Minor Ampullate Dragline Spider Silks. *Soft Matter* **2012**, *8* (25), 6713–6722.
- (38) Riekkel, C.; Bränden, C.; Craig, C.; Ferrero, C.; Heidelbach, F.; Müller, M. Aspects of X-Ray Diffraction on Single Spider Fibers. *Int. J. Biol. Macromol.* **1999**, *24* (2–3), 179–186.
- (39) Riekkel, C.; Vollrath, F. Spider Silk Fibre Extrusion: Combined Wide- and Small-Angle X-Ray Microdiffraction Experiments. *Int. J. Biol. Macromol.* **2001**, *29* (3), 203–210.
- (40) Riekkel, C.; Madsen, B.; Knight, D.; Vollrath, F. X-Ray Diffraction on Spider Silk during Controlled Extrusion under a Synchrotron Radiation X-Ray Beam. *Biomacromolecules* **2000**, *1* (4), 622–626.
- (41) Lefèvre, T.; Paquet-Mercier, F.; Rioux-Dubé, J.-F.; Pézolet, M. Structure of Silk by Raman Spectromicroscopy: From the Spinning Glands to the Fibers. *Biopolymers* **2012**, *97* (6), 322–336.
- (42) Lefèvre, T.; Rousseau, M.-E.; Pézolet, M. Protein Secondary Structure and Orientation in Silk as Revealed by Raman Spectromicroscopy. *Biophys. J.* **2007**, *92* (8), 2885–2895.
- (43) Lewis, R. V. Spider Silk: Ancient Ideas for New Biomaterials. *Chem. Rev.* **2006**, *106* (9), 3762–3774.
- (44) Holland, G. P.; Creager, M. S.; Jenkins, J. E.; Lewis, R. V.; Yarger, J. L. Determining Secondary Structure in Spider Dragline Silk by Carbon–Carbon Correlation Solid-State NMR Spectroscopy. *J. Am. Chem. Soc.* **2008**, *130* (30), 9871–9877.
- (45) Gosline, J. M.; Guerette, P. A.; Ortlepp, C. S.; Savage, K. N. The Mechanical Design of Spider Silks: From Fibroin Sequence to Mechanical Function. *J. Exp. Biol.* **1999**, *202* (23), 3295–3303.
- (46) Work, R. W. Mechanisms of Major Ampullate Silk Fiber Formation by Orb-Web-Spinning Spiders. *Trans. Am. Microsc. Soc.* **1977**, *96* (2), 170–189.
- (47) Shao, Z.; Vollrath, F.; Yang, Y.; Thøgersen, H. C. Structure and Behavior of Regenerated Spider Silk. *Macromolecules* **2003**, *36* (4), 1157–1161.
- (48) Colgin, M. A.; Lewis, R. V. Spider Minor Ampullate Silk Proteins Contain New Repetitive Sequences and Highly Conserved Non-Silk-like “Spacer Regions.” *Protein Sci.* **1998**, *7* (3), 667–672.
- (49) Lewis, R. V. Spider Silk: The Unraveling of a Mystery. *Acc. Chem. Res.* **1992**, *25* (9), 392–398.
- (50) Eisoldt, L.; Thamm, C.; Scheibel, T. The Role of Terminal Domains during Storage and Assembly of Spider Silk Proteins. *Biopolymers* **2012**, *97* (6), 355–361.
- (51) Motriuk-Smith, D.; Smith, A.; Hayashi, C. Y.; Lewis, R. V. Analysis of the Conserved N-Terminal Domains in Major Ampullate Spider Silk Proteins. *Biomacromolecules* **2005**, *6* (6), 3152–3159.
- (52) Hayashi, C. Y.; Lewis, R. V. Evidence from Flagelliform Silk cDNA for the Structural Basis of Elasticity and Modular Nature of Spider Silks. *J. Mol. Biol.* **1998**, *275* (5), 773–784.
- (53) Hayashi, C. Y.; Lewis, R. V. Spider Flagelliform Silk: Lessons in Protein Design, Gene Structure, and Molecular Evolution. *BioEssays News Rev. Mol. Cell. Dev. Biol.* **2001**, *23* (8), 750–756.
- (54) Teulé, F.; Cooper, A. R.; Furin, W. A.; Bittencourt, D.; Rech, E. L.; Brooks, A.; Lewis, R. V. A Protocol for the Production of Recombinant Spider Silk-like Proteins for Artificial Fiber

- Spinning. *Nat. Protoc.* **2009**, *4* (3), 341–355.
- (55) Teulé, F.; Addison, B.; Cooper, A. R.; Ayon, J.; Henning, R. W.; Benmore, C. J.; Holland, G. P.; Yarger, J. L.; Lewis, R. V. Combining Flagelliform and Dragline Spider Silk Motifs to Produce Tunable Synthetic Biopolymer Fibers. *Biopolymers* **2012**, *97* (6), 418–431.
- (56) Lewis, R. V.; Hinman, M.; Kothakota, S.; Fournier, M. J. Expression and Purification of a Spider Silk Protein: A New Strategy for Producing Repetitive Proteins. *Protein Expr. Purif.* **1996**, *7* (4), 400–406.
- (57) Exler, J. H.; Hümmerich, D.; Scheibel, T. The Amphiphilic Properties of Spider Silks Are Important for Spinning. *Angew. Chem. Int. Ed.* **2007**, *46* (19), 3559–3562.
- (58) Hinman, M. B.; Jones, J. A.; Lewis, R. V. Synthetic Spider Silk: A Modular Fiber. *Trends Biotechnol.* **2000**, *18* (9), 374–379.
- (59) Prince, J. T.; McGrath, K. P.; DiGirolamo, C. M.; Kaplan, D. L. Construction, Cloning, and Expression of Synthetic Genes Encoding Spider Dragline Silk. *Biochemistry (Mosc.)* **1995**, *34* (34), 10879–10885.
- (60) Huemmerich, D.; Scheibel, T.; Vollrath, F.; Cohen, S.; Gat, U.; Ittah, S. Novel Assembly Properties of Recombinant Spider Dragline Silk Proteins. *Curr. Biol.* **2004**, *14* (22), 2070–2074.
- (61) Fahnstock, S. R.; Bedzyk, L. A. Production of Synthetic Spider Dragline Silk Protein in *Pichia Pastoris*. *Appl. Microbiol. Biotechnol.* **1997**, *47* (1), 33–39.
- (62) Lazaris, A.; Arcidiacono, S.; Huang, Y.; Zhou, J.-F.; Duguay, F.; Chretien, N.; Welsh, E. A.; Soares, J. W.; Karatzas, C. N. Spider Silk Fibers Spun from Soluble Recombinant Silk Produced in Mammalian Cells. *Science* **2002**, *295* (5554), 472–476.
- (63) Teule, F.; Miao, Y.; Sohn, B.; Kim, Y.; Hull, J.; Fraser, M. J.; Lewis, R. V.; Jarvis, D. Silkworms Transformed with Chimeric Silkworm/Spider Silk Genes Spin Composite Silk Fibers with Improved Mechanical Properties. *Proc. Natl. Acad. Sci. USA* **2012**, *109* (3), 923.8.
- (64) Scheller, J.; Gührs, K.-H.; Grosse, F.; Conrad, U. Production of Spider Silk Proteins in Tobacco and Potato. *Nat. Biotechnol.* **2001**, *19* (6), 573–577.
- (65) Tucker, C. L.; Jones, J. A.; Bringham, H. N.; Copeland, C. G.; Addison, J. B.; Weber, W. S.; Mou, Q.; Yarger, J. L.; Lewis, R. V. Mechanical and Physical Properties of Recombinant Spider Silk Films Using Organic and Aqueous Solvents. *Biomacromolecules* **2014**, *15* (8), 3158–3170.
- (66) Jones, J. A.; Harris, T. I.; Tucker, C. L.; Berg, K. R.; Christy, S. Y.; Day, B. A.; Gaztambide, D. A.; Needham, N. J. C.; Ruben, A. L.; Oliveira, P. F.; et al. More Than Just Fibers: An Aqueous Method for the Production of Innovative Recombinant Spider Silk Protein Materials. *Biomacromolecules* **2015**.
- (67) Altman, G. H.; Diaz, F.; Jakuba, C.; Calabro, T.; Horan, R. L.; Chen, J.; Lu, H.; Richmond, J.; Kaplan, D. L. Silk-Based Biomaterials. *Biomaterials* **2003**, *24* (3), 401–416.
- (68) Dams-Kozłowska, H.; Majer, A.; Tomasiewicz, P.; Lozinska, J.; Kaplan, D. L.; Mackiewicz, A. Purification and Cytotoxicity of Tag-Free Bioengineered Spider Silk Proteins. *J. Biomed. Mater. Res.* **2013**, *101* (2), 456–464.
- (69) An, B.; Hinman, M. B.; Holland, G. P.; Yarger, J. L.; Lewis, R. V. Inducing  $\beta$ -Sheets Formation in Synthetic Spider Silk Fibers by Aqueous Post-Spin Stretching. *Biomacromolecules* **2011**, *12* (6), 2375–2381.
- (70) Seidel, A.; Liivak, O.; Calve, S.; Adaska, J.; Ji, G.; Yang, Z.; Grubb, D.; Zax, D. B.; Jelinski, L. W. Regenerated Spider Silk: Processing, Properties, and Structure. *Macromolecules*



- 2000**, 33 (3), 775–780.
- (71) Gilbert, W.; Mottelay, P. F.; Wright, E. *William Gilbert of Colchester, Physician of London, On the Load Stone and Magnetic Bodies, ...*; [New York, J. Wiley & Sons, 1893.
- (72) Boys, C. V. On the Production, Properties, and Some Suggested Uses of the Finest Threads. *Proc. Phys. Soc. Lond.* **1887**, 9 (1), 8.
- (73) Tucker, N.; Stanger, J.; Staiger, M.; Razzaq, H.; Hofman, K. The History of the Science and Technology of Electrospinning from 1600 to 1995. *J. Eng. Fibers Fabr.* **2012**, 7.
- (74) Taylor, S. G.; S, F. R. Disintegration of Water Drops in an Electric Field. *Proc R Soc Lond A* **1964**, 280 (1382), 383–397.
- (75) Doshi, J.; Reneker, D. H. Electrospinning Process and Applications of Electrospun Fibers. *J. Electrostat.* **1995**, 35 (2), 151–160.
- (76) Filatov, Y.; Budyka, A.; Kirichenko, V. *Electrospinning of Micro-and Nanofibers: Fundamentals and Applications in Separation and Filtration Processes*; Begell House: New York, 2007.
- (77) Persano, L.; Camposeo, A.; Tekmen, C.; Pisignano, D. Industrial Upscaling of Electrospinning and Applications of Polymer Nanofibers: A Review. *Macromol. Mater. Eng.* **2013**, 298 (5), 504–520.
- (78) Dotti, F.; Varesano, A.; Montarsolo, A.; Aluigi, A.; Tonin, C.; Mazzuchetti, G. Electrospun Porous Mats for High Efficiency Filtration. *J. Ind. Text.* **2007**, 37 (2), 151–162.
- (79) Bhardwaj, N.; Kundu, S. C. Electrospinning: A Fascinating Fiber Fabrication Technique. *Biotechnol. Adv.* **2010**, 28 (3), 325–347.
- (80) Wang, M.; Jin, H.-J.; Kaplan, D. L.; Rutledge, G. C. Mechanical Properties of Electrospun Silk Fibers. *Macromolecules* **2004**, 37 (18), 6856–6864.
- (81) Kim, J.; Reneker, D. H. Mechanical Properties of Composites Using Ultrafine Electrospun Fibers. *Polym. Compos.* **1999**, 20 (1), 124–131.
- (82) Wong, S.-C.; Baji, A.; Leng, S. Effect of Fiber Diameter on Tensile Properties of Electrospun Poly( $\epsilon$ -Caprolactone). *Polymer* **2008**, 49 (21), 4713–4722.
- (83) Mazinani, S.; Aiji, A.; Dubois, C. Morphology, Structure and Properties of Conductive PS/CNT Nanocomposite Electrospun Mat. *Polymer* **2009**, 50 (14), 3329–3342.
- (84) Cardwell, R. D.; Dahlgren, L. A.; Goldstein, A. S. Electrospun Fibre Diameter, Not Alignment, Affects Mesenchymal Stem Cell Differentiation into the Tendon/Ligament Lineage. *J. Tissue Eng. Regen. Med.* **2014**, 8 (12), 937–945.
- (85) Katta, P.; Alessandro, M.; Ramsier, R. D.; Chase, G. G. Continuous Electrospinning of Aligned Polymer Nanofibers onto a Wire Drum Collector. *Nano Lett.* **2004**, 4 (11), 2215–2218.
- (86) Huang, C.; Niu, H.; Wu, C.; Ke, Q.; Mo, X.; Lin, T. Disc-Electrospun Cellulose Acetate Butyrate Nanofibers Show Enhanced Cellular Growth Performances. *J. Biomed. Mater. Res. A* **2013**, 101 (1), 115–122.
- (87) Kartikowati, C. W.; Suhendi, A.; Zulhijah, R.; Ogi, T.; Iwaki, T.; Okuyama, K. Preparation and Evaluation of Magnetic Nanocomposite Fibers Containing  $\alpha$ -Fe<sub>16</sub>N<sub>2</sub> and  $\alpha$ -Fe Nanoparticles in Polyvinylpyrrolidone via Magneto-Electrospinning. *Nanotechnology* **2016**, 27 (2), 025601.
- (88) Teo, W.-E.; Gopal, R.; Ramaseshan, R.; Fujihara, K.; Ramakrishna, S. A Dynamic Liquid Support System for Continuous Electrospun Yarn Fabrication. *Polymer* **2007**, 48 (12), 3400–3405.
- (89) Ali, U.; Zhou, Y.; Wang, X.; Lin, T. Direct Electrospinning of Highly Twisted, Continuous

- Nanofiber Yarns. *J. Text. Inst.* **2012**, *103* (1), 80–88.
- (90) Zhang, X.; Reagan, M. R.; Kaplan, D. L. Electrospun Silk Biomaterial Scaffolds for Regenerative Medicine. *Adv. Drug Deliv. Rev.* **2009**, *61* (12), 988–1006.
- (91) Zarkoob, S.; Eby, R. .; Reneker, D. H.; Hudson, S. D.; Ertley, D.; Adams, W. W. Structure and Morphology of Electrospun Silk Nanofibers. *Polymer* **2004**, *45* (11), 3973–3977.
- (92) Amiraliyan, N.; Nouri, M.; Kish, M. H. Structural Characterization and Mechanical Properties of Electrospun Silk Fibroin Nanofiber Mats. *Polym. Sci. Ser. A* **2010**, *52* (4), 407–412.
- (93) Meechaisue, C.; Wutticharoenmongkol, P.; Waraput, R.; Huangjing, T.; Ketbumrung, N.; Pavasant, P.; Supaphol, P. Preparation of Electrospun Silk Fibroin Fiber Mats as Bone Scaffolds: A Preliminary Study. *Biomed. Mater. Bristol Engl.* **2007**, *2*, 181–188.
- (94) Wei, K.; Kim, B.-S.; Kim, I.-S. Fabrication and Biocompatibility of Electrospun Silk Biocomposites. *Membranes* **2011**, *1* (4), 275–298.
- (95) Das, S.; Sharma, M.; Saharia, D.; Sarma, K.; Muir, E.; Bora, U. Electrospun Silk-Polyaniline Conduits for Functional Nerve Regeneration in Rat Sciatic Nerve Injury Model. *Biomed. Mater. Bristol Engl.* **2017**.
- (96) Kim, U.-J.; Park, J.; Li, C.; Jin, H.-J.; Valluzzi, R.; Kaplan, D. L. Structure and Properties of Silk Hydrogels. *Biomacromolecules* **2004**, *5* (3), 786–792.
- (97) Hardy, J. G.; Romer, L. M.; Scheibel, T. R. Polymeric Materials Based on Silk Proteins. *Polymer* **2008**, *49*, 4309–4327.
- (98) Vepari, C.; Kaplan, D. L. Silk as a Biomaterial. *Prog. Polym. Sci.* **2007**, *32* (8), 991–1007.
- (99) Kundu, B.; Kurland, N. E.; Bano, S.; Patra, C.; Engel, F. B.; Yadavalli, V. K.; Kundu, S. C. Silk Proteins for Biomedical Applications: Bioengineering Perspectives. *Prog. Polym. Sci.* **2014**, *39* (2), 251–267.
- (100) Hardy, J. G.; Scheibel, T. R. Composite Materials Based on Silk Proteins. *Prog. Polym. Sci.* **2010**, *35* (9), 1093–1115.
- (101) Lee, K. Y.; Mooney, D. J. Hydrogels for Tissue Engineering. *Chem. Rev.* **2001**, *101* (7), 1869–1880.
- (102) Drury, J. L.; Mooney, D. J. Hydrogels for Tissue Engineering: Scaffold Design Variables and Applications. *Biomaterials* **2003**, *24* (24), 4337–4351.
- (103) Nguyen, K. T.; West, J. L. Photopolymerizable Hydrogels for Tissue Engineering Applications. *Biomaterials* **2002**, *23* (22), 4307–4314.
- (104) Khademhosseini, A.; Langer, R. Microengineered Hydrogels for Tissue Engineering. *Biomaterials* **2007**, *28* (34), 5087–5092.
- (105) Anseth, K. S.; Bowman, C. N.; Brannon-Peppas, L. Mechanical Properties of Hydrogels and Their Experimental Determination. *Biomaterials* **1996**, *17* (17), 1647–1657.
- (106) Tabata, Y.; Miyao, M.; Ozeki, M.; Ikada, Y. Controlled Release of Vascular Endothelial Growth Factor by Use of Collagen Hydrogels. *J. Biomater. Sci. Polym. Ed.* **2000**, *11* (9), 915–930.
- (107) Lyoo, W.; Lee, H. Synthesis of High-Molecular-Weight Poly(Vinyl Alcohol) with High Yield by Novel One-Batch Suspension Polymerization of Vinyl Acetate and Saponification. *Colloid Polym. Sci.* **2002**, *280* (9), 835–840.
- (108) Jikei, M.; Suga, T.; Yamadoi, Y.; Matsumoto, K. Synthesis and Properties of Poly(L-Lactide-Co-Glycolide)-b-Poly( $\epsilon$ -Caprolactone) Multiblock Copolymers Formed by Self-Polycondensation of Diblock Macromonomers. *Polym. J.* **2017**, *49* (4), 369–375.

- (109) Lee, B. P.; Dalsin, J. L.; Messersmith, P. B. Synthesis and Gelation of DOPA-Modified Poly(Ethylene Glycol) Hydrogels. *Biomacromolecules* **2002**, 3 (5), 1038–1047.
- (110) Preston, G. W.; Wilson, A. J. Photo-Induced Covalent Cross-Linking for the Analysis of Biomolecular Interactions. *Chem. Soc. Rev.* **2013**, 42 (8), 3289–3301.

## CHAPTER II

CONTINUOUS ELECTROSPINNING OF SPIDER SILK PROTEINS CREATES  
NANOFIBER YARNS WITH UNPRECEDENTED PROPERTIES

Co-Authors include: Bailey McFarland, Blake Taurone, Thomas I. Harris, Justin A. Jones, and Randy V. Lewis

## ABSTRACT

Traditional means of creating fibers from recombinant spider silk proteins (rSSp) have produced materials with properties that don't measure up to their natural counterpart (200 MPa versus 4,000 MPa). To address this, our laboratory has used a novel method of producing rSSp yarns composed of nanofibers known as electrospinning. By decreasing the fiber diameter of spider silk yarn, the number of stress focal points it contains decreases and thus, the mechanical properties increase. This method employs a large electrical field to create fibers from polymer or protein solutions when an elongation factor is initiated. This, in turn, increases the self-assembly of polymers, known as the chain entanglement property<sup>1</sup>, and initiates the formation of nanofibers that can be collected. Unfortunately, traditional electrospinning cannot create continuous products because current targets are limited in size. Our group has modified our electrospinner to be able to produce continuous yarns comprised of several hundred rSSp nanofibers (approximately 300-500). This continuous yarn is then reeled outside of the electrospinner and collected onto a spindle for post-processing, further enhancing the mechanical properties of the material. Using this technique, we have produced rSSp multi-nanofiber yarns with a stress of 3548 MPa and a diameter of 14  $\mu\text{m}$ .

## Introduction

Synthetic polymers such as Kevlar (max stress of 3600 MPa and max elongation of 2.4%)<sup>2</sup> are unmatched in mechanical properties when compared to natural materials, except for one. Spider silk has the potential to surpass the maximum stress and elongation of any other material known because of the protein structures found in the material. The mechanical properties range from absorbing massive amounts of stress (up to 4000 MPa) to extending 300% the original length before failure.<sup>2</sup> The structures within spider silk possess remarkable mechanical properties, as well as biocompatibility. For these reasons, spider silk has attracted the attention of the scientific community and the media. In nature, spiders are capable of producing up to six silk types and one glue that cover a wide range of mechanical properties, as each silk is designed for a specialized function. Unfortunately, it is relatively impossible to farm spiders for silk, forcing researchers to search for another method of attaining viable amounts of spider silk.

Currently, the main technique for creating synthetic spider silk is known as wet spinning. During this process, recombinant spider silk proteins are solubilized into a solution known as a dope. This is ejected into an alcohol bath, producing up to 8 fibers with diameters approaching those of natural silk. It was the goal of researchers to create synthetic spider silk fibers with mechanical properties close to the natural counterpart, eliminating the need to farm spiders. Unfortunately, these fibers possess decreased mechanical properties (200 MPa)<sup>3</sup>, possibly due to the truncated spider silk protein size (natural silk is 250 kDa while synthetic rSSp are 120 kDa) and to post-treatments of the material. To address the issue of performance, researchers have employed a novel technique used to create nanofibers out of recombinant spider silk proteins known as

electrospinning. Several groups have demonstrated successful electrospinning of silk proteins -- spider and *Bombyx mori*-- using HFIP as the solvent.

The ability of electrospinning to increase mechanical properties is based on the diameter of the fibers created. Fibers fail due to imperfections such as diameter inconsistencies or knots that become stress focal points. As the diameter decreases, so do the number of stress focal points enabling the fiber to distribute stress uniformly along its entire length and thus enhance its mechanical properties. During electrospinning of polymers and proteins, hundreds of nanofibers collect together to form a material that is dense yet porous due to its structure. For this reason, electrospun nanofibers have become the focus of material engineering due to their large surface area and superb mechanical properties. Electrospinning traditionally creates a “Taylor cone” of nanofibers collecting to form a mat, which is typically used for filtration purposes or processed into yarns.

To address the issue, our research group has employed the techniques developed by Deakin University<sup>4</sup> to modify the iMe electrospinner to create continuous electrospun yarns. Using rSSp to electrospin multi-nanofiber yarns, the resulting material and chemical properties will be applicable to the industrial, commercial, and medical settings. These multi-nanofiber yarns will possess impressive mechanical properties and biocompatibility similar to spider silk proteins. Decreasing the diameter of spider silk fibers and collecting them into a highly twisted yarn will result in mechanical properties surpassing those of natural silk, creating a novel material. The techniques and results for these experiments are presented below.

## **Methods and Materials**

### **Protein Purification**

Recombinant spider silk proteins (rSSp) were produced in the milk of genetically modified goats in *E.coli* as described in previous work.<sup>5-7</sup> The milk containing the rSSp was purified via tangential flow and lyophilization as described by Tucker et al.<sup>8</sup> A list of all the proteins used in these experiments is given in Table 2.1.

### **Preparation of Aqueous Electrospinning Dopes**

Several concentrations of aqueous-based rSSp dopes derived from goats and bacteria<sup>5-7</sup> were created for continuous electrospinning (Table 2.2). Aqueous dopes for fiber formation were created, as described in Jones et al.,<sup>9</sup> utilizing heat and pressure to solubilize the proteins. The dry weight of the proteins was measured into a vial, and the cap was tightened onto the vial and vortexed at maximum using a VWR Analog Vortex Mixer to ensure homogeneity of the components. Three milliliters of nanopure water from a NANOpure Diamond™ were added to the vial, and the components were sonicated with an energy output of 3-5 J for 1.5 minutes using a QSONICA Sonicator. The suspension was then sealed and heated using a 1000 W Magic Chef microwave oven in five second intervals to prevent overheating. This process was repeated until the contents were completely solubilized or the bottom of the vial temperature was a minimum of 130° C, verified using a Fluke 561 IR thermometer.<sup>9</sup> The vial was removed from the microwave and allowed to cool to room temperature. Once at room temperature, the dope was loaded into a plastic 1 ml slip fit syringe purchased from Grainger (part number 309659), and the appropriate syringe tip was attached, securing the connection with at least three layers of

electrical tape. The composition of the dopes and results from electrospinning are shown in Table 2.2.

### **Increasing Probability of Nanofiber Formation from Aqueous Dopes**

Not all aqueous dopes are appropriate for electrospinning, resulting in no nanofiber formation. To address this, several additives and techniques were used to modify the aqueous dope's composition to increase the likelihood of successful electrospinning. Modifying the dopes was accomplished by changing the protein and/or polymer concentration to higher ratios, resulting in a more viscous solution, shown in Table 2.3. Dopes were placed on the bench top overnight, allowing for partial gelation to increase viscosity. Glycerol and trehalose purchased from Sigma Aldrich (part numbers G7757-1L and PHR 1344-500mg) were added to aqueous dopes in quantities ranging from 1% to 15%. The pH of dopes was decreased by adding 10-20  $\mu$ m 0.2% propionic acid, listed in Table 2.3. The pH of dopes was increased by adding (10-20  $\mu$ m) of 0.5 M ammonium hydroxide, listed in Table 2.3. The conductivity was increased by adding small amounts of (10-20  $\mu$ m) 30 nm gold nano particles purchased from Ted Pella, Inc (part number: 15706-20) or small amounts of 10-20 nm -OH functionalized multiwall carbon nanotubes purchased from US Research Nanomaterials, Inc (part number: 99685-96-8). The temperature of dopes were decreased by placing them in a 0°C refrigerator for two hours. Small amounts of isopropyl alcohol, ethanol, and methanol were added to aqueous dopes up to 13% w/v, increasing gelation. After modifications, these dopes were vortexed on a medium setting for 2 minutes using a VWR Analog Vortex Mixer, ensuring homogeneity of the components. These dopes were loaded into plastic 1 ml slip fit syringes. Varying diameter syringe tips purchased from Grainger were used during electrospinning ranging



from 19 G to 27 G (part numbers: 5FVK3, 5FVH7, 5FVH9, 5FVJ1, 5FVJ3, 5FVJ5, 5FVG9, 5FVJ7).

### **Preparation of Composite Electrospinning Dopes**

Several concentrations of composite rSSp dopes derived from goats or bacteria<sup>5-7</sup> were created for continuous electrospinning, shown in Table 2.4. Composite aqueous dopes for electrospinning were created, as described in Jones et al.,<sup>9</sup> utilizing heat and pressure to solubilize the proteins with modifications. All solid polymers were processed into a fine powder using a Coffee Grinder purchased from Bodum (part number: 10903). The first composite dope was created by combining 240 mg of processed Mowiol® 40-88 (Polyvinyl Alcohol)(PVA) purchased from Sigma-Aldrich (part number: 324590-100G), and 60 mg of rMaSp1 (dry weight) into an 8 ml glass culture vial with a rubber-lined cap purchased from Wheaton (part number: 1615870), for a final concentration of 8% Mowiol and 2% MaSp1 (total 10% w/v). The cap was tightened onto the vial and vortexed vigorously using a VWR Analog Vortex Mixer, ensuring homogeneity of the components. Three milliliters of Nanopure water from a NANOpure Diamond™ were added to the vial, and the components were sonicated with an energy output of 3-5 J for 1.5 minutes using a QSONICA Sonicator. The suspension was then sealed and heated using a 1000 W Magic Chef microwave oven in five-second intervals to prevent overheating. This process was repeated until the contents were completely solubilized or the bottom of the vial temperature was a minimum of 130° C, verified using a Fluke 561 IR thermometer.<sup>9</sup> The vial was removed from the microwave and allowed to cool to room temperature. Once at room temperature, the dope was loaded into a plastic 1 ml slip fit syringe. Other aqueous-

based composite dopes were prepared using the same method, replacing PVA with Poly(ethylene oxide) (PEO) purchased from Sigma Aldrich (part number: 182001-250G).

Nylon 6-6 with rSSp dopes were created by adding 150 mg of Nylon 6-6 purchased from Sigma Aldrich (part number: 429201-250G) and 150 mg of rMaSp1 into an 8 ml glass culture vial with a rubber-lined cap. 3 ml of 98% Formic Acid purchased from Sigma Aldrich (part number: A13285-2500g) was added to the vial to create a 10% (w/v) dope. The cap was tightened onto the vial and wrapped with parafilm. This was vortexed vigorously using a VWR Analog Vortex Mixer to ensure homogeneity of the components. The vial was placed into a Labnet Mini Labroller (part number: H5500) and allowed to rotate overnight on the bench top. The dope was loaded into a plastic 1 ml slip fit syringe and the appropriate syringe tip was attached, securing the connection with at least 3 layers of electrical tape. The composition of the dopes and results from electrospinning are shown in Table 2.4

### **Preparation of HFIP Electrospinning Dopes**

Several HFIP rSSp dopes were created for continuous electrospinning with HFIP ranging from 5%-25% w/v, shown in Table 2.5. These dopes were created using the protocol from various sources.<sup>6,10,11</sup> A dry weight of 168 mg rMaSp1 and 42 mg rMaSp2 were placed into an 8 ml glass vial, the cap was tightened and the contents were vortexed vigorously using a VWR Analog Vortex. Three ml of 1,1,1,3,3,3-hexafluoro-2-propanol (HFIP) was combined with the rSSp. The cap was tightened and wrapped using parafilm. This was vortexed vigorously using a VWR Analog Vortex Mixer. The vial was placed into a Labnet Mini Labroller and allowed to rotate overnight on the bench top. With proteins in solution, the dope was centrifuged overnight at 6000 rpm using a Corning LSE

compact centrifuge (part number: 306.00). The liquid portion was transferred to a new 8 ml vial and loaded into a 1 ml glass syringe purchased from Grainger (part number: 19G359). A 19 G metal syringe tip purchased from Grainger (part number: 0609) was placed on the glass syringe and wrapped with 4 layers of electrical tape. All steps were performed in the fume hood. The composition of the dopes and results from electrospinning are shown in Table 2.5.

### **Continuous Electrospinning of rSSp Dopes**

Dopes were loaded into 1 ml plastic syringes (HFIP in glass syringes) with their appropriate syringe tip. The syringe was mounted into an 11 Elite Nanomite syringe pump, and the syringe pump was placed into the custom anti-static housing (appendix B, Figure B1&B2). This was then placed into the chamber of the modified (appendix A) EC-DIG electrospinner purchased from iMe (part number: P12043). The syringe pump was then raised to the appropriate position (dependent on dope used) relative to the funnel. The positive electrode was connected to the syringe tip using an alligator clip purchased from Grainger (part number: 9WDM8). Power to the funnel was adjusted to 0.2 volts for aqueous/composite dopes and 0.17 volts for HFIP dopes, rotating the funnel at 500 rpm and 310 rpm respectively. The syringe pump was primed, and the flow rate was turned on. The voltage was adjusted and applied initiating the Taylor cone from the syringe tip. Once a fibrous web formed on the mouth of the funnel, the reeling guide was raised to 6.35 cm below the funnel. The fibrous web then connected to the reeling rod and was allowed to stabilize into an inverted fibrous cone (IFC). With rotation of the funnel, the IFC turned into a fine yarn and was wrapped around the rod. The reeling rod was then carefully pulled out of the guide tube, aligning the yarn on the pulley system, and taped onto the reel for

collection. The power supply to the reel was adjusted keeping tension on the continuously produced yarn to increase stability of the IFC. Below in Figure 2.1 is a schematic of the continuous electrospinning setup.

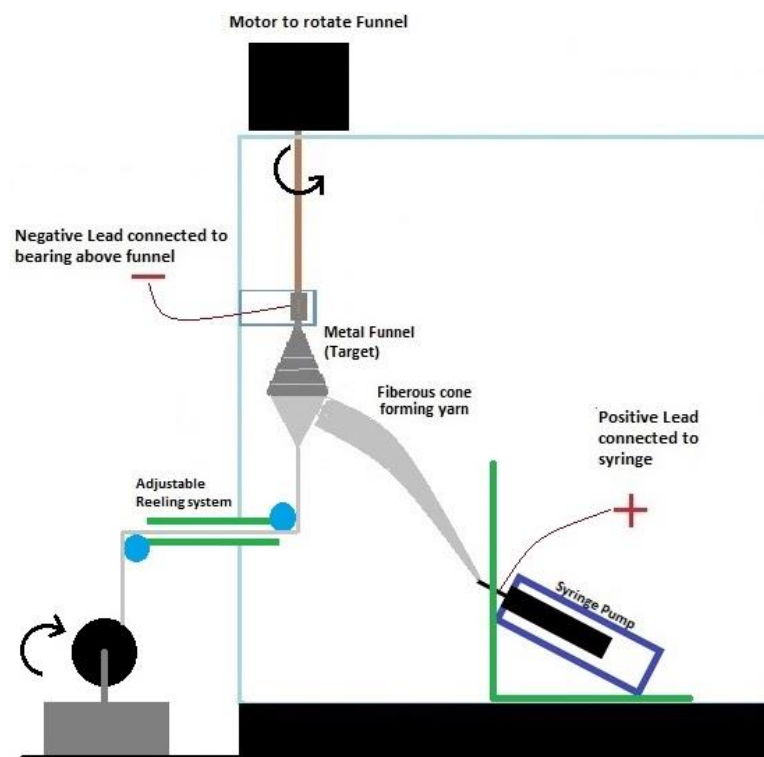


Figure 2.1: Continuous electrospinning setup

### Post-treatment of Continuous Electrospun Yarns

Samples were post-treated in varying concentrations of isopropyl alcohol (IPA), ethanol (EtOH), and methanol (MeOH) purchased from Pharmaco-AAPER, as shown in Table 2.6. During post-treatment, composite samples and HFIP samples were stretched from 1.2-1.5x their original length using a Pittsburgh 6 in. Digital Caliper purchased from Harbor Freight Tools (part number: 63731) These samples were then allowed to air dry and were placed into deionized water to assess if the yarns were water-insoluble.

## **Mechanical Testing of Continuous Electrospun Yarns**

Continuous electrospun yarns were carded on C-cards (38.5 cm x 26 cm) using scotch tape and super glue. The diameters were measured using a Motic BH 310 Digital microscope. A Synergie 100 MTS equipped with a 2 cm aluminum clamp and clip attached to a 10 N load cell were used to test the samples for tensile properties at a rate of 5 mm/min. The data was analyzed using Microsoft Excel. Best results are shown in Table 2.7

## **Novel Verification of Electrospun Spider silk Fibers**

An Azure Biosystems c200 gel imager using a wavelength of 302 nm was used to determine the presence of spider silk proteins in fiber form. Samples of powdered MaSp1, processed PVA, aqueous dopes, composite dopes, and HFIP dopes were placed on the stage, imaged and used as a control. Samples of electrospun PVA mats and yarns, composite rSSp mats and yarns, and HFIP rSSp yarns were placed onto the stage and imaged for verification of spider silk fibers created through electrospinning. The results can be seen in Table 2.8.

## **Results**

### **Polymers and rSSp for Continuous Electrospinning**

The goal of this research was to create continuous electrospun yarns from recombinant spider silk proteins, yielding materials with mechanical properties greater than or similar to those of natural spider silk.<sup>2</sup> By decreasing the diameter of fibers from microns to nanometers through continuous electrospinning, the mechanical properties of

rSSp fibers surpassed those of wet-spun rSSp fibers. Aqueous, composite, and HFIP dopes were created using proteins listed below in Table 2.1.

<b>Table 2.1- Polymers and rSSp Used for Electrospinning</b>	
<b>Protein</b>	<b>Ability to electrospin (0 worst- 5 best)</b>
PVA	5- quickly and readily forms fibers
PEO	4.5- readily forms fibers
rMaSp1	3.5- forms fibers at high concentrations
rMaSp2	2- occasionally forms fibers at high concentrations

Wet-spinning experiments of HFIP and aqueous-based rSSp<sup>10</sup> demonstrated that rMaSp1 and rMaSp2 (separately and combined), were capable of producing fibers with high stress and strain. For this reason, those proteins were used as the main components of electrospinning dopes. Two commonly used water-soluble polymers used in electrospinning were chosen to aid in the formation of nanofibers, PVA and PEO. At 10% (w/v), control dopes comprised only of the PVA or PEO readily make electrospun materials, which became our base concentration for composites (Table 2.4).

### **Electrospinning of Dopes (with and without additives)**

To assess the viability for each dope to make a continuous electrospun yarn, preliminary experiments utilized traditional techniques to collect the electrospun materials. This was accomplished by electrospinning onto a rotating drum. The goal was to create a

mat of rSSp nanofibers, pure or composite, that could be removed and assessed for post-treatment. Traditional means of producing viable fibers from HFIP or aqueous-based dopes are formed through wet-spinning. This is achieved when those dopes are loaded into a syringe with the tip submerged into an alcohol bath containing isopropyl alcohol (99%). As the dope exits the 0.01” orifice of the syringe, sheer stress is imparted on the proteins, inducing self-assembly into higher structures.<sup>12-15</sup> The IPA further induces beta-sheet formation causing the liquid dope to become a solid fiber.<sup>10</sup> Using this and the chain entanglement property seen with electrospinning, rSSp dopes should create materials composed of robust nanofibers.

The composition of aqueous based dopes and the results from electrospinning are shown in Table 2.2. Aqueous-based dopes ranging from 5%-25% (w/v) total protein content and varying rMaSp1/rMaSp2 ratios were tested. The concentrations of the dopes were varied because viscosity within a certain range is an essential parameter for successful electrospinning. Regardless of protein content, aqueous-based dopes were unable to form electrospun fibers. Above 18% (w/v) the target would be covered in droplets from the dope. Below that total protein content would result in a fine powder being formed with no fibers present.

Researchers use a number of techniques to aid solutions in electrospinning fibers. This is done by increasing the viscosity, adjusting the pH, and incorporating nanoparticles to increase the conductivity of the solution.<sup>1,16,17</sup> To increase the probability for aqueous-based dopes to form fibers through electrospinning, several additives were incorporated into the dopes (Table. 2.3). As stated above, wet-spinning employs a coagulation bath containing IPA to aid in the fiber maturation. Unfortunately, the large voltage used during

electrospinning makes it impossible to incorporate such a bath, which is a crucial step in wet-spinning. To compensate for this, we incorporated safe levels of three different alcohols into our aqueous dopes with the goal of inducing minor structural changes hypothesized to initiate self-assembly into fibers (Table 2.3). The effects of incorporating the alcohols into the dope were all similar. High levels (up to 13%) of methanol and ethanol would cause the protein to precipitate out of solution, becoming irreversible. IPA at this concentration would cause the dope to solidify, immediately becoming irreversible. None of these were eligible for electrospinning. At moderate levels (6%), all three alcohols would cause the dope to become more viscous, but over time it would solidify. When these were used to electrospin, only droplets would collect on the target with no fibers present. At low concentrations, all three alcohols had zero effect on the dopes. When electrospun, the results were the same — droplets collecting on the target with no fibers present.

To increase the viscosity of the dopes, glycerol and trehalose were incorporated in varying concentrations. At concentrations above 10%, the dope would not pass through the syringe tip due to the increased viscosity. When the viscosity was at an acceptable amount, 6% for glycerol and 8% for trehalose, droplets would collect on the target with no fibers formed. The same results were observed when aqueous dopes were refrigerated to increase viscosity.

Increasing the conductivity of solutions is hypothesized to further induce the chain entanglement property. To achieve this, gold nanoparticles and carbon nanotubes were incorporated at varying concentrations to aqueous-based dopes (Table 2.3). The effects of each concentration were the same: droplets would collect on the target and no fibers were produced.



Ammonium sulfate and propionic acid were used to raise and lower the pH of aqueous-based dopes. It has been observed that by altering the pH of dopes for wet-spinning, fibers would form from rSSp dopes that would not previously.<sup>10</sup> Regardless of the dope's protein concentration, when the pH of aqueous-based dopes was increased or decreased, the effect on electrospinning was the same. Only droplets would form and collect on the mat, with no fibers present.

From the experiments performed, it is hypothesized that aqueous-based dopes composed of only rSSp are incapable of creating electrospun fibers. For aqueous dopes to form fibers via wet-spinning, sheer stress and a coagulation bath are required. Without the ability to incorporate a coagulation bath into electrospinning, fibers cannot form via using aqueous-based dopes. The chain entanglement property is not enough to induce the self-assembly of spider silk proteins into fibers. To address this, our group utilized water-soluble polymers commonly used in electrospinning as a carrier for the rSSp to form fibers.

### **Electrospinning of Composite and HFIP Dopes**

PVA and PEO are commonly used in electrospinning to create water-soluble materials composed of nanofibers. Using this property, our research group created composite dopes consisting of rSSp and these polymers in varying concentrations. The goal was to use the polymers as carriers for the protein to form fibers during electrospinning. With successful electrospinning, the products will be composed of a mixture rSSp fibers and of polymer fibers. Post-treating the materials in alcohol baths will make rSSp fibers formed during electrospinning water insoluble. Using a water bath, the water-soluble polymers will be removed, leaving behind electrospun rSSp fibers. The two polymers were processed into a fine powder to increase homogeneity and solubility

of the solution. As stated above, 10% (w/v) was established as the base concentration. Several permutations of the composite dopes were created and electrospun, the results of which can be seen in Table 2.4. Composite dopes that electrospun successfully were used to create mats and continuous yarns that were subjected to post-treatment baths. Samples were taken for Scanning Electron Microscopy (SEM), an example of which can be seen in Figure 2.2. Previous experiments with Nylon 6-6 + rSSp solubilized in formic acid were successful in

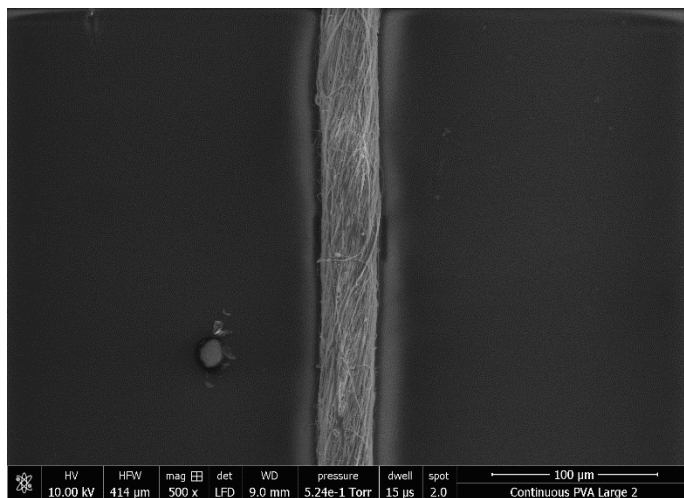


Figure 2.2: SEM image of continuous composite yarn.

creating a mat. The concentration of this dope was 5% Nylon and 5% rMaSp1. The mat would have a white appearance, with occasional spots due to droplets falling from the syringe. For unexplained reasons, these dopes were not successful in continuous electrospinning.

HFIP dopes were used as a control to create pure electrospun rSSp fibers, demonstrated by several research groups.<sup>18-21</sup> Observed during wet-spinning, high concentration HFIP dopes (20% and up) create fibers with high stress and strain, as stated before. The viscosity of these high-concentration dopes is a detriment to electrospinning and a common phenomenon is observed. With solutions of high viscosity, “tendrils” form at the end of the syringe. These form due to the elongation factor initiated during electrospinning, causing the solution to form several initiation points for the Taylor cone.

Fibers are inefficiently formed and do not collect onto the target when this occurs. Through experimentation it was observed that 7% (w/v) HFIP dopes were the most efficient for electrospinning, the results of which are shown in Table 2.5. Utilizing the rotating drum to assess the viability for fiber formation, the best dopes were used for continuous electrospinning to produce yarns. Seven dopes, five composites and one HFIP were used during continuous electrospinning, creating thin-diameter yarns as described in the methods section. These samples, as well as controls, were verified for spider silk fiber formation using a UV gel imager.

### **Post-treatment of Electrospun Yarns**

Electrospun mats and yarns were subjected to post-treatment listed in Table 2.6. As a control, pure PVA (10%) was electrospun and post-treated through steps 1 and 2. When placed into water, the materials dissolved, demonstrating water solubility. When composite materials were post-treated in steps one and two, their diameters decreased. However, when placed into water, these immediately dissolved, leading our group to believe that the rSSp fibers were not achieving high beta-sheet content or were not forming at all.

HFIP dopes were used to create continuous yarns via electrospinning. As described in the methods section, the yarns were post-treated and stretched 1.3x their original length in post-treatment baths to further mature proteins. These post-treated yarns became water insoluble, with diameters decreased by  $1/3^{\text{rd}}$ . Below, in Figure 2.3, is an SEM image of a 7% HFIP electrospun yarn without post-treatment. It is observed that the yarn is composed of several hundred highly twisted nanofibers. Samples from this set were mechanically tested and compared to that of post-treated samples.

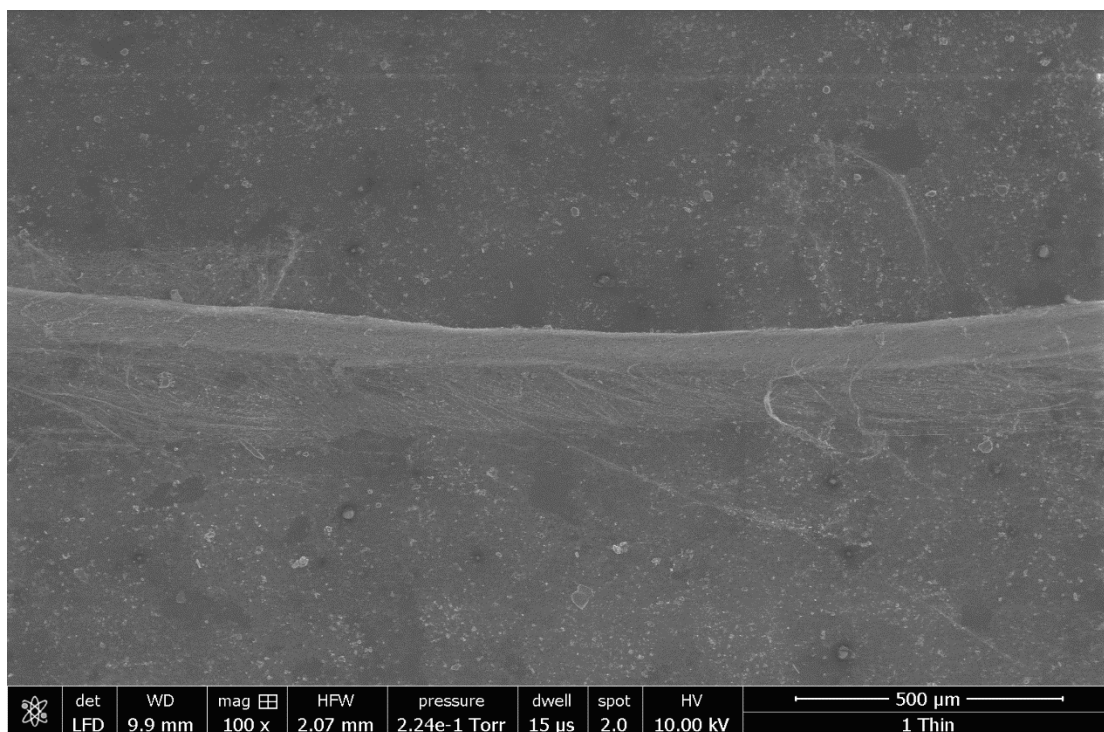


Figure 2.3: Unpost-treated HFIP yarn.

To increase the mechanical properties of these continuously electrospun yarns, samples were post-treated. The optimal results are compared against all continuous electrospun yarns, listed in Table 2.6. Originally hypothesized to surpass the mechanical properties of natural silk, the mechanical testing results of the continuously electrospun yarns fall just short.<sup>2,10</sup> Below, in Figure 2.3, is an SEM image of a sample from the same fiber with post-treatment. The most distinguishing observation is that the nanofibers have fused together, forming one solid yarn. This explains why the results were not as expected. To surpass the mechanical properties of natural silk, electrospun yarns must be composed of several hundred nanofibers working in conjunction to absorb energy. When the multi-nanofiber yarn fused together, it created a fiber with stress focal points, observed in Figure 2.4.

When composite dopes were used to electrospin the result was a fine diameter yarn

theorized to be composed of multiple nanofibers of PVA and rSSp. However, when these yarns were post-treated to induce water-insolubility of rSSp fibers, the results were unexpected. The fibers, regardless of post-treatments would dissolve in water. During electrospinning, if the rSSp were making fibers the end product would become water insoluble after post-treatment. It was also observed that unpost-treated composite yarns had decreased mechanical properties when compared to that of pure PVA yarns. This led us to believe that the rSSp are not forming fibers during electrospinning, instead interrupting the PVA polymer chains degrading the mechanical properties. This was verified using the gel imager mentioned in the methods section.

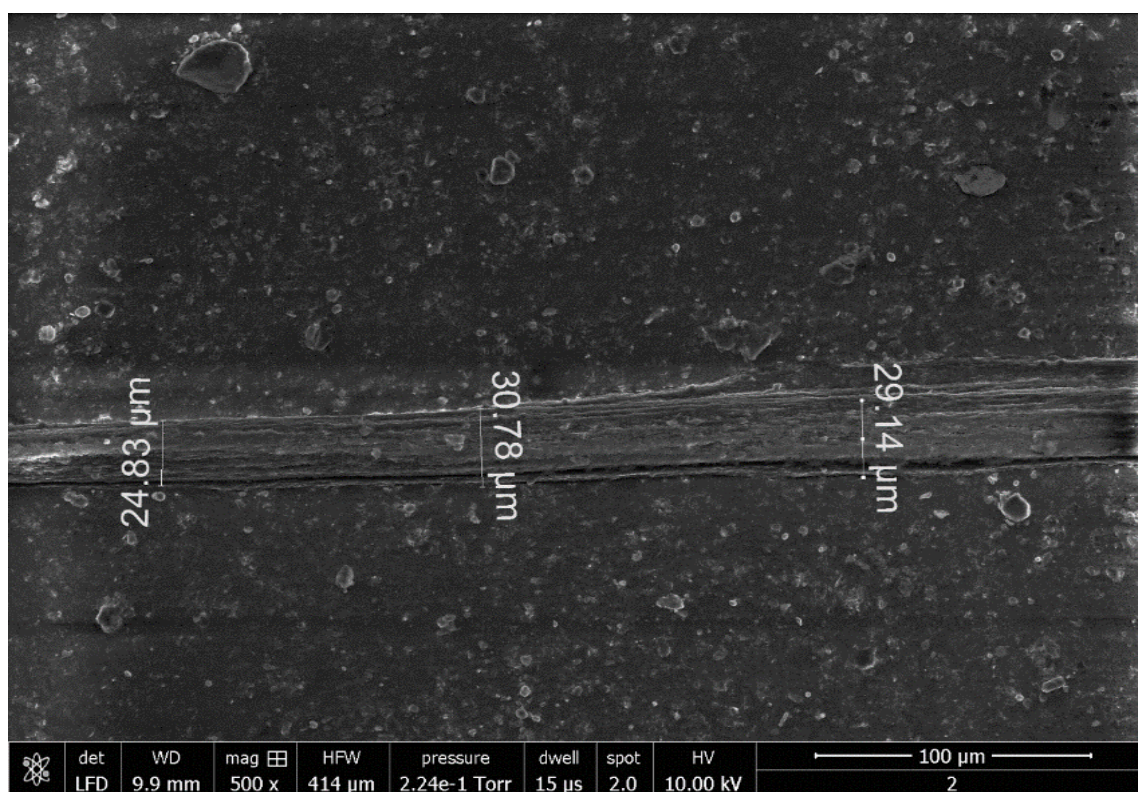


Figure 2.4: Post-treated continuous electrospun HFIP rSSp yarn

### Mechanical Properties

The best mechanical properties for continuously electrospun yarns from pure PVA,

HFIP rSSp, and composite dopes are reported in Table 2.7. It was observed that when increasing the concentration of rSSp in composite dopes, the mechanical properties would decrease compared to pure polymer samples, which is counterintuitive to prior hypotheses. The cause for this decrease in mechanical properties was hypothesized to be caused by the rSSp interrupting the polymer chains instead of forming nanofibers. This was confirmed using an Azure Biosystems c200 gel imager in a novel manner.

### **Verification of rSSp Fiber Formation**

The Azure Biosystems c200 gel imager is traditionally used to excite proteins and take images of gels containing samples of proteins of unknown size and a molecular ladder for comparison. Our group used this machine in a novel manner to image several controls and electrospun samples to verify the presence of electrospun rSSp, listed in Table 2.8. As described in the methods sections, images were taken of controls and samples to verify the presence of rSSp. The results elucidated the mechanical property results. One of the original hypotheses was that by incorporating rSSp into polymers such as PVA and Nylon, the mechanical properties would increase due to the presence of nanofibers composed of rSSp. Below — in Figures 2.5, 2.6, 2.7, 2.8, and 2.9 — the presence of rSSp is highlighted, while the polymers are not captured. The figures demonstrate that the composite materials only show fluorescence at the droplets, where rSSp are present. Powdered rSSp, as well as HFIP dopes, wet and electrospun products, show up clearly.

### **Discussion**

Utilizing electrospinning, traditional and continuous, our group has established parameters for successful electrospinning of rSSp dopes. With the rSSp currently available,

aqueous-based dopes (pure or composite) are not capable of electrospinning fibers. The maturation step associated with wet-spinning cannot be incorporated into electrospinning. Through extensive experimentation, the only method currently available for producing continuously electrospun yarns utilizes HFIP rSSp dopes. Unfortunately, using this chaotropic agent makes it impossible to upscale the process to create viable amounts of electrospun yarns with the desirable mechanical properties. However, the HFIP yarns produced through continuous electrospinning did achieve mechanical properties approaching those of natural silk fibers, shown in Table 2.7. The properties of our yarns did not surpass that of natural silk due to the fusion of fibers observed during stretching and post-treatment. To achieve properties greater than natural silk, the rSSp must be modified and methods must be devised to stretch and post-treat electrospun samples that will not result in fused fibers. This will create a yarn composed of individual nanofibers, creating in a material with mechanical properties greater than natural silk.

<b>Table 2.2- Aqueous Dopes Composition and Electrospun Results</b>		
<b>Total % (w/v)</b>	<b>Composition</b>	<b>Electrospinning Results</b>
25%	80% rMaSp1 + 20%rMaSp2	Droplets, no fibers
	70% rMaSp1 + 30%rMaSp2	Droplets, no fibers
	60% rMaSp1 + 40%rMaSp2	Droplets, no fibers
	100% rMaSp1	Droplets, no fibers
	100% rMaSp2	Droplets, no fibers
20%	80% rMaSp1 + 20%rMaSp2	Droplets, no fibers
	70% rMaSp1 + 30%rMaSp2	Droplets, no fibers
	60% rMaSp1 + 40%rMaSp2	Droplets, no fibers
	100% rMaSp1	Droplets, no fibers
	100% rMaSp2	Droplets, no fibers
18%	80% rMaSp1 + 20%rMaSp2	Fine powder, no fibers
	70% rMaSp1 + 30%rMaSp2	Fine powder, no fibers
	60% rMaSp1 + 40%rMaSp2	Fine powder, no fibers
	100% rMaSp1	Fine powder, no fibers



	100% rMaSp2	Fine powder, no fibers
15%	80% rMaSp1 + 20%rMaSp2	Fine powder, no fibers
	70% rMaSp1 + 30%rMaSp2	Fine powder, no fibers
	60% rMaSp1 + 40%rMaSp2	Fine powder, no fibers
	100% rMaSp1	Fine powder, no fibers
	100% rMaSp2	Fine powder, no fibers
12%	80% rMaSp1 + 20%rMaSp2	Fine powder, no fibers
	70% rMaSp1 + 30%rMaSp2	Fine powder, no fibers
	60% rMaSp1 + 40%rMaSp2	Fine powder, no fibers
	100% rMaSp1	Fine powder, no fibers
	100% rMaSp2	Fine powder, no fibers
10%	80% rMaSp1 + 20%rMaSp2	Fine powder, no fibers
	70% rMaSp1 + 30%rMaSp2	Fine powder, no fibers
	60% rMaSp1 + 40%rMaSp2	Fine powder, no fibers
	100% rMaSp1	Fine powder, no fibers
	100% rMaSp2	Droplets, no fibers

5%	80% rMaSp1 + 20%rMaSp2	Fine powder, no fibers
	70% rMaSp1 + 30%rMaSp2	Fine powder, no fibers
	60% rMaSp1 + 40%rMaSp2	Fine powder, no fibers
	100% rMaSp1	Fine powder, no fibers
	100% rMaSp2	Fine powder, no fibers

<b>Table 2.3- Effects of Additives on Aqueous Dope Electrospinning</b>		
<b>Additive % (w/v)</b>	<b>Effect</b>	<b>Electrospinning Results</b>
1% Isopropyl Alcohol	No visible effect	Droplets, no fibers
7% IPA	Viscosity increased	Droplets, no fibers
13% IPA	Solidified	Impossible to electrospin
1% Methanol	No visible effect	Droplets, no fibers
7% MeOH	Viscosity increased	Droplets, no fibers
13% MeOH	Protein precipitated, irreversible	Impossible to electrospin
1% Ethanol	No visible effect	Droplets, no fibers
7% EtOH	Viscosity increased	Droplets, no fibers
13% EtOH	Protein precipitated, irreversible	Impossible to electrospin
1% Glycerol	No visible effect	Droplets, no fibers
5% Glycerol	Viscosity increased	Droplets, no fibers
10% Glycerol	Solidified	Impossible to electrospin
15% Glycerol	Solidified	Impossible to electrospin
1% Trehalose	No visible effect	Droplets, no fibers

5% Trehalose	Viscosity increased	Droplets, no fibers
10% Trehalose	Solidified	Impossible to electrospin
15% Trehalose	Solidified	Impossible to electrospin
Gold nanoparticles (30 nm)	No visible effect	Droplets, no fibers
Carbon nanotubes (10-20 nm)	No visible effect	Droplets, no fibers
Propionic acid (2.0%)	pH decreased- 4.0, Inc. viscosity	Droplets, no fibers
Ammonium hydroxide (0.5 M)	pH increased- 10.0, Inc. viscosity	Droplets, no fibers
Refrigeration	Temp lowered- 0°C, Inc. viscosity	Droplets, no fibers

<b>Table 2.4- Composition of Composite Dopes and Electrospinning Results</b>		
<b>Total %</b>	<b>Composition</b>	<b>Results</b>
10% (w/v)	8% Poly(vinyl-alcohol) PVA + 2% rMaSp1	Fibers formed
	7% PVA + 3% rMaSp1	Fibers formed
	6% PVA + 4% rMaSp1	Fibers formed
	5% PVA + 5% rMaSp1	Powder, no fibers
	8% PVA + 2% rMaSp2	Powder, no fibers
	7% PVA + 3% rMaSp2	Powder, no fibers
	6% PVA + 4% rMaSp2	Powder, no fibers
	5% PVA + 5% rMaSp2	Powder, no fibers
	8% PVA + 2% rSSp (80% rMaSp1+ 20% rMaSp2)	Fibers formed
	7% PVA + 3% rSSp (80% rMaSp1+ 20% rMaSp2)	Fibers formed
	6% PVA + 4% rSSp (80% rMaSp1+ 20% rMaSp2)	Powder, no fibers
	5% PVA + 5% rSSp (80% rMaSp1+ 20% rMaSp2)	Powder, no fibers
	8% PVA + 2% rSSp (70% rMaSp1+ 30% rMaSp2)	Powder, no fibers
7% PVA + 3% rSSp (70% rMaSp1+ 30% rMaSp2)	Powder, no fibers	

	6% PVA + 4% rSSp (70% rMaSp1+ 30% rMaSp2)	Powder, no fibers
	5% PVA + 5% rSSp (70% rMaSp1+ 30% rMaSp2)	Powder, no fibers
10% (w/v)	8% Poly(ethylene oxide) (PEO) + 2% rMaSp1	Powder, no fibers
	7% PEO + 3% rMaSp1	Powder, no fibers
	6% PEO + 4% rMaSp1	Powder, no fibers
	5% PEO + 5% rMaSp1	Powder, no fibers
	8% PEO + 2% rMaSp2	Powder, no fibers
	7% PEO + 3% rMaSp2	Powder, no fibers
	6% PEO + 4% rMaSp2	Powder, no fibers
	5% PEO + 5% rMaSp2	Powder, no fibers
	8% PEO + 2% rSSp (80% rMaSp1+ 20% rMaSp2)	Powder, no fibers
	7% PEO + 3% rSSp (80% rMaSp1+ 20% rMaSp2)	Powder, no fibers
	6% PEO + 4% rSSp (80% rMaSp1+ 20% rMaSp2)	Powder, no fibers
	5% PEO + 5% rSSp (80% rMaSp1+ 20% rMaSp2)	Powder, no fibers

<b>Table 2.5- Results of 80/20 HFIP Dopes at Different Concentrations</b>	
<b>Concentration</b>	<b>Results</b>
25% (w/v)	Solution is too viscous, forms “tendrils” from droplet at syringe tip causing few fibers to form but do not collect onto target.
20% (w/v)	Solution is too viscous, forms “tendrils” from droplet at syringe tip causing few fibers to form but do not collect onto target.
15% (w/v)	Solution is less viscous, fewer “tendrils” form at syringe tip. More fibers are produced but do not collect onto target.
10% (w/v)	Fewer “tendrils” form. Fibers are produced but not in great quantities, approximately 50% of fibers formed collect on target.
8% (w/v)	Droplet forms far fewer “tendrils”, less interference of fiber formation. Fibers gather on target more readily.
7% (w/v)	Best concentration for electrospinning, little to no tendrils present, fibers formed efficiently and collected onto target.
6.5% (w/v)	Decreased fibers formed, requires a minimum of 45 minutes to collect a thin layer of fibers.
6% (w/v)	Decreased fibers formed, requires a minimum of 1 hour and 30 minutes to collect a thin layer of fibers.

<b>Table 2.6- Optimal Post-treatment Results on Continuous Electrospun Yarns</b>			
<b>Sample</b>	<b>Post-treatment Process (1<sup>st</sup> →2<sup>nd</sup>→3<sup>rd</sup>)</b>	<b>Max Stretch</b>	<b>H<sub>2</sub>O Insoluble</b>
Mowiol- 10% (w/v)	80% IPA→20% IPA→H <sub>2</sub> O 80% EtOh→20% EtOh→H <sub>2</sub> O 80% MeOh→20% MeOh→H <sub>2</sub> O	1.5x	No
Composite- 8% Mowiol + 2% rMaSp1	80% IPA→20% IPA→H <sub>2</sub> O 80% EtOh→20% EtOH→H <sub>2</sub> O 80% MeOh→20% MeOh→H <sub>2</sub> O	1.25x	No
Composite- 7% Mowiol + 3% rMaSp1	80% IPA→20% IPA→H <sub>2</sub> O 80% EtOh→20% EtOh→H <sub>2</sub> O 80% EtOh→20% EtOh→H <sub>2</sub> O	1.2x	No
Composite- 6% Mowiol + 4% rMaSp1	80% IPA→20% IPA→H <sub>2</sub> O 80% EtOh→20% EtOh→H <sub>2</sub> O 80% MeOh→20% MeOh→H <sub>2</sub> O	1.2x	No
HFIP- 7% w/v (80% rMaSp1 + 20% rMaSp2)	80% IPA→20% IPA→H <sub>2</sub> O 80% EtOh→20% EtOh→H <sub>2</sub> O 80% MeOh→20% MeOh→H <sub>2</sub> O	1.3x	Yes



**Table 2.7 - Mechanical Properties of Natural Silk and Continuous Electrospun Yarns**

<b>Sample</b>	<b>Diameter (<math>\mu\text{m}</math>)</b>	<b>Max Stress (MPa)</b>	<b>Max Strain (mm/mm)</b>	<b>Energy to Break (MJ/m<sup>3</sup>)</b>
Natural Dragline (~80% MaSp1 + 20% MaSp2)	15	4000	35	40
PVA Dope- 10% (w/v)	40.42	75.38	0.49	60.19
Composite Dope- 8% PVA + 2% rMaSp1 (w/v)	52.84	31.12	0.24	6.19
Composite Dope- 7% PVA + 3% rMaSp1 (w/v)	135.76	7.96	0.64	4.39
Composite Dope- 6% PVA + 4% rMaSp1 (w/v)	63.52	6.15	0.75	4.14
HFIP Dope- 7% w/v (80% rMaSp1 + 20% rMaSp2)	14.44	3548.58	0.02	41.82

<b>Table 2.8- Results from rSSo Fiber Verification</b>			
<b>Sample</b>	<b>Form</b>	<b>Protein Present</b>	<b>Visible</b>
rMaSp1	Powder	Yes	Yes
Processed Mowiol® 40-88 (Polyvinyl Alcohol)	Powder	No	No
Mowiol dope (10% w/v)	Liquid	No	No
Composite dope 10% w/v (8% Mowiol + 2% rMaSp1)	Liquid	Yes	Yes
HEIP dope 7% w/v (80% rMaSp1 + 20% rMaSp2)	Liquid	Yes	Yes
Electrospun Mowiol mat 10% w/v	Mat	No	No
Electrospun composite mat 1 (8% Mowiol + 2% rMaSp1)	Mat w/ spots	Yes	Only spots
Electrospun composite mat 2 (7% Mowiol + 3% rMaSp1)	Mat w/ spots	Yes	Only spots
Electrospun composite yarn 1 (8% Mowiol + 2% rMaSp1)	Yarn w/ spots	Yes	Only spots
Electrospun composite yarn 2 (8% Mowiol + 2% rMaSp1)	Yarn w/ spots	Yes	Only spots
HEIP wetspun rSSo fibers 20% w/v (80% rMaSp1 + 20% rMaSp2)	Single Fiber	Yes	All material
HEIP wetspun rSSo fibers 20% w/v (80% rMaSp1 + 20% rMaSp2)	Fiber bundle	Yes	All material
HEIP electrospun rSSP mat 7% w/v (80% rMaSp1 + 20% rMaSp2)	Fiber bundle	Yes	All material
HEIP electrospun rSSP fibers 7% w/v (80% rMaSp1 + 20%)	Yarn	Yes	All material

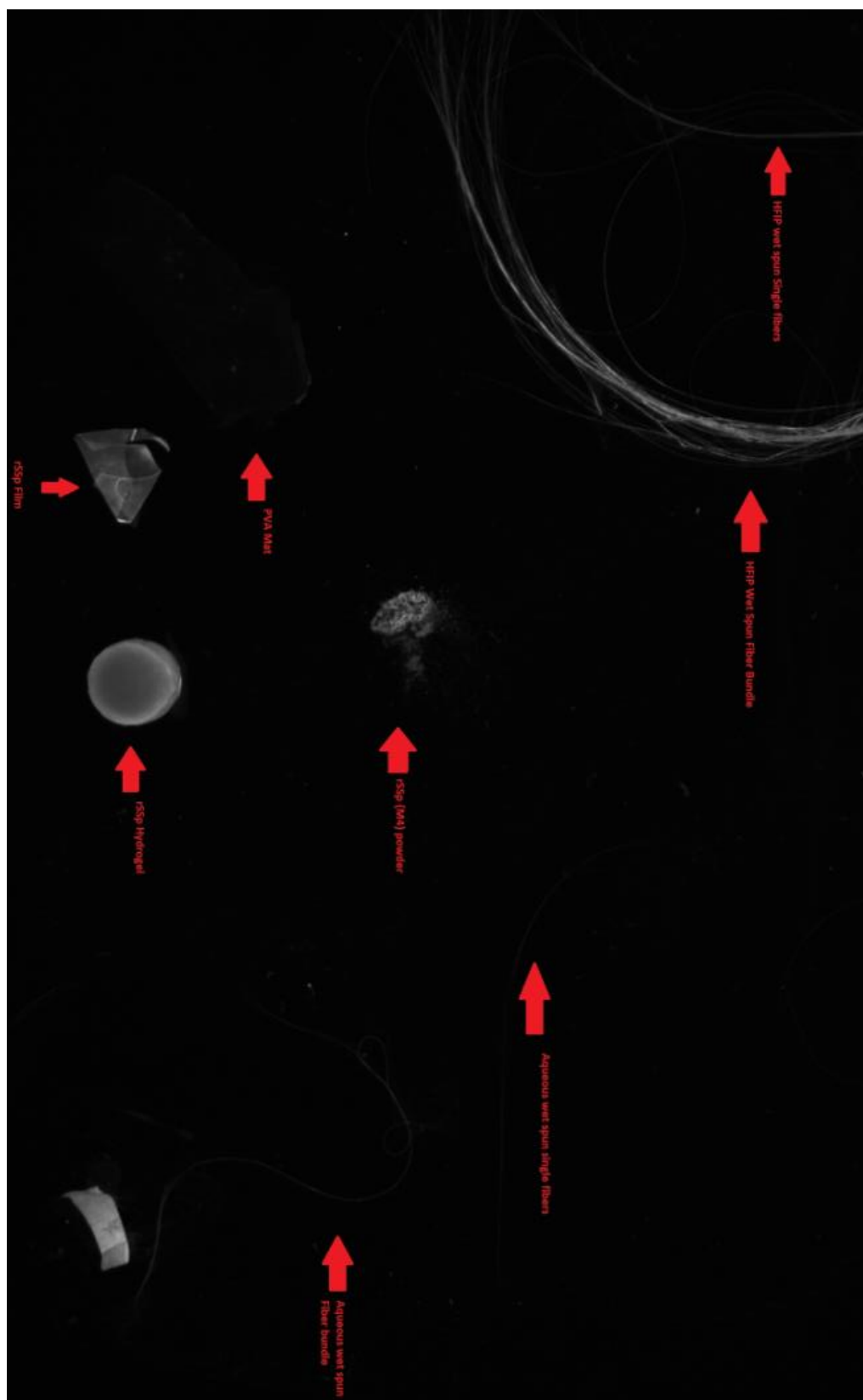


Figure 2.5: rSSp verification 1-5.

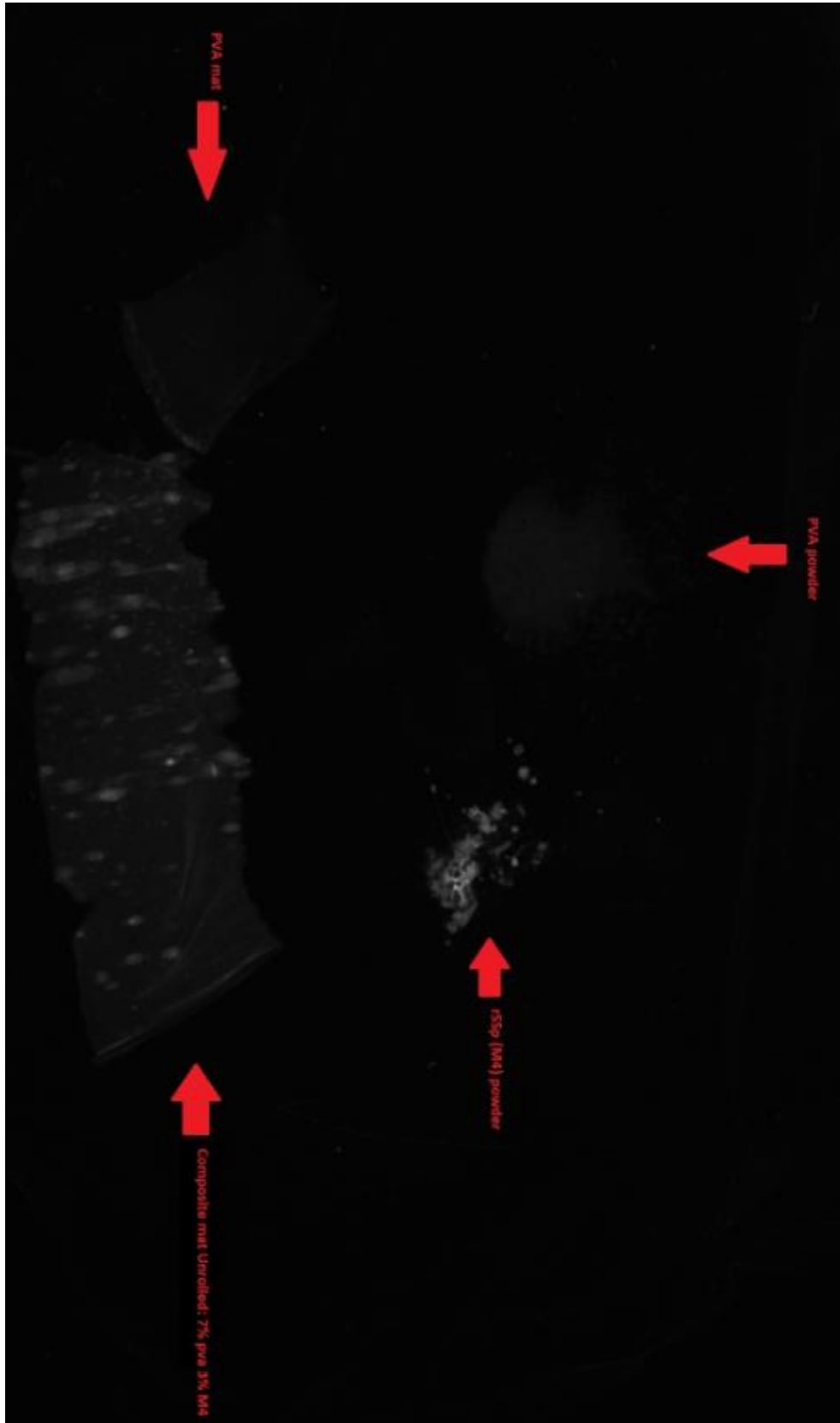


Figure 2.6: rSSp verification 2-5.

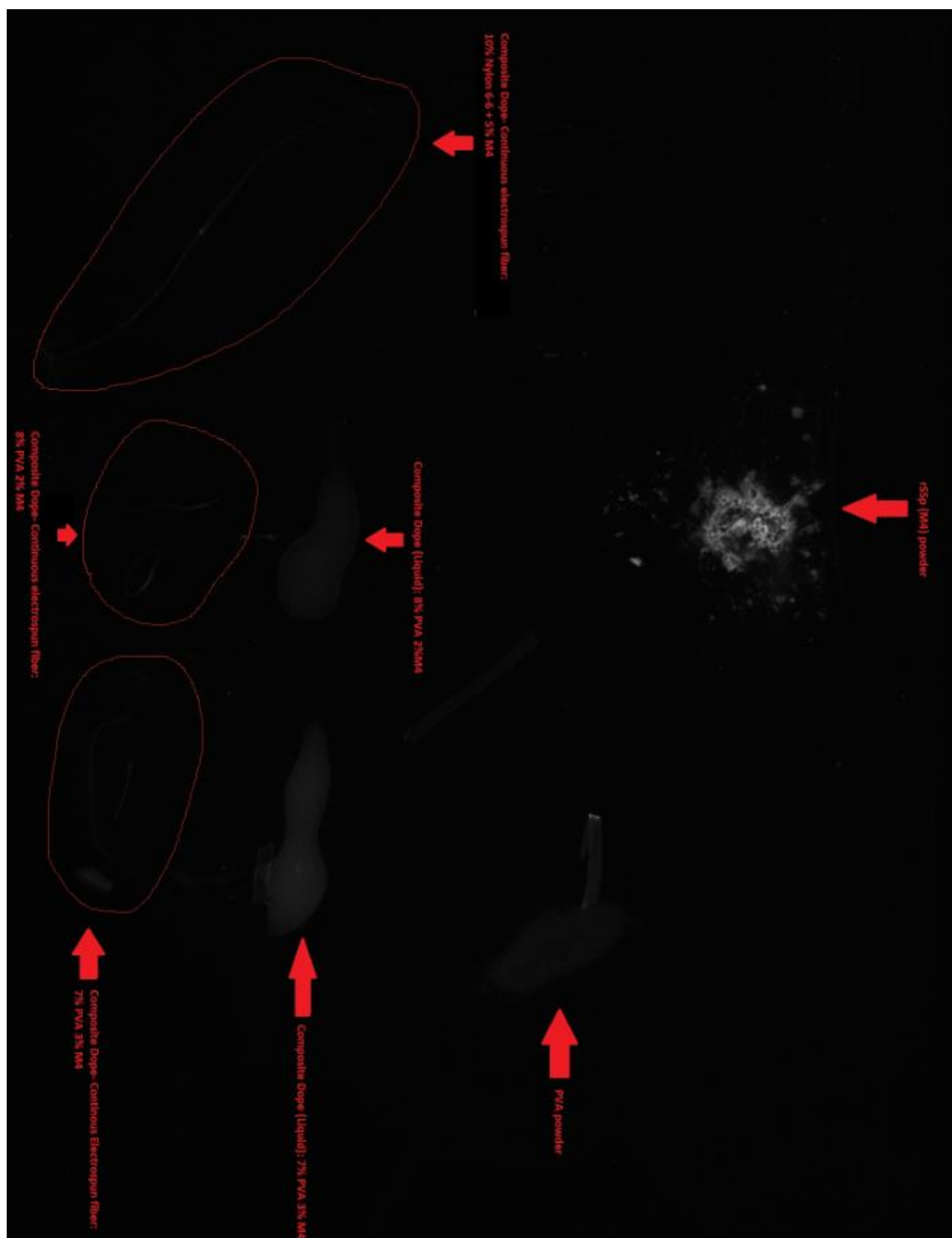


Figure 2.7: rSSp verification 3-5.

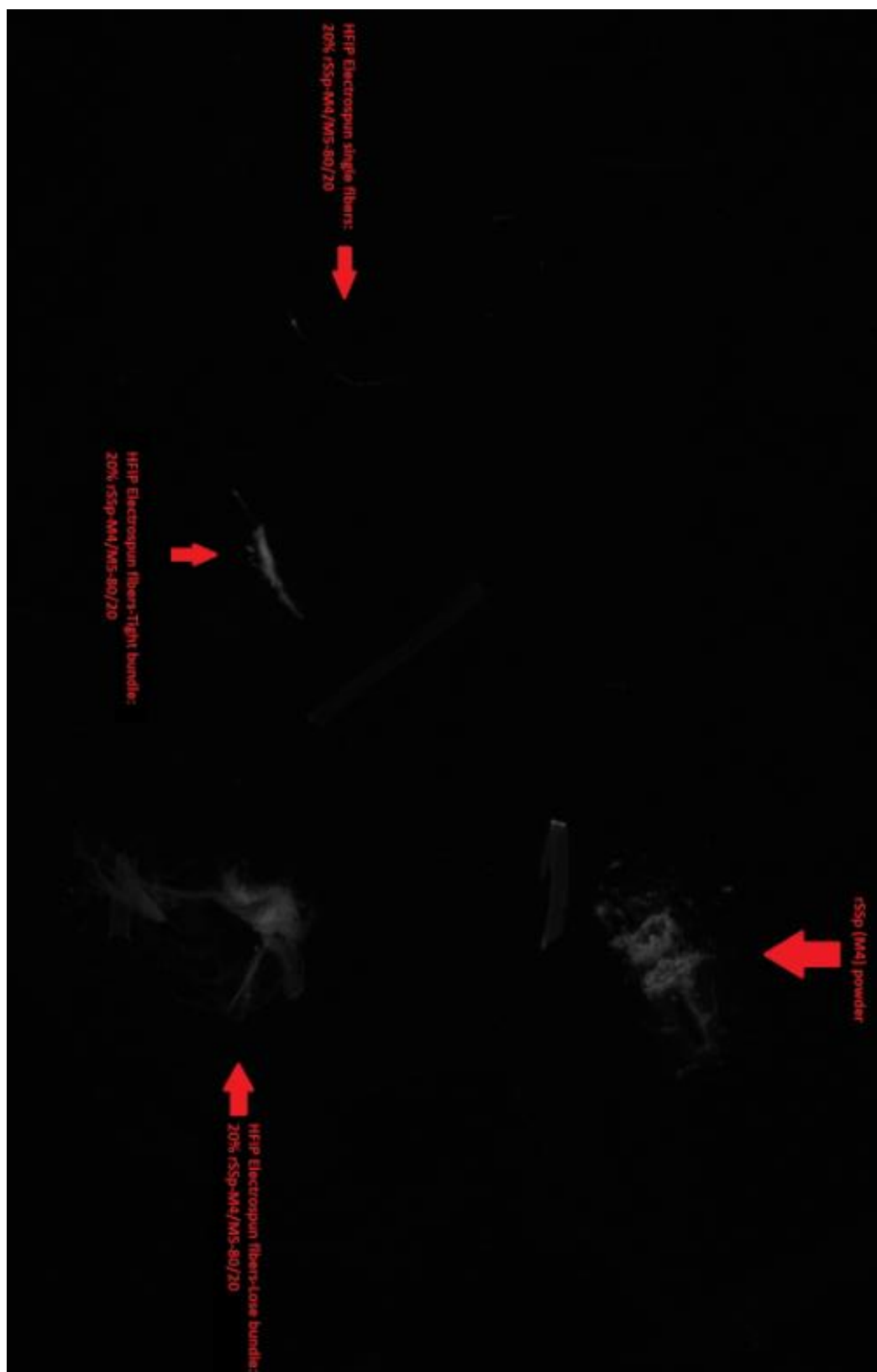


Figure 2.8: rSSp verification 4-5.

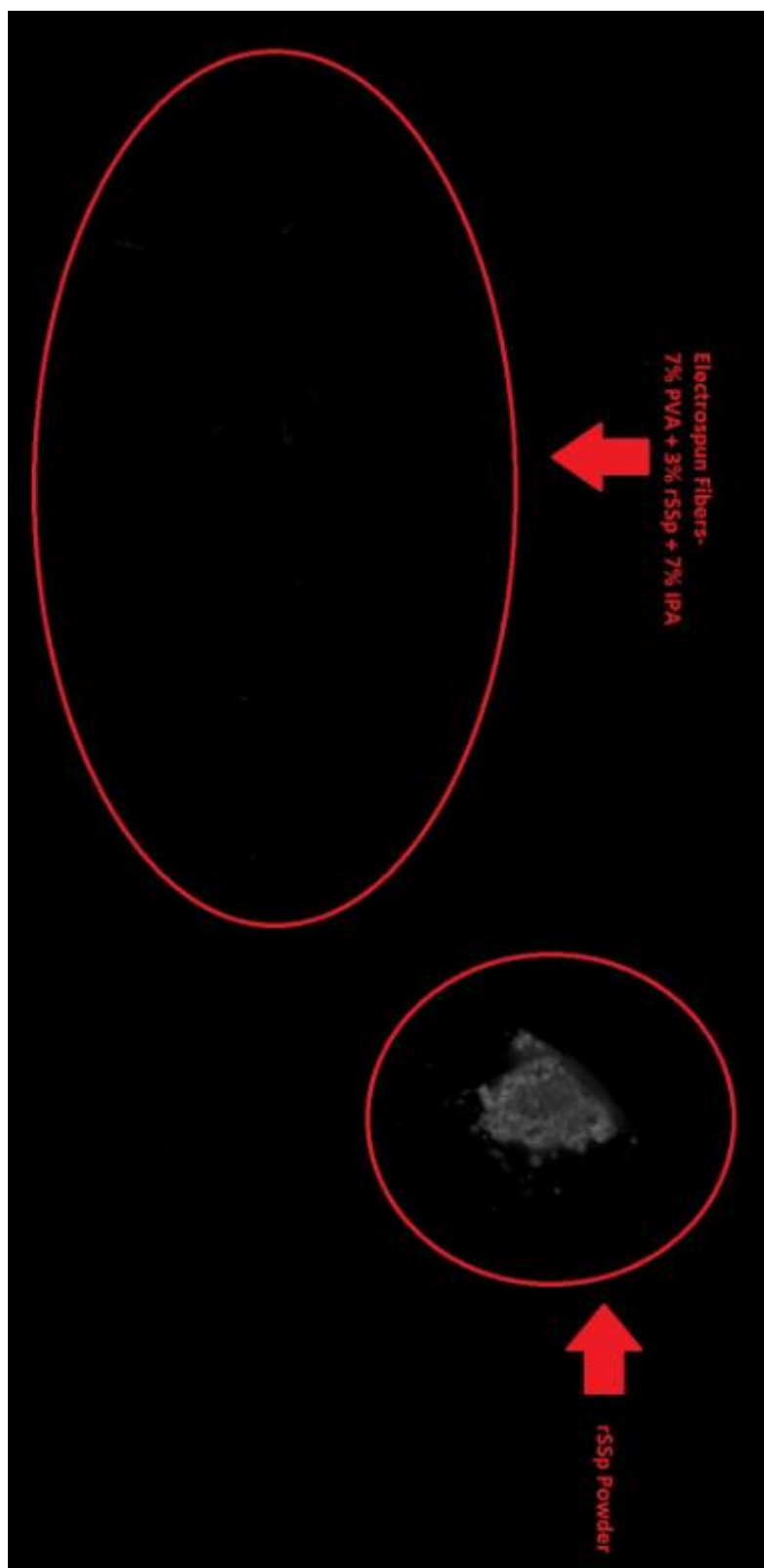


Figure 2.9: rSSp verification 5-5.

## References

- (1) Shenoy, S. L.; Bates, W. D.; Frisch, H. L.; Wnek, G. E. Role of Chain Entanglements on Fiber Formation during Electrospinning of Polymer Solutions: Good Solvent, Non-Specific Polymer–polymer Interaction Limit. *Polymer* **2005**, *46* (10), 3372–3384.
- (2) Lewis, R. V. Spider Silk: Ancient Ideas for New Biomaterials. *Chem. Rev.* **2006**, *106* (9), 3762–3774.
- (3) Copeland, C. G.; Bell, B. E.; Christensen, C. D.; Lewis, R. V. Development of a Process for the Spinning of Synthetic Spider Silk. *ACS Biomater. Sci. Eng.* **2015**, *1* (7), 577–584.
- (4) Ali, U.; Zhou, Y.; Wang, X.; Lin, T. Direct Electrospinning of Highly Twisted, Continuous Nanofiber Yarns. *The Journal of The Textile Institute* **2012**, *103* (1), 80–88.
- (5) Costas N, K.; Jeffrey D, T.; Anthoula, K. Production of Biofilaments in Transgenic Animals, US Patent 7,157,615. US Patent 7157615, June 27, 2001.
- (6) Teulé, F.; Cooper, A. R.; Furin, W. A.; Bittencourt, D.; Rech, E. L.; Brooks, A.; Lewis, R. V. A Protocol for the Production of Recombinant Spider Silk-like Proteins for Artificial Fiber Spinning. *Nature Protocols* **2009**, *4* (3), 341–355.
- (7) Teulé, F.; Addison, B.; Cooper, A. R.; Ayon, J.; Henning, R. W.; Benmore, C. J.; Holland, G. P.; Yarger, J. L.; Lewis, R. V. Combining Flagelliform and Dragline Spider Silk Motifs to Produce Tunable Synthetic Biopolymer Fibers. *Biopolymers* **2012**, *97* (6), 418–431.
- (8) Tucker, C. L.; Jones, J. A.; Bringham, H. N.; Copeland, C. G.; Addison, J. B.; Weber, W. S.; Mou, Q.; Yarger, J. L.; Lewis, R. V. Mechanical and Physical Properties of Recombinant Spider Silk Films Using Organic and Aqueous Solvents. *Biomacromolecules* **2014**, *15* (8), 3158–3170.
- (9) Jones, J. A.; Harris, T. I.; Tucker, C. L.; Berg, K. R.; Christy, S. Y.; Day, B. A.; Gaztambide, D. A.; Needham, N. J. C.; Ruben, A. L.; Oliveira, P. F.; et al. More Than Just Fibers: An Aqueous Method for the Production of Innovative Recombinant Spider Silk Protein Materials. *Biomacromolecules* **2015**, *16* (4), 1418–1425.
- (10) Copeland, C. G.; Bell, B. E.; Christensen, C. D.; Lewis, R. V. Development of a Process for the Spinning of Synthetic Spider Silk. *ACS Biomaterials Science & Engineering* **2015**.
- (11) Xia, X.-X.; Qian, Z.-G.; Ki, C. S.; Park, Y. H.; Kaplan, D. L.; Lee, S. Y. Native-Sized Recombinant Spider Silk Protein Produced in Metabolically Engineered *Escherichia Coli* Results in a Strong Fiber. *PNAS* **2010**, *107* (32), 14059–14063.



- (12) Askarieh, G.; Hedhammar, M.; Nordling, K.; Saenz, A.; Casals, C.; Rising, A.; Johansson, J.; Knight, S. D. Self-Assembly of Spider Silk Proteins Is Controlled by a PH-Sensitive Relay. *Nature* **2010**, *465* (7295), 236–238.
- (13) Rabotyagova, O. S.; Cebe, P.; Kaplan, D. L. Self-Assembly of Genetically Engineered Spider Silk Block Copolymers. *Biomacromolecules* **2009**, *10* (2), 229–236.
- (14) Stark, M.; Grip, S.; Rising, A.; Hedhammar, M.; Engström, W.; Hjälms, G.; Johansson, J. Macroscopic Fibers Self-Assembled from Recombinant Miniature Spider Silk Proteins. *Biomacromolecules* **2007**, *8* (5), 1695–1701.
- (15) Wu, Y.; Shah, D. U.; Liu, C.; Yu, Z.; Liu, J.; Ren, X.; Rowland, M. J.; Abell, C.; Ramage, M. H.; Scherman, O. A. Bioinspired Supramolecular Fibers Drawn from a Multiphase Self-Assembled Hydrogel. *PNAS* **2017**, 201705380.
- (16) Sill, T. J.; von Recum, H. A. Electrospinning: Applications in Drug Delivery and Tissue Engineering. *Biomaterials* **2008**, *29* (13), 1989–2006.
- (17) Zhu, J.; Shao, H.; Hu, X. Morphology and Structure of Electrospun Mats from Regenerated Silk Fibroin Aqueous Solutions with Adjusting PH. *International Journal of Biological Macromolecules* **2007**, *41* (4), 469–474.
- (18) Li, C.; Vepari, C.; Jin, H.-J.; Kim, H. J.; Kaplan, D. L. Electrospun Silk-BMP-2 Scaffolds for Bone Tissue Engineering. *Biomaterials* **2006**, *27* (16), 3115–3124.
- (19) Jin, H.-J.; Fridrikh, S. V.; Rutledge, G. C.; Kaplan, D. L. Electrospinning Bombyx Mori Silk with Poly(Ethylene Oxide). *Biomacromolecules* **2002**, *3* (6), 1233–1239.
- (20) Sukigara, S.; Gandhi, M.; Ayutsede, J.; Micklus, M.; Ko, F. Regeneration of Bombyx Mori Silk by Electrospinning—part 1: Processing Parameters and Geometric Properties. *Polymer* **2003**, *44* (19), 5721–5727.
- (21) Jin, H.-J.; Chen, J.; Karageorgiou, V.; Altman, G. H.; Kaplan, D. L. Human Bone Marrow Stromal Cell Responses on Electrospun Silk Fibroin Mats. *Biomaterials* **2004**, *25* (6), 1039–1047.

CHAPTER III  
ENHANCING SPIDER SILK PROTEIN MATERIALS THROUGH  
PHOTO-INITIATED CROSS-LINKING

Co-Authors include: Blake Taurone, Bailey McFarland, Thomas I. Harris, Justin A. Jones, and Randy V. Lewis

ABSTRACT

Spider silk materials are known for their robust and diverse mechanical properties. To further enhance spider silk materials, our group has employed photo-induced cross-linking of unmodified proteins (PICUP). By incorporating tris(2,2'-bipyridyl) dichlororuthenium(II) hexahydrate (ruthenium), ammonium persulfate (APS) to our dopes then irradiating them with a high lumen light source, tyrosines are covalently cross-linked, enhancing the spider silk proteins and creating a novel material. To increase the efficiency of this reaction, we created the cross-link initiating photodiode (CLIP), a 18,000 lumen LED light source. Using the CLIP in combination with PICUP, our spider-silk hydrogels demonstrate up to a 500% increase in strain and tensile strength. The cross-linked hydrogels can further be modified using post-treatment baths. This method of treatment result in materials with a range of mechanical properties that can be used in applications not available to spider silk materials prior to cross-linking.

Keywords: Proteins, Spider Silk, Cross-linking, Photo-initiated, Biomaterial

## Introduction

Spiders, specifically orb weaving spiders like *Nephila clavipes*, can create up to six different spider silks and one adhesive.<sup>1</sup> Each silk has a specialized function within the web such as: support (web spokes and safety line), prey capture (elongation up to 300%), egg sac (protection), adhesive, prey wrapping, and anchoring<sup>2,3</sup> These properties are derived from four protein structures:  $\beta$ -sheets, Gly II-helices,  $\beta$ -spirals and random coils<sup>4-8</sup>. For this reason, spider silk proteins are tunable materials that rival the properties of commonly used polymers. Dragline silk derived from the major ampullate glands have an energy to break greater than that of Kevlar, 4 GPa and 3 MPa respectively. This difference is attributed to dragline silk's ability to elongate up to 35% prior to failure where Kevlar will elongate 5% at most.<sup>1,9</sup> In addition to possessing desirable mechanical properties, spider silk protein materials are biocompatible and have been found to promote healthy cell growth, in addition to being biodegradable.<sup>10-12</sup>

Recombinant spider silk proteins (rSSp) are remarkable biomaterials with the potential to meet the needs of commercial, industrial, and medical markets.<sup>1,13-24</sup> Kaplan's group has successfully developed hydrogels from silkworm proteins through vortexing, causing the solution to become a hydrogel within the container, limiting the shapes created (REF). Other methods include increasing the protein content or adding an acid in low concentrations, but must go through a gelation process to solidify into a hydrogel.<sup>25-31</sup> Even with these advances, silk protein hydrogels lack the mechanical properties for certain applications. Our group has utilized a method for cross-linking proteins to modify our spider silk materials enhancing their mechanical properties.

Photo-induced cross-linking of unmodified proteins, or PICUP, is traditionally used to observe protein-to-protein interactions.<sup>32,33</sup> This reaction requires proteins, tris(2,2'-bipyridyl) dichlororuthenium(II) hexahydrate (ruthenium), ammonium persulfate (APS), and a high-intensity light source.<sup>26,34,34-40</sup> The reaction is initiated when irradiated by a high lumen light source, a direct carbon-to-carbon bond forms between tyrosines, causing intramolecular cross-linking. We applied this standard analytical technique to our spider silk protein materials. Reported here is a new method for solubilizing the spider silk proteins with cross-linking reagents to form the dope solution. These dopes can be used to produce hydrogels, foams, and sponges, which can be activated with the CLIP to crosslink the rSSp material into robust and stable forms. These cross-linked materials have been studied for their mechanical properties, ability to be grow cells, and their protein structure.

## **Experimental (Materials and Methods)**

### **Protein Purification**

Recombinant spider silk proteins (rSSp) were produced in the milk of genetically modified goats as described in previous work.<sup>41</sup> The rSSp was purified via tangential flow, washed and lyophilized as described by Tucker et al.<sup>42</sup> Recombinant major ampullate spidroin 1 (rMaSp1) was used for these experiments due to the abundance of the protein in our laboratory, and the presence of tyrosine.

### **Solubilization of Cross-linking Dope**

Purified rMaSp1<sup>42</sup> was used to create cross-linking dopes. For a 10% (w/v) dope at a 4 mL volume 400 mg of rMaSp1 was placed into an 8 mL glass culture vial with rubber lined cap purchased from VWR (catalog number: 66014-240). Tris(2,2'-bipyridyl) dichlororuthenium(II) hexahydrate (ruthenium) (part number: 544981-1G) was purchased from Sigma-Aldrich and used to create a stock solution (62.7  $\mu$ M). The ruthenium stock solution (2mL) and Nano-pure water (1mL) from a Nanopure Diamond™ were added to the dry rSSp in the vial. This mixture was sonicated with an energy output of 5 W for 90 s using a QSONICA Sonicator with microtip. The vial was tightly sealed with its lid and rubber insert, then microwaved (Magic Chef 1000 W) in 5 s intervals until the temperature reached an excess of 130 °C (checked with a Fluke 561 IR thermometer on the bottom of the vial following the methods of Jones et al<sup>25</sup>) and all the rSSp was solubilized and then removed from the microwave and allowed to cool to room temperature. A 21.5 mM solution of Ammonium persulfate (part number: 0486-100G, Amresco Inc.) was created

and 1 mL of this solution was added to the vial and vortexed, bringing the final concentrations of ruthenium and APS to 31.35  $\mu\text{M}$  and 5.0375 mM respectively.

### **Photo Cross-linking rSSp Materials**

The cross-link initiating Photodiode (CLIP) was designed and constructed as indicated in supplementary materials (Figure S1). A polydimethylsiloxane (PDMS) substrate (90 mm by 50 mm by 10 mm) was placed on the stage of the CLIP. A silicone dog bone mold (49 mm long, 13 mm head, and 2.68 mm neck) was placed on top of the PDMS substrate and 1 mL of cross-linking dope was pipetted into the mold. The CLIP was illuminated for 30 seconds per sample and repeated a total of four times to generate crosslinked hydrogels.

To create cross-linked foams, a 4 mL cross-linking dope (described above) was distributed into four separate vials containing 1 ml each and vortexed for 3-5 minutes until the contents were a foamy consistency, with no liquid present. The vials were placed onto the stage of the CLIP and irradiated for 30 seconds and removed from the vials.

### **Post Treatments of Cross-linked Materials**

The cross-linked hydrogels were removed from the dog bone mold and placed into three different baths for 1min: 100% isopropyl alcohol (IPA), 100% methanol (MeOH), and 100% ethanol (EtOH) (all alcohols purchased from Pharmaco-AAPER). To remove excess ruthenium the hydrogels and foams were placed into 100 mL glass bottles with 50 mL of deionized water. These were autoclaved using a Tuttnauer Autoclave-Steam Sterilizer Model 2340M for one hour, two separate times, changing the

water in the bottle between autoclaving. The post-treated cross-linked hydrogels were placed back into their respective post-treatment baths, one of the 100% IPA post-treated cross-linked hydrogels was immediately placed into a -80 °C freezer for 24 h.

### **Additional Steps to Create Cross-linked Foams and Sponges**

Cross-linked foams were placed into individual 50 mL conical tubes with and without 40 mL of deionized water and labeled either wet frozen and dry frozen, respectively. These tubes were placed in the -80 °C freezer for 24 h then lyophilized. One of each (wet frozen and dry frozen) cross-linked foam was placed in water for one hour, to produce cross-linked sponges.

### **Mechanical Testing of Cross-linked Materials**

A Synergie 100 MTS, running TestWorks 4 software, equipped with a 50 g load cell was used to test the post-treated cross-linked hydrogels for mechanical properties. The post-treated cross-linked hydrogels were tested under compression and uniaxial tension. The cross-linked foams were tested only under compression, and the cross-linked sponges were tested using cyclical compression with 50 mm diameter aluminum compression platens. The data was exported and analyzed in Microsoft Excel.

### **FTIR Spectroscopy**

FT-IR spectra of cross-linked materials were measured with an attenuated total reflectance Fourier-transform (Varian 660) spectrophotometer. Samples were placed directly on the stage of the ATR-FTIR, each spectrum was acquired in absorbance mode with 32 scans, a resolution of 4  $\text{cm}^{-1}$ , and a spectral range of 4000-600  $\text{cm}^{-1}$ . The FTIR spectra of cross-linked hydrogels were deconvoluted as described by Zhou.<sup>43</sup> (Figures 9,

10, S2, S3).

## Results and Discussion

### Solubilization and Cross-linking rSSp Dopes

To incorporate ruthenium and APS into spider silk materials for cross-linking, researchers have traditionally relied on diffusivity.<sup>44,45</sup> Samples are placed into a bath containing liquid ruthenium and APS and allowed to diffuse overnight. Preliminary results indicated enhanced mechanical properties however, a core-shell structure was observed, indicating that the cross-linking reagents were not penetrating the interior of the hydrogel. To address this, we developed a method to incorporate ruthenium and APS in the solvating agent for our rSSp. Experiments using varying concentrations of stock solution of ruthenium and APS were used to determine the optimal concentrations for solubilization. The solutions of ruthenium and APS ( $62.7 \mu\text{M}$  and  $20.15 \text{ mM}$ , respectively) are combined with nanopure water to solubilize the proteins in a 2:1:1 ratio. The key to avoiding premature cross-linking was incorporating the APS after the proteins were solubilized. Otherwise, the cross-linking reaction would be prematurely initiated through prolonged heat from the solubilization step.

Preliminary experiments using this solvation method employed a 1000 lumen Maglite to initiate the cross-linking reaction.

Using this light source, samples had to be irradiated for 5 minutes while rotating the samples to ensure thorough cross-linking. Irradiation time was decreased to 2.5 minutes using a 1600 lumen Duracell



**Figure 3.1.** CLIP activated. (A) Cooling unit (B) Staging area for samples.








flashlight. It was also observed that all cross-linked hydrogels formed with a core-shell structure. The outer most layer being more robust than the interior indicating the light source was not penetrating through the entire material. To minimize irradiation time and increase the efficiency of the reaction to create a hydrogel that was cross-linked uniformly, our group constructed the CLIP (**Figure 1**). The CLIP uses an 18,000 lumen 465 nm LED which is cooled by a liquid cooling unit typically used for CPU's. To minimize environmental irradiation and focus the light onto the substrate, a staging chamber was mounted onto the LED. Moso bamboo was chosen as the material for the staging chamber due to its high heat capacity, shape,., enabling it to withstand the heat generated by the LED.<sup>46</sup> The design and construction of the CLIP are detailed in the supporting information. With the CLIPs high irradiation level, the reaction was nearly instantaneous


### **Effects of Post-treatment on Cross-linked rSSp Hydrogels**

Cross-linked hydrogels can be post-treated to produce materials with varying properties. When the cross-linked hydrogels are post-treated in IPA they turn opaque and white, rigid with some flexibility (Table 1). To generate greater flexibility, the hydrogel can be placed into IPA and then into a -80°C freezer for 24 h. (Table 1).

Post-treating in methanol results in an opaque material that has increased strain when compared to the IPA materials. Post-treating in ethanol results in a material that appears to be between the IPA and methanol post-treated hydrogels in terms of materials properties which is slightly translucent with decreased strain compared to methanol post-treated materials. When samples were post-treated in MeOH and EtOH then frozen, there were no observable differences unlike the IPA frozen samples, seen in Figure S4. Each of these permutations can be cast as any shape and post-treated to yield materials with varying

properties through post-treatment. Presented in Table 1, are the effects of post-treatment of cross-linked hydrogels.

<b>Table 3.1. Post-treated Cross-linked Hydrogels, Foams and Sponges</b>		
<b>Post-treatment</b>	<b>Physical properties</b>	<b>Picture</b>
IPA	Opaque white, glass-like, Rigid with minor flexibility	
IPA frozen	White, translucent edges, Cartilage-like, pulls apart in striations	
Methanol	Solid white, flexible, stretches, compressed has rebound	
Ethanol	Solid white, decreased flexibility, stretches less than methanol	
Foam	White, airy, “packing-peanut”, soft, floats	

Sponge	Translucent white, porous, retakes form when compressed with addition of water	
--------	--	---

### Mechanical Testing of Cross-linked rSSp Materials

The mechanical properties of post-treated cross-linked rSSp hydrogels, foams, and spongers were assessed through mechanical testing. Cylindrical hydrogels, post-treated in IPA, methanol, and ethanol exceeded the load cell of our compression tests. These samples were compressed into discs, Figure 2a. The average stress-strain curves for these are compared to an uncross-linked hydrogel and presented in Figure 3a and Table 2. All samples were tested in sets of 10, except the sample set of 6 for uncross-linked hydrogels. Utilizing our cross-linking technique, our cylindrical hydrogels mechanical properties have increase by a minimum of 16% and maximum of 217%. The Young's modulus surpassed that of PEG hydrogels and was increased to values similar to rubber (small strain- 0.01 GPa)<sup>47</sup> and low-density polyethylene (0.11 GPa),<sup>48</sup> creating new applications for our cross-linked materials.

<b>Table 3.2.</b> Average Mechanical Results for Compression of Uncross-linked Hydrogels and Post-treated Cross-linked Hydrogels				
<b>Sample</b>	<b>Max Stress (MPa)</b>	<b>Max Strain (mm/mm)</b>	<b>Energy to Break (MJ/m<sup>3</sup>)</b>	<b>Young's Modulus (MPa)</b>
Uncross-linked	0.23 ± 0.05	0.24 ± 0.17	0.03 ± 0.02	1.88 ± 0.63
IPA	49.82 ± 12.95	9.03 ± 1.23	4.97 ± 0.79	115.00 ± 20.70

IPA frozen	$49.85 \pm 9.97$	$5.01 \pm 0.90$	$3.95 \pm 0.59$	$91.4 \pm 13.17$
Methanol	$50.07 \pm 9.01$	$5.45 \pm 0.71$	$3.36 \pm 0.37$	$3.41 \pm 0.51$
Ethanol	$35.50 \pm 5.33$	$5.85 \pm 0.87$	$2.56 \pm 0.15$	$3.03 \pm 0.45$

With no stress fractures observed, the post-treated cross-linked hydrogels were tested for uniaxial tension in the form of dog bones (Figure 2b). The average stress-strain for these are presented in Figure 3b and c. All samples were tested in sets of 10. Unpost-treated cross-linked hydrogels were not testable due to becoming too soft after the rinse methods. Cross-linked hydrogels post-treated in IPA achieved the highest stress and energy

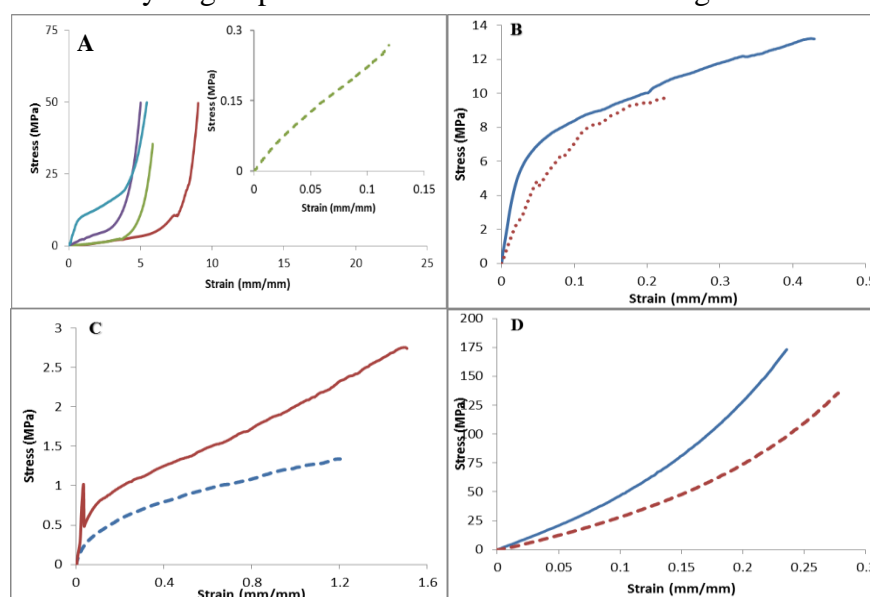


**Figure 3.2.** Average mechanical properties of cross-linked hydrogels, foams, and sponges. (A) Compression stress-strain graph of uncross-linked hydrogels (green, dashed) compared against cross-linked hydrogels: IPA (purple), IPA frozen (blue), MeOH (green), and EtOH (red). (B) Uniaxial tension stress-strain graph of IPA (blue, solid) and IPA frozen (red, dashed) post-treated hydrogels. (C) Uniaxial tension stress-strain graph of EtOH (red, solid) and MeOH (blue, dashed) post-treated hydrogels \*sharp peak observed in EtOH due to clamp tightened during testing. (D) Uniaxial tension stress-strain graph of wet frozen (blue, solid) and dry frozen (red, dashed) foams. (D) Compression stress-strain graph of wet frozen (blue, solid) and dry frozen (red, dashed) sponges.



**Figure 3.3.** (A) Compressed post-treated cross-linked cylindrical hydrogel with no stress fractures. (B) Post-treated cross-linked hydrogel as dog bone for uniaxial tension testing.

to break, at 13.23 MPa and 4.27 KJ/m<sup>3</sup>. All other post-treatments achieved far less stress and energy to break, with EtOH achieving the greatest strain at 151% (Table 3a). The mechanical properties of our rSSp hydrogels have been enhanced through cross-linking, demonstrating that we can tune the mechanical properties to applications.

<b>Table 3.3a.</b> Avg Mechanical Results for Post-treated Cross-linked Hydrogels Tested in Uniaxial Tension				
<b>Sample</b>	<b>Max Stress (MPa)</b>	<b>Max Strain (mm/mm)</b>	<b>Energy to Break (MJ/m<sup>3</sup>)</b>	<b>Young's Modulus (MPa)</b>
IPA	13.23 ± 2.42	0.43 ± 0.18	4.27 ± 0.96	101.00 ± 18.66
IPA frozen	9.72 ± 2.13	0.23 ± 0.06	3.77 ± 0.41	78.4 ± 10.08
Methanol	3.09 ± 0.52	0.26 ± 0.08	0.82 ± 0.02	5.22 ± 0.65
Ethanol	2.75 ± 0.38	1.51 ± 0.30	2.61 ± 0.31	4.07 ± 0.48

The average stress-strain for cross-linked foams is presented in Figure 3d. The freezing method, wet and dry, had a substantial impact on the foams mechanical properties. The strain of wet frozen foams increased by 187% with the energy to break increasing by 359% when compared to dry frozen foams (Table 3b). These cross-linked foams, wet and dry frozen, have surpassed the Young's modulus of IMPAXX foams (56 MPa)<sup>49</sup> commonly used in automotive safety to absorb energy moments of impact. The mechanical properties

of our cross-linked foams indicate they could be applied to a wide variety of applications.

<b>Table 3.3b.</b> Average Mechanical Results for Cross-linked Foams Tested in Compression.				
<b>Method</b>	<b>Max Stress (KPa)</b>	<b>Max Strain (mm/mm)</b>	<b>Energy to Break (KJ/m<sup>3</sup>)</b>	<b>Young's Modulus (KPa)</b>
Wet frozen foam	173.14 ± 30.27	0.24 ± 0.08	15.84 ± 2.62	370 ± 55.50
Dry frozen foam	137.01 ± 25.08	0.28 ± 0.07	14.29 ± 2.33	322 ± 51.52

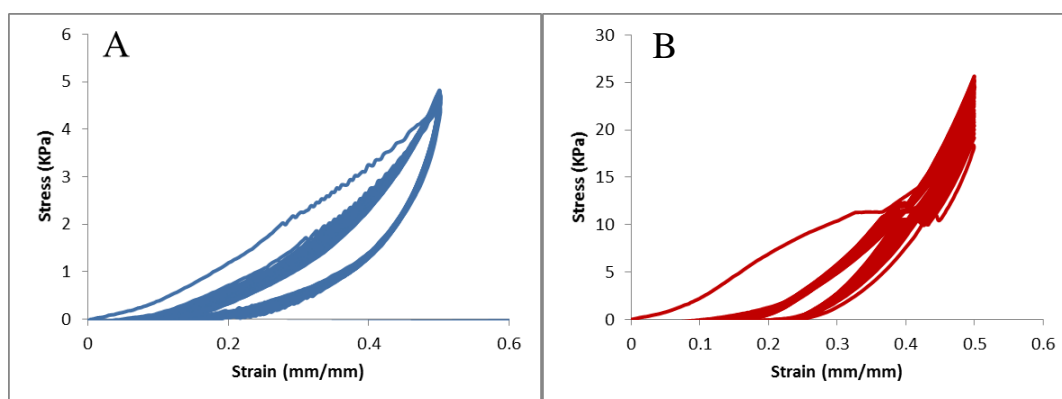


**Figure 3.4.** Average mechanical properties for cross-linked sponges tested in cyclical compression at 50% for 50 cycles. (A) Wet frozen sponge. (B) Dry frozen sponge.

The average stress-strain for cross-linked sponges mechanical testing results are presented graphically in Figure 4 and tabulated results presented in Table 4. The wet and dry frozen sponges were we compressed to 50% of maximum strain for 50 cycles. The stress of the wet frozen sponges did not decrease, demonstrating minimal deformation. The initial stress of the dry frozen sponges was 5.3x more than that of wet frozen sponges, however after the 50 cycles the stress decreased by 36%.

<b>Table 3.3c. Average Results for Cross-linked Sponges Tested in Cyclical Compressions.</b>				
<b>Method</b>	<b>Max Stress (KPa)</b>	<b>Strain</b>	<b>Energy to Break (KJ/m<sup>3</sup>)</b>	<b>Young's Modulus (KPa)</b>
Wet frozen sponge	4.82 ± 0.86	50%	13.42 ± 3.51	7.80 ± 1.40
Dry frozen sponge	25.66 ± 4.05	50%	37.32 ± 7.13	49.4 ± 8.39

### **Structural Characterization of Cross-linked rSSp Materials**

Post-treated cross-linked hydrogels, foams, and sponges were characterized using FTIR spectroscopy. The Amide I and II spectra of the post-treated cross-linked hydrogels was deconvoluted using Savitsky-Golay second derivative function, presented in Figure 5a and 5b, respectively. The most noticeable difference is the  $\beta$ -sheet content of each spectra. In Amide I, the IPA and frozen IPA samples contain the highest levels of  $\beta$ -sheets. One of the most noticeable differences in the Amide I region is observed with the ethanol post-treated cross-linked hydrogels. The Gly II helical content increased while the random coils almost completely disappear. Methanol post-treated cross-linked hydrogels are also observed to have a significant increase in random-coil content, Figure 5c.

In the Amide II region, the post-treatment with the highest  $\beta$ -sheet was methanol. When cross-linked hydrogels were frozen in IPA, there was a decrease in  $\beta$ -sheet and Gly II helical content when compared to unfrozen IPA hydrogels, explaining the decrease in all mechanical properties. The most noticeable difference was the increase in random coil content for ethanol post-treatments, exceeding all other post-treatments. This contributes to the ability of the EtOH post-treated samples to elongate 175% prior to failure. The increase in beta-sheet content for IPA explains why these materials are more rigid than

frozen IPA, methanol, and ethanol post-treated materials.

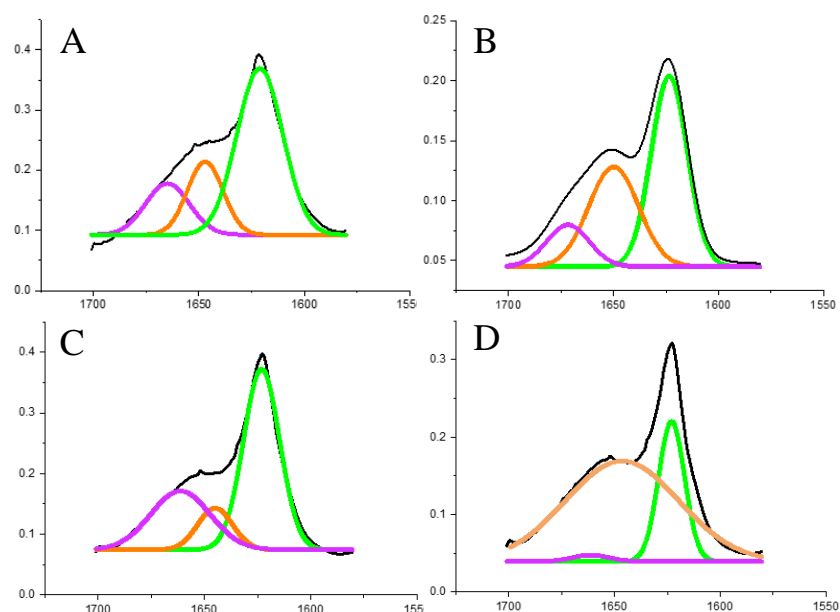


**Figure 3.5a.** Deconvoluted FT-IR Amide I of post-treated cross-linked hydrogels;  $1600\text{-}1700\text{cm}^{-1}$  (A) IPA (B) IPA frozen (C) MeOH (D) EtOH. (purple)- random coil, (orange)- Gly II helices, (green)-  $\beta$ -sheet

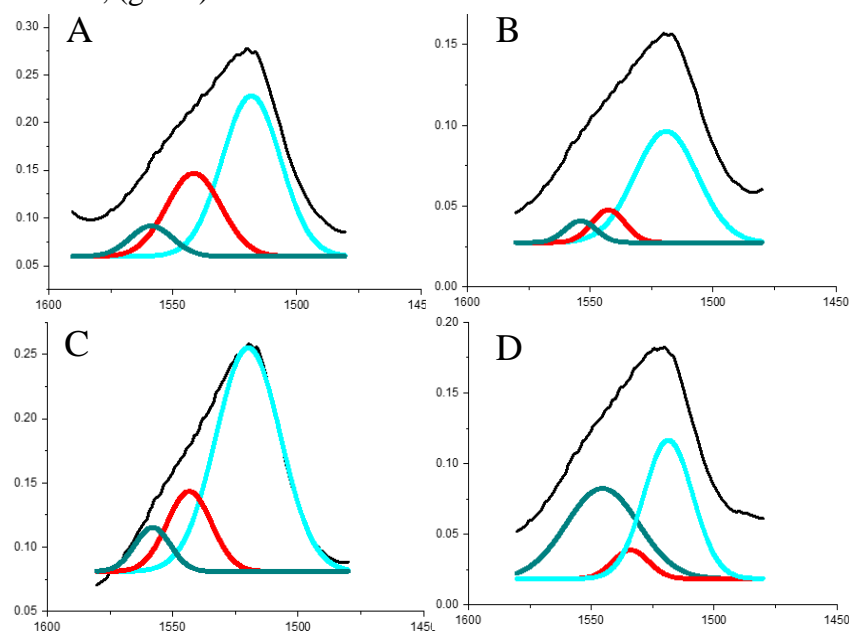


**Figure 3.5b.** Deconvoluted FT-IR Amide II of post-treated cross-linked hydrogels;  $1500\text{-}1600\text{cm}^{-1}$  (A) IPA (B) IPA Frozen (C) MeOH (D) EtOH. (dark blue)- random coil, (red)- Gly II helices, (light blue)-  $\beta$ -sheet



The Amide I and II regions, from 1400-1800  $\text{cm}^{-1}$ , were scanned and deconvoluted to elucidate the secondary structure of the materials. The spectra for the sponges and foams are presented in Figure 6a and b, respectively. Observed in the Amide I region, the wet frozen foams and sponges are almost identical in their beta-sheet, random coil, and Gly II helical content. The dry frozen foams and sponges also have identical peaks. The only difference in the spectra between foams and sponges was due to the freezing method. In the Amide I region, wet frozen sponges have a decrease in Gly II-helices and an increase in  $\beta$ -sheet content, explaining why the wet frozen sponges are more rigid and do not recoil to the extent of the dry frozen sponges.

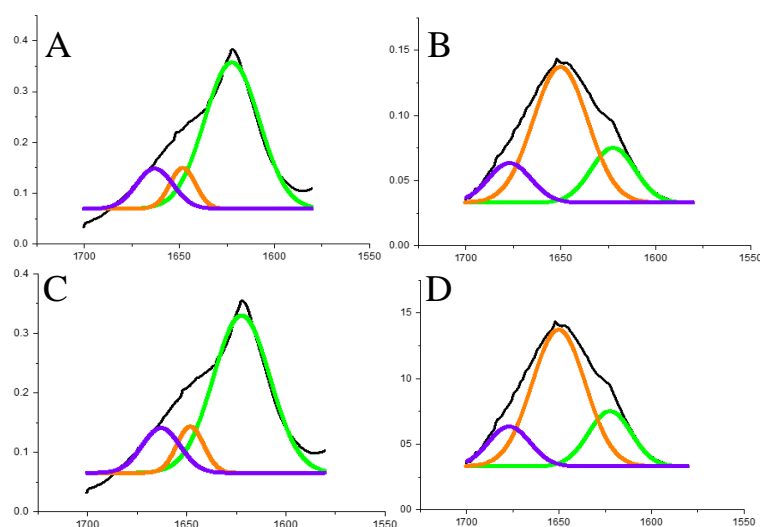


**Figure 3.6a.** Deconvoluted FT-IR Amide I of post-treated cross-linked hydrogels; 1600-1700 $\text{cm}^{-1}$  (A) Wet frozen foam (B) Dry frozen foam (C) Wet frozen sponge (D) Dry frozen sponge. (purple)- random coil, (orange)- Gly II helices, (green)-  $\beta$ -sheet

The most noticeable differences are within the Amide II region. The dry frozen foams have increased beta-sheet and random coil. This is hypothesized to be why the stress and strain are similar to wet frozen foams even with decreased  $\beta$ -sheet content in the Amide I region. The Amide II regions of dry frozen sponges were observed to increase in

$\beta$  -sheet content, hypothesized to be why the stress and energy to break increased in comparison to wet frozen sponges.

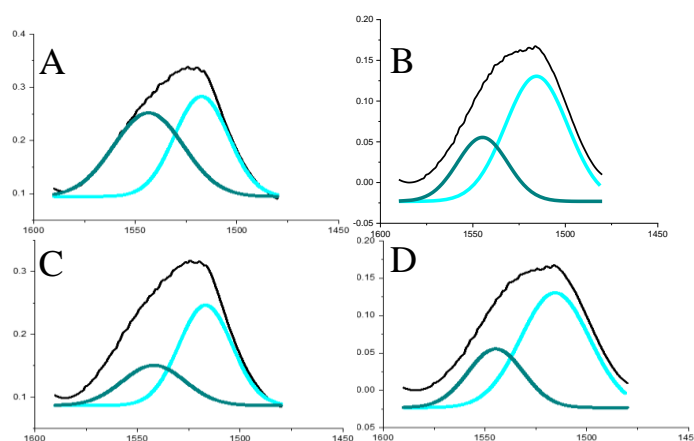


**Figure 3.6b.** Deconvoluted FT-IR Amide II of cross-linked foams and sponges; 1500-1600 $\text{cm}^{-1}$  (A)Wet frozen foam (B) Dry frozen foam (C)Wet frozen sponge (D) Dry frozen sponge. (dark blue)- random coil, (light blue)-  $\beta$ -sheet

### Increasing Biocompatibility by Removal of Excess Ruthenium

The presence of ruthenium can decrease the biocompatibility of cross-linked rSSp materials.<sup>50-52</sup> We utilized two methods for removal of excess ruthenium, a slow and expedited diffusivity rinse. Presented in Figure 7A and C, are examples of an unwashed and washed cross-linked hydrogels. For the slow rinse, cross-linked rSSp materials were placed into 50 mL conical tubes filled with deionized water and rotated for 24 hr. Since the ruthenium fluoresces orange,<sup>53-55</sup> the cross-linked materials were placed on the clip stage after each rinse. With the clip activated, materials that fluoresced orange, presented in Figure 7C (top hydrogel A), were rinsed using new water for another 24 hr. It was observed that after three days, all ruthenium was removed as shown in Figure 7C, hydrogel B.

To increase the rate of diffusivity, samples were autoclaved. Uncross-linked hydrogels do not have the strain and stress necessary to withstand being autoclaved, but the crosslinked materials show no damage. The expedited method utilizing autoclaving reduced rinsing time from three days to two hours. It was observed that unpost-treated cross-linked hydrogels had a volume increase of 65% making the hydrogel too soft to be mechanically tested. After two autoclave cycles, the materials no longer fluoresced orange. Utilizing the slow and expedited rinse methods, the *in vitro* biocompatibility of cross-linked rSSp materials was tested *in vitro*.

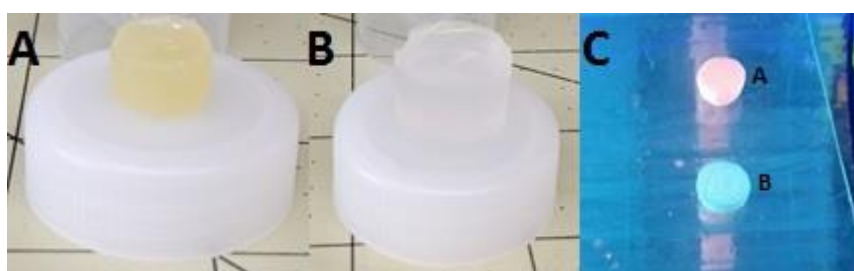


**Figure 3.7.** Rinse results of Cross-linked hydrogels. (A) Unwashed (B) Washed (C) CLIP used to excite excess Ruthenium.

### ***In vitro* Biocompatibility Testing of Washed Cross-linked Hydrogels**

To demonstrate the improved biocompatibility as a result of the rinse methods, two cell growth studies were performed. Two sets of cross-linked hydrogels were cast, cross-linked and post-treated in IPA, and MeOH. Ethanol post-treated samples were omitted due to an inability to promote healthy cell growth. One set was left unwashed, while the other set was washed using the expedited method described previously. Unpost-treated hydrogels were not used in this study because they were too weak and could not be mechanically tested on our system. Both sets of cross-linked hydrogels were cut into 1.15 mm thin wafers, placed into petri dishes and seeded with cells. Baby hamster kidney cells (Clone 31, Sigma Aldrich, 85011433-1VL) were used as they are genetically stable, grow

well in adherent and submerged cultures, and are virally resistant.<sup>56-62</sup> The cells were observed for proliferation and passaged several times onto the two sets of wafers, unwashed post-treated and washed post-treated, to observe the growth effects. The presence of the cross-linking reagents decreased the biocompatibility of the post-treated cross-linked hydrogels observed in Figure 8. The control well, Figure 8a has healthy cells while there is little to no cell growth in the unwashed cross-linked post treated hydrogel samples in Figure 8b and 8c. All cross-linked post-treated hydrogels did not hinder cell growth and created a matrix for the cells to grow upon observed in Figures 9b, and 9c.

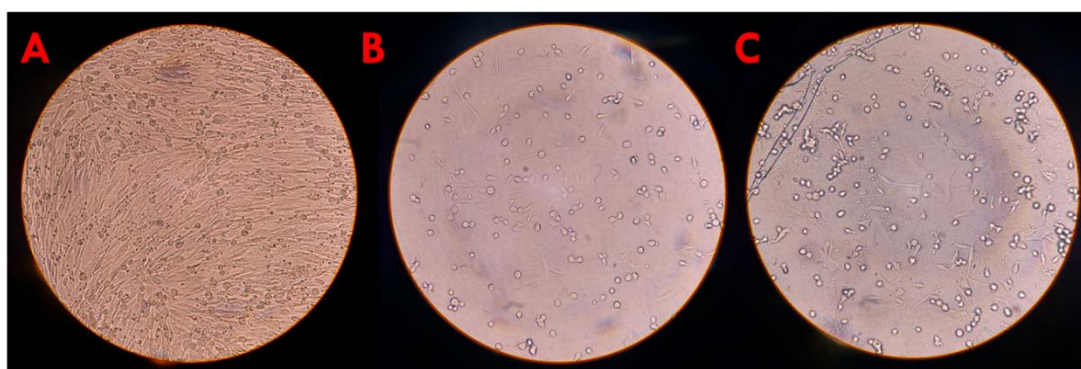


**Figure 3.8.** BHK cell growth study using unwashed cross-linked post-treated hydrogels. (A) Control well (B) IPA post-treated (C) methanol post-treated.

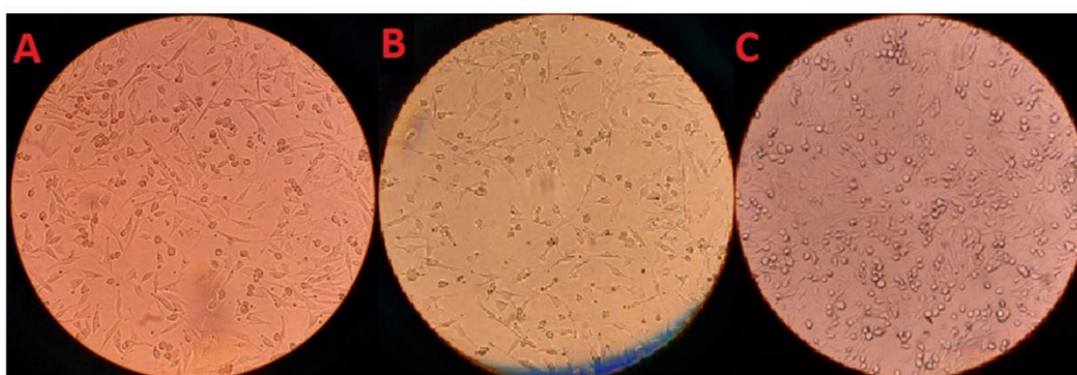


**Figure 3.9.** BHK cell growth study using washed cross-linked post-treated hydrogels. (A) Control well (B) IPA post-treated (C) methanol post-treated.

## Conclusion

To enhance our rSSp hydrogels, foams, and sponges, photo-induced cross-linking of unmodified proteins (PICUP) was used to generate intramolecular dityrosine cross-links. The cross-linked proteins generate materials with new properties. The cross-links resulted in a 200x, 21x, and 61x increase in the max stress, strain, and Young's modulus respectively of our hydrogels. This technique has also decreased the time necessary to form an rSSp hydrogel to just seconds. Traditional means of creating rSSp hydrogels such as increasing protein concentration, addition of propionic acid, and vigorous vortexing need to go through a gelation process to solidify into a hydrogel.<sup>12,25,26,29,31</sup> Using our modified techniques and the CLIP, we are able to create rSSp hydrogels virtually instantaneously when the samples are irradiated. This has enabled our group to create hydrogels, foams, and sponges of any shape. Our technique has also demonstrated a proof of concept for 3D printing applications. These materials stress, strain, and tensile strength can further be enhanced when post-treated in alcohol baths. Through mechanical testing and initial *in vitro* biocompatibility testing, we have demonstrated the properties of the cross-linked materials for potential future uses.

## References

- (1) Lewis, R. V. Spider Silk: Ancient Ideas for New Biomaterials. *Chem. Rev.* **2006**, *106* (9), 3762–3774.
- (2) Gatesy, J.; Hayashi, C.; Motriuk, D.; Woods, J.; Lewis, R. Extreme Diversity, Conservation, and Convergence of Spider Silk Fibroin Sequences. *Science* **2001**, *291* (5513), 2603–2605.
- (3) Brunetta, L.; Craig, C. L. *Spider Silk: Evolution and 400 Million Years of Spinning, Waiting, Snagging, and Mating*; Yale University Press, 2010.
- (4) Hayashi, C. Y.; Shipley, N. H.; Lewis, R. V. Hypotheses That Correlate the Sequence, Structure, and Mechanical Properties of Spider Silk Proteins. *Int. J. Biol. Macromol.* **1999**, *24* (2–3), 271–275.
- (5) Jenkins, J. E.; Creager, M. S.; Lewis, R. V.; Holland, G. P.; Yarger, J. L. Quantitative Correlation between the Protein Primary Sequences and Secondary Structures in Spider Dragline Silks. *Biomacromolecules* **2010**, *11* (1), 192–200.
- (6) Lefèvre, T.; Rousseau, M.-E.; Pézolet, M. Protein Secondary Structure and Orientation in Silk as Revealed by Raman Spectromicroscopy. *Biophys. J.* **2007**, *92* (8), 2885–2895.
- (7) Hinman, M. B.; Jones, J. A.; Lewis, R. V. Synthetic Spider Silk: A Modular Fiber. *Trends Biotechnol.* **2000**, *18* (9), 374–379.
- (8) Vollrath, F.; Knight, D. P. Liquid Crystalline Spinning of Spider Silk. *Nature* **2001**, *410* (6828), 541–548.
- (9) Stauffer, S. L.; Coguill, S. L.; Lewis, R. V. Comparison of Physical Properties of Three Silks from *Nephila clavipes* and *Araneus gemmoides*. *J. Arachnol.* **1994**, *22* (1), 5–11.
- (10) Dams-Kozłowska, H.; Majer, A.; Tomaszewicz, P.; Lozinska, J.; Kaplan, D. L.; Mackiewicz, A. Purification and Cytotoxicity of Tag-Free Bioengineered Spider Silk Proteins. *J. Biomed. Mater. Res.* **2013**, *101* (2), 456–464.
- (11) Gomes, S.; Gallego-Llamas, J.; Leonor, I. B.; Mano, J. F.; Reis, R. L.; Kaplan, D. L. In Vivo Biological Responses to Silk Proteins Functionalized with Bone Sialoprotein. *Macromol. Biosci.* **2013**, *13* (4), 444–454.
- (12) Chao, P.-H. G.; Yodmuang, S.; Wang, X.; Sun, L.; Kaplan, D. L.; Vunjak-Novakovic, G. Silk Hydrogel for Cartilage Tissue Engineering. *J. Biomed. Mater. Res. B Appl. Biomater.* **2010**, *95B* (1), 84–90.
- (13) Wang, Y.; Kim, H.-J.; Vunjak-Novakovic, G.; Kaplan, D. L. Stem Cell-Based Tissue Engineering with Silk Biomaterials. *Biomaterials* **2006**, *27* (36), 6064–6082.
- (14) Altman, G. H.; Diaz, F.; Jakuba, C.; Calabro, T.; Horan, R. L.; Chen, J.; Lu, H.; Richmond, J.; Kaplan, D. L. Silk-Based Biomaterials. *Biomaterials* **2003**, *24* (3), 401–416.
- (15) Vepari, C.; Kaplan, D. L. Silk as a Biomaterial. *Prog. Polym. Sci.* **2007**, *32* (8), 991–1007.
- (16) Spiess, K.; Lammel, A.; Scheibel, T. Recombinant Spider Silk Proteins for Applications in Biomaterials. *Macromol. Biosci.* **2010**, *10* (9), 998–1007.
- (17) MacIntosh, A. C.; Kearns, V. R.; Crawford, A.; Hatton, P. V. Skeletal Tissue Engineering Using Silk Biomaterials. *J. Tissue Eng. Regen. Med.* **2008**, *2* (2–3), 71–80.
- (18) Cao, Y.; Wang, B. Biodegradation of Silk Biomaterials. *Int. J. Mol. Sci.* **2009**, *10* (4), 1514–1524.
- (19) Slotta, U. K.; Rammensee, S.; Gorb, S.; Scheibel, T. An Engineered Spider Silk Protein Forms Microspheres. *Angew. Chem. Int. Ed.* **2008**, *47* (24), 4592–4594.
- (20) Huang, J.; Wong, C.; George, A.; Kaplan, D. L. The Effect of Genetically Engineered Spider Silk-Dentin Matrix Protein 1 Chimeric Protein on Hydroxyapatite Nucleation. *Biomaterials* **2007**, *28* (14), 2358–2367.
- (21) Porter, D.; Vollrath, F. Nanoscale Toughness of Spider Silk. *Nano Today* **2007**, *2* (3), 6.

- (22) Gould, P. Exploiting Spiders' Silk. *Mater. Today* **2002**, *5* (12), 42–47.
- (23) Miller, J. A.; Nagarajan, V. The Impact of Biotechnology on the Chemical Industry in the 21st Century. *Trends Biotechnol.* **2000**, *18* (5), 190–191.
- (24) Florczak, A.; Mackiewicz, A.; Dams-Kozłowska, H. Functionalized Spider Silk Spheres As Drug Carriers for Targeted Cancer Therapy. *Biomacromolecules* **2014**, *15* (8), 2971–2981.
- (25) Jones, J. A.; Harris, T. I.; Tucker, C. L.; Berg, K. R.; Christy, S. Y.; Day, B. A.; Gaztambide, D. A.; Needham, N. J. C.; Ruben, A. L.; Oliveira, P. F.; et al. More Than Just Fibers: An Aqueous Method for the Production of Innovative Recombinant Spider Silk Protein Materials. *Biomacromolecules* **2015**.
- (26) Schacht, K.; Scheibel, T. Controlled Hydrogel Formation of a Recombinant Spider Silk Protein. *Biomacromolecules* **2011**, *12*, 2488–2495.
- (27) Rammensee, S.; Huemmerich, D.; Hermanson, K. D.; Scheibel, T.; Bausch, A. R. Rheological Characterization of Hydrogels Formed by Recombinantly Produced Spider Silk. *Appl. Phys. A* **2006**, *82* (2), 261–264.
- (28) Schacht, K.; Jüngst, T.; Schweinlin, M.; Ewald, A.; Groll, J.; Scheibel, T. Biofabrication of Cell-Loaded 3D Spider Silk Constructs. *Angew. Chem. Int. Ed.* **2015**, *54* (9), 2816–2820.
- (29) Yucel, T.; Cebe, P.; Kaplan, D. L. Vortex-Induced Injectable Silk Fibroin Hydrogels. *Biophys. J.* **2009**, *97* (7), 2044–2050.
- (30) Vendrely, C.; Scheibel, T. Biotechnological Production of Spider-Silk Proteins Enables New Applications. *Macromol. Biosci.* **2007**, *7* (4), 401–409.
- (31) Numata, K.; Yamazaki, S.; Naga, N. Biocompatible and Biodegradable Dual-Drug Release System Based on Silk Hydrogel Containing Silk Nanoparticles. *Biomacromolecules* **2012**, *13* (5), 1383–1389.
- (32) Rahimi, F.; Maiti, P.; Bitan, G. Photo-Induced Cross-Linking of Unmodified Proteins (PICUP) Applied to Amyloidogenic Peptides. *J. Vis. Exp. JoVE* **2009**, No. 23.
- (33) Fancy, D. A.; Denison, C.; Kim, K.; Xie, Y.; Holdeman, T.; Amini, F.; Kodadek, T. Scope, Limitations and Mechanistic Aspects of the Photo-Induced Cross-Linking of Proteins by Water-Soluble Metal Complexes. *Chem. Biol.* **2000**, *7* (9), 697–708.
- (34) Preston, G. W.; Wilson, A. J. Photo-Induced Covalent Cross-Linking for the Analysis of Biomolecular Interactions. *Chem. Soc. Rev.* **2013**, *42* (8), 3289–3301.
- (35) Shetlar, M. D. Cross-Linking of Proteins to Nucleic Acids by Ultraviolet Light. In *Photochemical and Photobiological Reviews*; Springer, Boston, MA, 1980; pp 105–197.
- (36) Truong, M. Y.; Dutta, N. K.; Choudhury, N. R.; Kim, M.; Elvin, C. M.; Nairn, K. M.; Hill, A. J. The Effect of Hydration on Molecular Chain Mobility and the Viscoelastic Behavior of Resilin-Mimetic Protein-Based Hydrogels. *Biomaterials* **2011**, *32* (33), 8462–8473.
- (37) Fancy, D. A.; Kodadek, T. Chemistry for the Analysis of Protein–protein Interactions: Rapid and Efficient Cross-Linking Triggered by Long Wavelength Light. *Proc. Natl. Acad. Sci.* **1999**, *96* (11), 6020–6024.
- (38) Bitan, G. Structural Study of Metastable Amyloidogenic Protein Oligomers by Photo-Induced Cross-Linking of Unmodified Proteins. In *Methods in Enzymology*; Amyloid, Prions, and Other Protein Aggregates, Part C; Academic Press, 2006; Vol. 413, pp 217–236.
- (39) Sinz, A. Chemical Cross-Linking and Mass Spectrometry to Map Three-Dimensional Protein Structures and Protein–protein Interactions. *Mass Spectrom. Rev.* **2006**, *25* (4), 663–682.
- (40) Howerton, B. S.; Heidary, D. K.; Glazer, E. C. Strained Ruthenium Complexes Are Potent Light-Activated Anticancer Agents. *J. Am. Chem. Soc.* **2012**, *134* (20), 8324–8327.

- (41) Costas N, K.; Jeffrey D, T.; Anthoula, K. Production of Biofilaments in Transgenic Animals, US Patent 7,157,615. US Patent 7157615, June 27, 2001.
- (42) Tucker, C. L.; Jones, J. A.; Bringham, H. N.; Copeland, C. G.; Addison, J. B.; Weber, W. S.; Mou, Q.; Yarger, J. L.; Lewis, R. V. Mechanical and Physical Properties of Recombinant Spider Silk Films Using Organic and Aqueous Solvents. *Biomacromolecules* **2014**, *15* (8), 3158–3170.
- (43) Zhou, Y.; Rising, A.; Johansson, J.; Meng, Q. Production and Properties of Triple Chimeric Spidroins. *Biomacromolecules* **2018**.
- (44) Whittaker, J. L.; Choudhury, N. R.; Dutta, N. K.; Zannettino, A. Facile and Rapid Ruthenium Mediated Photo-Crosslinking of Bombyx Mori Silk Fibroin. *J. Mater. Chem. B* **2014**, *2* (37), 6259.
- (45) Ding, D.; Guerette, P. A.; Fu, J.; Zhang, L.; Irvine, S. A.; Miserez, A. From Soft Self-Healing Gels to Stiff Films in Suckerin-Based Materials Through Modulation of Crosslink Density and  $\beta$ -Sheet Content. *Adv. Mater.* **2015**, *27* (26), 3953–3961.
- (46) Huang, P.; Zeidler, A.; Chang, W.; Ansell, M. P.; Chew, Y. M. J.; Shea, A. Specific Heat Capacity Measurement of Phyllostachys Edulis (Moso Bamboo) by Differential Scanning Calorimetry. *Constr. Build. Mater.* **2016**, *125*, 821–831.
- (47) Young's Modulus - Tensile and Yield Strength for common Materials  
[https://www.engineeringtoolbox.com/young-modulus-d\\_417.html](https://www.engineeringtoolbox.com/young-modulus-d_417.html) (accessed May 18, 2018).
- (48) Overview of materials for Low Density Polyethylene (LDPE), Molded  
<https://web.archive.org/web/20110101084650/http://www.matweb.com/search/dataset.aspx?MatGUID=557b96c10e0843dbb1e830ceedeb35b0> (accessed May 18, 2018).
- (49) de Vries, D. V. W. M. Characterization of Polymeric Foams.pdf  
<https://pdfs.semanticscholar.org/008e/a87620d0f87d9ea4d17d74bd41722c0c6ffd.pdf> (accessed May 18, 2018).
- (50) Brabec, V.; Nováková, O. DNA Binding Mode of Ruthenium Complexes and Relationship to Tumor Cell Toxicity. *Drug Resist. Updat.* **2006**, *9* (3), 111–122.
- (51) Frasca, D.; Ciampa, J.; Emerson, J.; Umans, R. S.; Clarke, M. J. Effects of Hypoxia and Transferrin on Toxicity and DNA Binding of Ruthenium Antitumor Agents in Hela Cells  
<https://www.hindawi.com/journals/mbd/1996/973585/abs/> (accessed May 15, 2018).
- (52) Elvin, C. M.; Vuocolo, T.; Brownlee, A. G.; Sando, L.; Huson, M. G.; Liyou, N. E.; Stockwell, P. R.; Lyons, R. E.; Kim, M.; Edwards, G. A.; et al. A Highly Elastic Tissue Sealant Based on Photopolymerised Gelatin. *Biomaterials* **2010**, *31* (32), 8323–8331.
- (53) Chuang, H.; Arnold, M. A. Linear Calibration Function for Optical Oxygen Sensors Based on Quenching of Ruthenium Fluorescence. *Anal. Chim. Acta* **1998**, *368* (1), 83–89.
- (54) Razeq, T. M. A.; Spear, S.; Hassan, S. S. M.; Arnold, M. A. Selective Measurement of Chromium(VI) by Fluorescence Quenching of Ruthenium. *Talanta* **1999**, *48* (2), 269–275.
- (55) Bhasikuttan, A. C.; Suzuki, M.; Nakashima, S.; Okada, T. Ultrafast Fluorescence Detection in Tris(2,2'-Bipyridine)Ruthenium(II) Complex in Solution: Relaxation Dynamics Involving Higher Excited States. *J. Am. Chem. Soc.* **2002**, *124* (28), 8398–8405.
- (56) Lazaris, A.; Arcidiacono, S.; Huang, Y.; Zhou, J.-F.; Duguay, F.; Chretien, N.; Welsh, E. A.; Soares, J. W.; Karatzas, C. N. Spider Silk Fibers Spun from Soluble Recombinant Silk Produced in Mammalian Cells. *Science* **2002**, *295* (5554), 472–476.
- (57) Dumont, J.; Eewart, D.; Mei, B.; Estes, S.; Kshirsagar, R. Human Cell Lines for Biopharmaceutical Manufacturing: History, Status, and Future Perspectives. *Crit. Rev. Biotechnol.* **2016**, *36* (6), 1110–1122.



- (58) Garcia, L.; Viaplana, E.; Urniza, A. Comparison of BHK-21 Cell Growth on Microcarriers vs in Suspension at 2L Scale Both in Conventional Bioreactor and Single-Use Bioreactor (Univessel® SU). *BMC Proc.* **2013**, *7* (Suppl 6), P40.
- (59) Bradshaw, G. L.; Sato, G. H.; McClure, D. B.; Dubes, G. R. The Growth Requirements of BHK-21 Cells in Serum-free Culture. *J. Cell. Physiol.* **1983**, *114* (2), 215–221.
- (60) J. Radlett, P. The Use of BHK Suspension Cells for the Production of Foot and Mouth Disease Vaccines. In *Adv. Biochem. Eng. Biotechnol.*; 1970; Vol. 34, pp 129–146.
- (61) Bouck, N.; di Mayorca, G. [24] Evaluation of Chemical Carcinogenicity by in Vitro Neoplastic Transformation. In *Methods in Enzymology*; Cell Culture; Academic Press, 1979; Vol. 58, pp 296–302.
- (62) Kamal, T.; Naeem, K.; Munir, A.; Ali, M.; Ullah, A. Comparative Study for the Sensitivity of BHK-21 and Bovine Kidney Cell Line for the Isolation of FMD Viruses. In *Proceedings of 2014 11th International Bhurban Conference on Applied Sciences Technology (IBCAST) Islamabad, Pakistan, 14th - 18th January, 2014*; 2014; pp 59–64.

## CHAPTER IV

### CONCLUSION

Modifying the iMe electrospinner has enabled our group to create continuous electrospun yarns composed of HFIP solubilized rSSp. Through extensive experimentation of electrospinning rSSp, we have concluded that aqueous-based and composite dopes are incapable of creating fibers. The polymers used as a carrier in the composite dopes believed to aid in rSSp to form fibers. However, without the incorporation of a coagulation bath, the shear stress is not enough to mature the rSSp into fibers, resulting in composite material with randomly distributed rSSp. This, in turn, decreases the mechanical properties due to the rSSp interrupting the polymer chains.

Wet-spinning is able to create fibers from aqueous-based dopes by incorporating a coagulation bath containing alcohols that mature the proteins into fibers. Without being able to safely incorporate a coagulation bath into electrospinning, it is impossible to force the aqueous-based dopes to form their secondary, tertiary, and quaternary structures to create a mature fiber. Using HFIP as the solvent, rSSp are kept in a transitional state, enabling us to create yarns using continuous electrospinning without the incorporation of a coagulation bath. These yarns are composed of hundreds of nanofibers possessing no stress focal points. This results in yarns with mechanical properties surpassing those of natural silk, enabling us to create yarns with novel properties.

Recombinant spider-silk protein materials already possess desirable properties that can be applied in the medical field. However, they do not always meet the need for certain applications, such as bone or cartilage replacement. To further enhance the mechanical properties of non-fiber rSSp materials, we have utilized PICUP in a novel manner. Through

extensive experimentation, the optimal concentrations of ruthenium and APS were used to create stock solutions. Using a method developed in our lab, these stock solutions are used to solubilize our proteins, creating a dope that has the cross-linking components within. This step removes the overnight diffusivity commonly used in PICUP. This method has also increased the efficiency of our cross-linking reaction, enabling the materials to be cross-linked throughout the entire substance instead of creating a core-shell structure seen with diffusivity.

The creation of the CLIP enabled our group to drive the cross-linking reaction to maximum efficiency, instantaneously initiating the reaction resulting in novel materials. The increased efficiency of our technique has also created a method for 3D printing with our rSSp. This removes the need for molds and decreases the time needed for solidification of hydrogels. Post-treating these cross-linked materials further enhances their mechanical properties, creating a wide array of materials with varying physical and chemical properties. Utilizing continuous electrospinning and PICUP, our group has created novel rSSp materials with robust and tunable properties.

### **Future Work**

Research will continue to devise a method for creating continuously electrospun yarns from aqueous-based dopes. This is critical to upscale the process to produce viable amounts of robust rSSp yarns that will surpass the mechanical properties of natural silk. Using computational programs, the electric field will be studied with the goal of understanding the physics of electrospinning. This will give us a better insight as to why fibers do not always collect onto the target and why certain dopes do not electrospin. Modifying the iMe electrospinner further will enable us to efficiently create and collect

yarns for further post-treatment with the goal of upscaling the process.

The cross-linked rSSp materials studied in this research are just a few of the possible permutations. Using different post-treatment baths can result in materials with novel properties. 3D printing using the CLIP will also be explored, creating shapes that could be used in the medical setting as replacements for cartilage, bone, etc. These new cross-linked materials will be characterized using mechanical testing, structural analysis (FT-IR, Raman, NMR), and biocompatibility studies, assessing the possible applications.

## APPENDICES

## APPENDIX A

MODIFICATIONS TO IME ELECTROSPINNER TO PRODUCE CONTINUOUS  
YARNS

The iMe electrospinner (Model: EC-DIG/P12043) was purchased by our group to create electrospun materials composed of pure rSSp or composites with polymers. The machine came with two targets, a stationary circular target and a rotating drum. The stationary target is used to assess whether the solution is capable of forming fibers. When the solutions have been deemed appropriate for electrospinning, they are used to electrospin onto the rotating drum. The rotating drum creates mats composed of oriented nanofibers, resulting in a porous mat. These mats can be used as is or can further be processed into yarns. This is done by cutting 2 mm strips — oriented with fiber direction — then rotating the yarn in either direction to create a twisted yarn. This process can result in yarns with cuts and diameter inconsistencies, resulting in stress focal points that cause the yarns to fail. For this reason, continuously produced electrospun yarns are of interest to our group.

The modifications to our iMe electrospinner are derived from the design created at Deakin University by Dr. Tong Lin. His design consists of two syringe pumps with polymers loaded into syringes, as well as a grounded metal funnel that is used as the target. When voltage is applied, the oppositely charged nanofibers collect onto the grounded metal funnel. This, in turn, creates a highly twisted, continuous electrospun yarn.

Our modifications are based on this design, with alterations to enable us to use our rSSp for electrospinning. A DC motor purchased from Dayton (model number: 3LCH7) was used to rotate the metal funnel. The power supply was purchased from Amazon.com (model number: S-360-12) to control the motor attached to the funnel using an attached potentiometer. The funnel was custom made by Lunazul Gallery on Etsy. The funnel has an



Figure A1:  
Metal funnel

opening of 63 mm, a bell height of 30 mm and a stem height of 50 mm (Figure A1). The stem has an opening of 12.5 mm that's designed to slip onto a 12.5 mm oak dowel purchased from Lowes. Wood was chosen as the connector from the motor to the funnel to prevent any charge from shorting out the motor.

Preliminary trials used two syringe pumps that were loaded with our rSSp dopes and had one electrode connected to each syringe tip. This was unsuccessful. Fibers did not collect onto the rotating funnel or form within the electrospinning chamber. To address this, our group removed the ground from the rotating funnel and attached the negative electrode to the funnel. A stabilizing chamber with a connector for the electrode was created using ¼ inch thick polycarbonate sheets (Figure A2). When the voltage was applied,

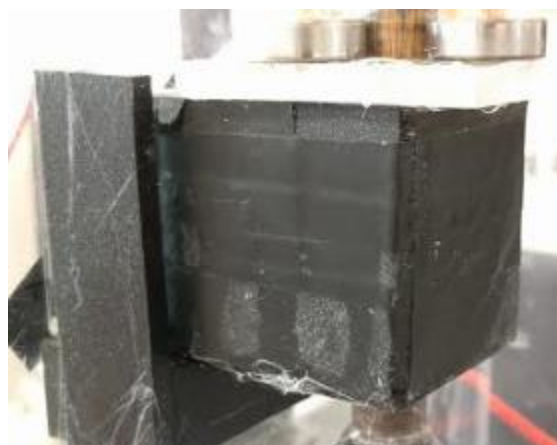


Figure A2: Stabilizing chamber with electrode attachment

fibers were seen to collect onto the mouth of the funnel, successfully creating electrospun fibers from our solutions. To collect the continuous electrospun yarn produced, we created a reeling system located outside of the electrospinning chamber. The reeling system consists of an 18 cm long, 2.14 cm wide PVC tube purchased from Lowe's. The yarn retriever that slides into and out of the PVC tube is a 31 cm long, 6.5 mm thick oak dowel that has a glass rod attached at the end. The glass rod is used to attract the yarn, while the wooden dowel prevents the researcher from being shocked. Pulley systems were created using polycarbonate to maintain the yarn's tension and alignment. With the yarn pulled through the PVC tube, it is attached to a rotating motor outside the system (Figure A3).





Figure A3: Reeling system for continuous electrospinning

## APPENDIX B

## INSULATING IME ELECTROSPINNER TO REDUCE STATIC INTERFERENCE

Several factors contribute to successful electrospinning. One of the main factors that decreases the efficiency of electrospinning is static charge. To efficiently electrospin, humidity has to be within a narrow range — 20-30% relative humidity. When this range is not met, a static charge is present throughout the chamber. Any materials that can hold a charge will attract electrospun fibers, reducing the efficiency of collecting them onto a target. To address this, our group created an anti-static housing for our syringe pumps, reducing the affinity for fibers to attach on the metal of the pump. This housing was covered in an anti-static rubber spray purchased from Lowe's (Performix, Plasti Dip). The housing was then covered completely using electrical tape to further reduce any static charge (Figure B1 and B2). This Plasti Dip was also used to coat the stabilizing chamber and the outside of the funnel.

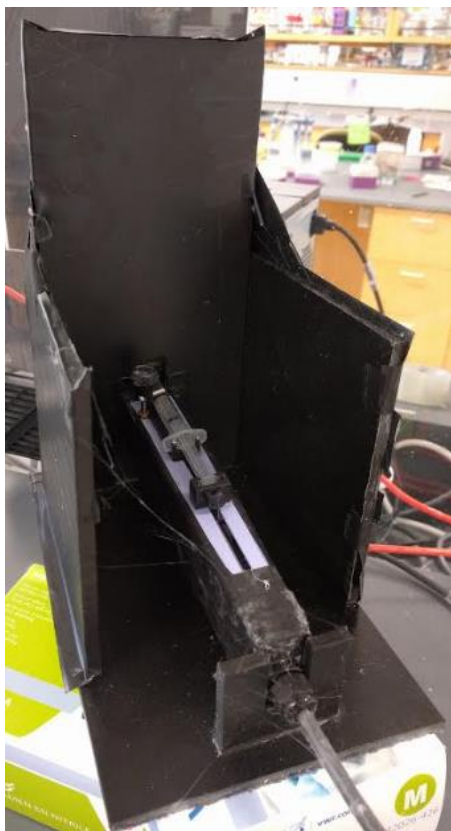


Figure B1: Back- opening for syringe pump



Figure B2: Front end of housing with syringe tip exposed.

## APPENDIX C

PRELIMINARY CROSS-LINKING EXPERIMENTS USING HAND-HELD  
FLASHLIGHTS

Preliminary cross-linking experiments utilized a 1000 lumen Maglite. Using this light source, materials had to be irradiated for 5 minutes to drive the reaction to completion. To decrease irradiation time, and thus increase the reaction's efficiency, we used a 1600 lumen Duracell flashlight. Experiments using this light source required only 2.5 minutes of irradiation time. By increasing the light intensity, we were able to successfully increase the efficiency of the reaction. However, hydrogels that were cross-linked using these handheld light sources all had a common characteristic. When compressed through mechanical testing, all cross-linked hydrogels would break apart in two distinguishing parts: a core and shell. This led our group to believe our materials were being cross-linked, but the reaction was not fully penetrating the substance. To address this, our group set out to create a light source specifically designed to maximize the efficiency of the cross-linking reaction.

## APPENDIX D

## CONSTRUCTION OF CROSS-LINK INITIATING PHOTODIODE (CLIP)

Most research groups that perform PICUP to modify proteins employ a 200 W Xenon arc lamp, ranging in cost from \$1,500 to \$4,000. Due to the heat generated from the light, they cannot be activated for prolonged periods of time. We set out to create our own high-intensity light source for a fraction of the cost. To further increase the efficiency of our experiments, we created the cross-link initiated photodiode (CLIP). The CLIP has been designed for maximum efficiency of our cross-linking experiments. The CLIP housing is composed of a box made up of ½ inch thick polycarbonate sheets with air vents cut into them to ensure proper air flow. The CLIP originally consisted of a 200 w Bright White LED (broad spectrum) purchased on Amazon. This LED is equivalent to 16,000 lumens. The LED is attached to a Corsair Hydro Series Extreme Performance Liquid CPU Cooler H100I, also purchased from Amazon, to reduce heat and prolong the life of the LED. The supplies for the LED and cooling unit were purchased from eBay. Extra fans were mounted to the cooling unit to further increase efficiency. A two-way switch was purchased from Lowe's and integrated into the LED and cooling system. This enabled us to power the LED and cooling system separately. Chinese moso bamboo, which is approximately 8 inches in diameter and ½ inch in thickness, was used for the stage of the CLIP due to bamboo's heat resistance. Plastics used prior to the staging area would melt due to the extreme heat produced. To further reduce heat, two 3-inch fans were mounted onto either side of the staging area. Preliminary experiments using the CLIP instantaneously cross-linked our materials, solidifying them into a gel upon being irradiated. This enabled our group to essentially 3D print using the CLIP and cross-linking dopes. Research into the cross-linking components revealed that ruthenium is activated at a specific wavelength, 460 nm.

With this knowledge, the original 200 w bright white LED was exchanged for a 200 w Blue LED with a wavelength of 465 nm (Figure D1).



Figure D1: CLIP with 465 nm LED. Red arrow indicates cooling system.

Using this updated CLIP, our materials have surpassed the mechanical load cell of 50 N. The efficiency of the CLIP has driven the cross-linking reaction into a cascading effect. When attempting to 3D print, the syringe must be moved quickly — otherwise, the cross-linking will travel up the syringe tip, solidifying the contents. When cross-linked hydrogels are compressed, we no longer observe the core-shell structure seen with handheld light sources. Instead, the cross-linked hydrogels compress into a disc with no visible stress fractures on any side.



## APPENDIX D

## COPYRIGHTS AND PERMISSIONS FOR REPLICATION

4/24/2018

Rightslink® by Copyright Clearance Center

**RightsLink®****SPRINGER NATURE**

**Title:** Efficient protein production inspired by how spiders make silk

**Author:** Nina Kronqvist, Médoune Sarr, Anton Lindqvist, Kerstin Nordling, Martins Otikovs et al.

**Publication:** Nature Communications

**Publisher:** Springer Nature

**Date:** May 23, 2017

Copyright © 2017, Springer Nature

### Creative Commons

This is an open access article distributed under the terms of the [Creative Commons CC BY](#) license, which permits unrestricted use, distribution, and reproduction in any medium, provided the original work is properly cited.

You are not required to obtain permission to reuse this article.

Are you the [author](#) of this Springer Nature article?

To order reprints of this content, please contact Springer Nature by e-mail at [reprintswarehouse@springernature.com](mailto:reprintswarehouse@springernature.com), and you will be contacted very shortly with a quote.

4/24/2018

Rightslink® by Copyright Clearance Center



# RightsLink®

[Home](#)
[Create Account](#)
[Help](#)


**Title:** Nephila clavipes Flagelliform Silk-Like GGX Motifs Contribute to Extensibility and Spacer Motifs Contribute to Strength in Synthetic Spider Silk Fibers

**Author:** Sherry L. Adrianos, Florence Teulé, Michael B. Hinman, et al

**Publication:** Biomacromolecules

**Publisher:** American Chemical Society

**Date:** Jun 1, 2013

Copyright © 2013, American Chemical Society

#### LOGIN

If you're a [copyright.com](#) user, you can login to RightsLink using your [copyright.com](#) credentials. Already a RightsLink user or want to [learn more?](#)

### PERMISSION/LICENSE IS GRANTED FOR YOUR ORDER AT NO CHARGE

This type of permission/license, instead of the standard Terms & Conditions, is sent to you because no fee is being charged for your order. Please note the following:

- Permission is granted for your request in both print and electronic formats, and translations.
- If figures and/or tables were requested, they may be adapted or used in part.
- Please print this page for your records and send a copy of it to your publisher/graduate school.
- Appropriate credit for the requested material should be given as follows: "Reprinted (adapted) with permission from (COMPLETE REFERENCE CITATION). Copyright (YEAR) American Chemical Society." Insert appropriate information in place of the capitalized words.
- One-time permission is granted only for the use specified in your request. No additional uses are granted (such as derivative works or other editions). For any other uses, please submit a new request.

If credit is given to another source for the material you requested, permission must be obtained from that source.

[BACK](#)
[CLOSE WINDOW](#)

Copyright © 2018 [Copyright Clearance Center, Inc.](#) All Rights Reserved. [Privacy statement](#), [Terms and Conditions](#). Comments? We would like to hear from you. E-mail us at [customercare@copyright.com](mailto:customercare@copyright.com)

4/24/2018

Rightslink® by Copyright Clearance Center



# RightsLink®

[Home](#)
[Create Account](#)
[Help](#)


**ACS Publications**  
Most Trusted. Most Cited. Most Read.

**Title:** Conformation of Spider Silk Proteins In Situ in the Intact Major Ampullate Gland and in Solution

**Author:** Thierry Lefèvre, Jérémie Leclerc, Jean-François Rioux-Dubé, et al

**Publication:** Biomacromolecules

**Publisher:** American Chemical Society

**Date:** Aug 1, 2007

Copyright © 2007, American Chemical Society

**LOGIN**

If you're a [copyright.com](#) user, you can login to RightsLink using your [copyright.com](#) credentials. Already a RightsLink user or want to [learn more?](#)

## PERMISSION/LICENSE IS GRANTED FOR YOUR ORDER AT NO CHARGE

This type of permission/license, instead of the standard Terms & Conditions, is sent to you because no fee is being charged for your order. Please note the following:

- Permission is granted for your request in both print and electronic formats, and translations.
- If figures and/or tables were requested, they may be adapted or used in part.
- Please print this page for your records and send a copy of it to your publisher/graduate school.
- Appropriate credit for the requested material should be given as follows: "Reprinted (adapted) with permission from (COMPLETE REFERENCE CITATION). Copyright (YEAR) American Chemical Society." Insert appropriate information in place of the capitalized words.
- One-time permission is granted only for the use specified in your request. No additional uses are granted (such as derivative works or other editions). For any other uses, please submit a new request.

If credit is given to another source for the material you requested, permission must be obtained from that source.

[BACK](#)
[CLOSE WINDOW](#)

Copyright © 2018 [Copyright Clearance Center, Inc.](#) All Rights Reserved. [Privacy statement](#). [Terms and Conditions](#). Comments? We would like to hear from you. E-mail us at [customer@copyright.com](mailto:customer@copyright.com)

5/11/2018

Rightslink® by Copyright Clearance Center



RightsLink®

Home

Account  
Info

Help



**Title:** Electrospinning: A fascinating fiber fabrication technique  
**Author:** Nandana Bhardwaj, Subhas C. Kundu  
**Publication:** Biotechnology Advances  
**Publisher:** Elsevier  
**Date:** May-June 2010

Logged in as:  
 Dan Gil  
 Home

LOGOUT

Copyright © 2010 Elsevier Inc. All rights reserved.

**Order Completed**

Thank you for your order.

This Agreement between Home -- Dan Gil ("You") and Elsevier ("Elsevier") consists of your license details and the terms and conditions provided by Elsevier and Copyright Clearance Center.

Your confirmation email will contain your order number for future reference.

[printable details](#)

License Number	4346090018241
License date	May 11, 2018
Licensed Content Publisher	Elsevier
Licensed Content Publication	Biotechnology Advances
Licensed Content Title	Electrospinning: A fascinating fiber fabrication technique
Licensed Content Author	Nandana Bhardwaj, Subhas C. Kundu
Licensed Content Date	May-June 2010
Licensed Content Volume	28
Licensed Content Issue	3
Licensed Content Pages	23
Type of Use	reuse in a thesis/dissertation
Portion	figures/tables/illustrations
Number of figures/tables/illustrations	1
Format	both print and electronic
Are you the author of this Elsevier article?	No
Will you be translating?	No
Original figure numbers	Figure 1
Title of your thesis/dissertation	Enhancing spider-silk protein materials through continuous electrospinning and photo-initiated cross-linking
Expected completion date	May 2018
Estimated size (number of pages)	100
Attachment	
Requestor Location	Home 803 Avalon Hills dr  OGDEN, UT 84404 United States Attn: Dan Gil
Publisher Tax ID	98-0397604
Total	0.00 USD

4/24/2018

Rightslink® by Copyright Clearance Center



# RightsLink®

[Home](#)
[Create Account](#)
[Help](#)


**Title:** Spider Silk: Ancient Ideas for New Biomaterials  
**Author:** Randolph V. Lewis  
**Publication:** Chemical Reviews  
**Publisher:** American Chemical Society  
**Date:** Sep 1, 2006

Copyright © 2006, American Chemical Society

#### LOGIN

If you're a [copyright.com](#) user, you can login to RightsLink using your [copyright.com](#) credentials. Already a [RightsLink](#) user or want to [learn more?](#)

#### PERMISSION/LICENSE IS GRANTED FOR YOUR ORDER AT NO CHARGE

This type of permission/license, instead of the standard Terms & Conditions, is sent to you because no fee is being charged for your order. Please note the following:

- Permission is granted for your request in both print and electronic formats, and translations.
- If figures and/or tables were requested, they may be adapted or used in part.
- Please print this page for your records and send a copy of it to your publisher/graduate school.
- Appropriate credit for the requested material should be given as follows: "Reprinted (adapted) with permission from (COMPLETE REFERENCE CITATION). Copyright (YEAR) American Chemical Society." Insert appropriate information in place of the capitalized words.
- One-time permission is granted only for the use specified in your request. No additional uses are granted (such as derivative works or other editions). For any other uses, please submit a new request.

If credit is given to another source for the material you requested, permission must be obtained from that source.

[BACK](#)
[CLOSE WINDOW](#)

Copyright © 2018 [Copyright Clearance Center, Inc.](#) All Rights Reserved. [Privacy statement.](#) [Terms and Conditions.](#) Comments? We would like to hear from you. E-mail us at [customer-care@copyright.com](mailto:customer-care@copyright.com)

4/27/2018

Rightslink® by Copyright Clearance Center



RightsLink®

Home

Create  
Account

Help



**Taylor & Francis**  
Taylor & Francis Group

**Title:** Direct electrospinning of highly twisted, continuous nanofiber yarns

**Author:** Usman Ali, Yaqiong Zhou, Xungai Wang, et al

**Publication:** The Journal of the Textile Institute

**Publisher:** Taylor & Francis

**Date:** Jan 1, 2012

Rights managed by Taylor & Francis

**LOGIN**

If you're a [copyright.com user](#), you can login to RightsLink using your copyright.com credentials. Already a [RightsLink user](#) or want to [learn more?](#)

**Thesis/Dissertation Reuse Request**

Taylor & Francis is pleased to offer reuses of its content for a thesis or dissertation free of charge contingent on resubmission of permission request if work is published.

BACK

CLOSE WINDOW

Copyright © 2018 [Copyright Clearance Center, Inc.](#) All Rights Reserved. [Privacy statement](#). [Terms and Conditions](#).  
Comments? We would like to hear from you. E-mail us at [customercare@copyright.com](mailto:customercare@copyright.com)

## Curriculum Vitae

**Dan Gil**

803 Avalon Hills Drive, Ogden, UT 84404  
(Cell) 973-598-5478 • [Dangil86@gmail.com](mailto:Dangil86@gmail.com)

**Education**

---

- PhD Candidate in Biology, Utah State University, Logan, UT 2014 – 2018  
Advisor: Dr. Randy Lewis, USTAR Professor of Biology  
Dissertation Title: “Enhancing Spider-silk Protein Materials Through Continuous Electrospinning and Photo-initiated Cross-linking”
- Bachelor of Art in Biology – Rutgers University, New Brunswick, NJ  
2012  
Minor in Biochemistry
- Associate in Applied Science – County College of Morris, Randolph, NJ  
2010  
Biotechnology

**Doctoral Degree Research and Experience**

---

- Designed and developed novel techniques and applications for biomaterials using recombinant spider-silk proteins, such as electrospinning producing fibers with novel properties that otherwise would not be possible.
- Designed and developed novel techniques and applications for biomaterials using recombinant spider silk proteins by means of a modified cross-linking method through a light-induced reaction
- Developed techniques to increase biocompatibility of biomaterials and determined biocompatibility of said biomaterials through cell culture, leading to in-vivo testing
- Led team of undergraduates, mentored them in research experimentation and design, conducted data acquisition and analysis, carried out trouble shooting

**Technical Skills**

---

- **Materials Science:** Protein chemistry, electrospinning, materials testing and analysis, cross-link modifications, sample preparation, mechanical testing and data analysis, Fourier-transform infrared spectroscopy and analysis, scanning electron microscopy, confocal microscopy
- **Cellular Biology:** Biocompatibility testing, cell culture, cell-based assays, transfection (electro and chemical)
- **Molecular Biology:** Plasmid design/construction/mini-prep, restriction enzyme digestion, DNA sequencing, polymerase chain reaction, molecular cloning, immunodetection (Western, Southern, and Northern blot)
- **Other Skills:** Electrical engineering, practical computer skills (building and configuring Windows/Linux based systems), equipment calibration, cGMP/cGLP, organization and accounting, Microsoft Word, Excel, PowerPoint, Spanish (fluent)



## Scholarships and Awards

---

- County College of Morris, dean's list  
2010
- County College of Morris, Phi Theta Kappa Honor Society  
2010

## Additional Academic Activities

---

- County College of Morris, Head Science Tutor  
2006-2010
- Rutgers University: Animal micro-techniques and tissue culture, Intern  
2010
- Skylands Medical Group, Intern  
2010

## Working Experience

---

- Integrated Analytical Laboratories, Microbiologist/Organic Extractionist  
2012-2013
- Akorn Pharmaceuticals, Metrologist  
2013-2014

## Presentations in Scientific Meetings

---

- Synthetic Biomanufacturing Institute Science and Technology Review, Logan, UT: "Electrospinning: Silk and Composite Fibers," 2014, Dan Gil, Ibrahim Hassounah, Justin Jones, Randy Lewis
- Student Research Symposium, Logan, UT: "Electrospinning: Silk and Composite Fibers," 2014, Dan Gil, Ibrahim Hassounah, Justin Jones, Randy Lewis
- Synthetic Biomanufacturing Institute Science and Technology Review: "Electrospinning: Silk and Composite Fibers," 2015, Dan Gil, Ibrahim Hassounah, Justin Jones, Randy Lewis
- Student Research Symposium, Logan, UT: "Modified Electrospinning and Cross-Linking of Recombinant Spider Silk Proteins," 2015, Dan Gil, Ibrahim Hassounah, Justin Jones, Randy Lewis
- Student Research Symposium, Logan, UT: "Modified Electrospinning and Cross-Linking of Recombinant Spider Silk Proteins," 2016, Dan Gil, Blake Taurone, Justin Jones, Randy Lewis
- Materials Research Society, Phoenix, AZ: "Making Electrospun Spider Silk Fibers Stronger," 2016, Dan Gil, Blake Taurone, Justin Jones, Randy Lewis

## Publications and Manuscripts in Preparation

---

- "Enhancing the Mechanical Properties of Nylon 66 Electrospun Yarns by Annealing and Addition of Spider Silk Proteins," 2017, Ibrahim Hassounah, Ethan Abbott, Dan Gil, Cameron Copeland, Thomas Harris, Justin Jones, Jeff Yarger, Randolph V. Lewis

- “Enhancing Spider-silk Protein Materials Through Photo-Initiated Cross-linking,” 2018, Dan Gil, Blake Taurone, Bailey McFarland, Thomas Harris, Justin Jones, Randy Lewis
- “Continuous Electrospinning of Spider-silk Proteins Creates Nanofiber Yarns with Unprecedented Properties,” 2018, Dan Gil, Bailey McFarland, Blake Taurone, Justin Jones, Randy Lewis

## References

---

Dr. Randy Lewis  
USTAR Professor of Biology  
Utah State University  
Email: [randy.lewis@usu.edu](mailto:randy.lewis@usu.edu)  
Phone: 435-797-9291

Dr. Justin Jones  
Research Assistant Professor, Biology Department  
Utah State University  
Email: [justin.a.jones@usu.edu](mailto:justin.a.jones@usu.edu)  
Phone: 435-797-9292

Dr. Lee Rickords  
Associate Professor of Animal, Dairy, and Veterinary Sciences  
Utah State University  
Email: [lee.rickords@usu.edu](mailto:lee.rickords@usu.edu)  
Phone: 848-932-9095

Joe Li  
Former Manager of Metrology, Senior Validation Engineer  
Akron Pharmaceuticals  
Email: [joe.li@akorn.com](mailto:joe.li@akorn.com)  
Phone: 631-789-8228 ext:4109

Robert Blank  
Manager of Microbiology  
Integrated Analytical Laboratories  
Email: [rblank@ialonline.com](mailto:rblank@ialonline.com)  
Phone: 908-625-7197